THE

LONDON, EDINBURGH, AND DUBLIN

PHILOSOPHICAL MAGAZINE

AND

JOURNAL OF SCIENCE.

[SEVENTH SERIES.]

JULY 1935.

I. *The Influence of Impurities in the Core-metal on the Thermionic Emission from Oxide-coated Nickel.*

(Part I. of a Thesis * approved for the Degree of Doctor of Philosophy in the University of London.) *By* M. BENJAMIN, *B.Sc.*, *Ph.D.*† (Communication from the Research Staff of the M.O. Valve Company, Limited, at Wembley.)

SUMMARY.

THE commoner metallic impurities have been added in turn to a pure nickel, and the emission from the oxide-coated cores compared. It is found that these additions can profoundly affect the emission. An explanation put forward is that the amount of barium metal in the coating is dependent on the reducing power of the additive. This theory is supported by the results obtained when the addition is a powerful reducing agent such as aluminium. It is found, also, that at very low temperatures non-saturation of the emission occurs, and that the critical temperature depends on the nature of the additive. The results obtained are explained by

* The thesis has been somewhat abbreviated for the purposes of publication.

† Communicated by C. C. Paterson, M.I.E.E.

the theories of the mechanism of emission, due to Becker and Sears, and Fowler and Wilson, which regard the coating as a semi-electronic conductor, whose conductivities and emission depend on the concentration of barium metal in the coating.

Introduction.

OXIDE-COATED cathodes, the coatings being composed of a mixture of BaO and SrO, have displaced to a very large extent tungsten, thoriated tungsten, and "barium vapour process" cathodes in broadcast receiving valves. The first oxide cathodes had platinum or platinum alloy cores, but in the past few years nickel has superseded platinum as the core-metal, mainly on the grounds of economy.

The use of nickel has shown that, under carefully controlled conditions, wide variations in thermionic emission occur. Further, these variations are generally coincident with a change in the batch of core-metal. This has necessitated a rigid testing of each batch of nickel before it could be passed for general use.

The commercially pure nickel commonly used contains generally about 0·5 per cent. of metallic impurities, the nature and quantity of which vary with the processes of manufacture. It seemed reasonable, therefore, to suppose that it was differences in the impurity content of the nickel which were responsible for the observed variations. A series of experiments was carried out in order to determine the effects, if any, of the commoner metallic impurities on the thermionic activity from oxide-coated nickel.

In a very early study of oxide cathodes Deininger [1] found the emission to be independent of the nature of core-metal. That the addition of small amounts of other metals to the core-metal can influence the activity was, however, demonstrated by C. J. Smithells [2] in these laboratories. Working with coated platinum he found, in 1925, that the thermionic activity was increased by the addition of up to five per cent. of iron or chromium to the platinum. These results form the basis of a patent relating to improvements in oxide cathodes, but are otherwise unpublished.

E. W. Lowry [3], in 1930, found that the emission of an oxide coating could be altered considerably by completely changing the nature of the core-metal. He obtained greatly increased emissions with coated "konel," a nickel-cobalt-iron-titanium alloy, as compared with coated platinum.

Experimental.

(a) The method adopted was to prepare nickel of a very high standard of purity, and to add to it small quantities of the commoner impurities, viz., magnesium, manganese, iron, and ferro-titanium.

The thermionic properties of the coated pure nickel and the coated alloys were then directly compared.

(b) *Preparation of Core-metals.*

The methods by which the various wires used were prepared are described in detail in a paper by Ransley and Smithells [4]. The alloys, together with a sample of the pure nickel, were drawn down into wires of 0·0425 mm. in diameter.

The results of chemical analyses of the different wires are shown in Table I., together with the analysis of a typical commercial nickel. The alloys were analyzed only for the impurity added, the composition otherwise was assumed to be that of the pure nickel. The magnesium alloy, although 0·5 per cent. magnesium was added originally, contained less than 0·1 per cent. magnesium, due to the volatilization of the additive during melting. The other analyses were in close agreement with the expected composition. The ferro-titanium was added as such, since it is extremely difficult to obtain titanium free from iron, and the two metals normally occur together in nickel.

(c) *Coating of the Core-wires.*

The wires were coated with a mixture of $BaCO_3$ and $SrCO_3$, the oxides being obtained by subsequent decomposition in vacuum. The continuous coating process used has been described in a previous paper [5]. To ensure similar conditions for each wire the wires were joined together and coated as a single wire and then separated. The carbonate coating was such that, on

TABLE I.

Chemical Analyses of the Different Core-metals.

Material.	Nickel and cobalt (by difference), per cent.	Cobalt, per cent.	Manganese, per cent.	Magnesium, per cent.	Iron, per cent.	Titanium, per cent.	Aluminium, per cent.	Calcium, per cent.	Silicon, per cent.	Carbon, per cent.	Sulphur, per cent.
Commercially pure nickel	99·39	0·45	0·21	0·09	0·22	—	—	—	0·024	0·036	0·033
Pure electrolytic nickel	99·91	0·29	trace	0·006	0·004	—	0·024	0·083	0 016	0·022	0·003
Nickel and magnesium	—	—	—	0·07							
Nickel and ferro-titanium	—	—	—	—	0·37	0·10					
Nickel and manganese	—	—	0·34								
Nickel and iron	—	—	—	—	2·33						

decomposition, a solid solution of oxides was obtained, the chemical composition of which was 46 per cent. BaO to 54 per cent. SrO by weight.

(d) *Description of Apparatus.*

In order to obtain a comparison of two coated cathodes under identical conditions it is essential to place them inside the same electrode system. First attempts with two cathodes mounted side by side in a common anode revealed the fact that, with both cathodes in an active state, each tended to poison, temporarily, its neighbour. (By poisoning it is meant that gas evolved from the

Fig. 1.

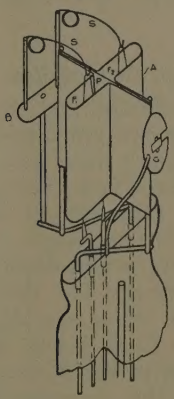

Tubes used for direct comparison of the various oxide-coated core-wires.

cathode under test settles on its neighbour and reduces the emission.) The apparatus shown in fig. 1 was found to overcome this defect, and it also prevents the possibility of evaporation of coating from either cathode on to its neighbour.

Each tube contained a coated alloy cathode F_1 and a coated pure nickel cathode F_2 in the form of filaments each 68 mm. in length. The filaments were mounted from a glass pinch in the shape of inverted V's, and were suspended by molybdenum springs S, S from a glass bead B. Both filaments were surrounded by a nickel anode A, of rectangular section, 2×20 mm.,

and 32 mm. in length. The two filaments were separated, however, by the nickel partition P, which ran the length of the anode and so divided it into two separate compartments. This device effectively prevented each filament from " seeing " its neighbour.

Placed parallel to the face of the anode, and several mm. from its centre, was the nickel disk G, on to which was clipped a piece of magnesium for gettering purposes.

The electrode system described was sealed into a pre-baked glass bulb, which could be evacuated by means of a foot-tube in the glass pinch.

Before the tube was assembled, the anode, disk, and springs were vacuum cooked at 1000° C. in order to outgas them. The magnesium was similarly treated, but at 500° C.

(e) *Initial Treatment of the Cathodes.*

Each tube was evacuated and the filaments activated together by the processes previously described [5]. The activation temperatures * were, as before, 1250° K. and 1150° K. The temperatures were measured on the coated pure nickel filament, it being assumed that, since the coatings were the same on each filament, the brightness temperature would depend only on the watts supplied to the filament. The differences in hot resistances of the various wires was allowed for by running each filament at a fixed input watts equal to that supplied to the pure nickel filament at any particular temperature. Since the constructions were the same in each case, and the conductivities are not very different, end-cooling was the same for each filament.

Emission measurements were made at 1020° K., 40 volts applied to the anode being sufficient to ensure good saturation.

The filaments, during all the processes described, were run on alternating current, to minimize the emission-heating effect. It is necessary to appreciate that at 1020° K. the heating current is only 90 ma., whilst the emission current is 30–50 ma., that is, of the same order as the heating current, and the use of a D.C. supply would result in the heating up of one end of the filament. The

* The temperatures given in the test are brightness temperatures measured by an optical pyrometer, and are only approximate.

arrangement described ensures that this heating effect is distributed uniformly over the filament.

The emissions obtained are shown in Table II. Six filaments of each coated wire were measured. Each

TABLE II.

Data showing Emissions obtained from the Various Core-wires at 1020° K.

Core-wire.	Emissions in ma.	Average emissions in ma.	Emission from pure nickel filament in same tube in ma.	Average emission in ma.
Nickel +0·5 per cent. ferro-titanium.	42·5 46·0 44·5 46·0 44·0 47·0	45·0 ±6·0 per cent.	27·0 32·0 30·0 29·5 30·5 32·0	31·0 ±13 per cent.
Nickel +0·07 per cent. magnesium.	48·0 44·0 43·0 45·0 47·0 43·5	45·0 ±7·0 per cent.	31·0 29·0 27·0 34·0 32·0 27·5	
Nickel +2·0 per cent. iron.	24·0 24·0 20·0 23·0 23·0 21·0	22·5 ±11 per cent.	30·0 33·0 31·0 28·0 27·5 29·5	
Nickel +0·4 per cent. manganese.	22·0 18·5 20·0 21·0 18·5 19·5	20·0 ±10 per cent.	31·0 34·0 32·0 27·0 29·0 29·0	

filament had a pure nickel filament next to it, as described in the previous section.

It will be seen from the table that the emissions vary considerably with the nature of the core-metal.

The presence of less than 0·1 per cent. magnesium and of 0·5 per cent. ferro-titanium has increased the emission obtained from the pure nickel core by about 50 per cent.

The presence of 2·0 per cent. Fe and of 0·4 per cent. manganese has reduced the emission by 30 per cent. These results are of great interest and importance, for manganese and magnesium are the two most common impurities in commercially pure nickel, since they are used as deoxidizing agents in the melting process.

The increase in emission, due to ferro-titanium, must be attributed to the titanium, since the presence of iron alone results in a lowered thermionic emission. This was established by repeating the experiment, using a nickel containing 0·1 per cent. Ti free from iron.

Fig. 2.

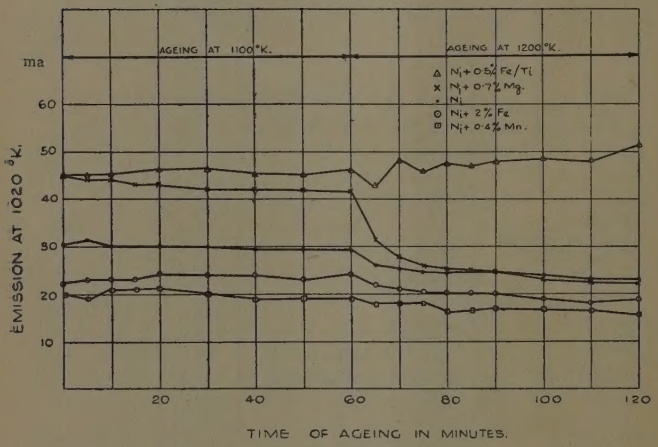

Effect of high-temperature ageing on emissions of alloy filaments.

(f) *Prolonged Ageing at High Temperature and the Effect on the Thermionic Emission.*

The emissions given above are those obtained after an activation period of 15 minutes. In order to determine whether the emissions obtained were permanent in character, several tubes of each type were run with the filaments maintained at 1100° K. for one hour, and then at 1200° K. for one hour. In each case about 10 ma. space-current was drawn from each filament. Emission measurements at 1020° K. were made every few minutes, and in fig. 2

are shown the curves obtained relating the emission with time of ageing.

It will be seen that during the first hour very little change in the respective emissions has occurred. On raising the temperature, however, a decline in the emission value is observed in every case. With the ferro-titanium alloy this fall is not continued, and with further running the emission returns to its original value and then shows a tendency to improve further. The magnesium alloy, however, shows a very sharp initial fall in emission, and it then declines steadily until it reaches a value of the same order as that obtained from the pure nickel cathode at the same point. The pure nickel emission, after the initial drop, also decays, but the rate of decay is slight. The manganese and iron alloys show a very slight decrease in emission throughout.

Attempt to prolong the ageing beyond the one hour at 1200° K. resulted in mechanical failure of the majority of the filaments.

(g) *Prolonged Running at Normal Temperatures.*

A number of the tubes were run, with their filaments maintained at 1020° K., for several hundred hours. Small space currents were again drawn from the filaments the whole of the time. The emission-time curves obtained are shown in fig. 3, and it will be seen that the results are very much the same as those obtained at the higher temperatures.

(h) *Increased Titanium Content.*

The result obtained with an alloy containing 1·1 per cent. iron, 0·39 per cent. titanium is shown in fig. 4, together with the curve due to the 0·5 per cent. ferro-titanium. It will be observed that the tendency for the emission from the 0·5 per cent. alloy to rise with prolonged ageing is accelerated when the titanium content is increased from 0·1 per cent. to 0·4 per cent., and the ultimate emission obtained was 70 ma. This emission did not saturate at the measuring temperature. It will be observed that, on raising the ageing temperature from 1100° K. to 1200° K., the initial fall in emission seen in fig. 2 again occurs. The fall occurs with all the core-metals, and may be due to an upsetting of the equilibrium

conditions prevailing, due to an increased rate of evaporation of active material from the coating, which

Fig. 3.

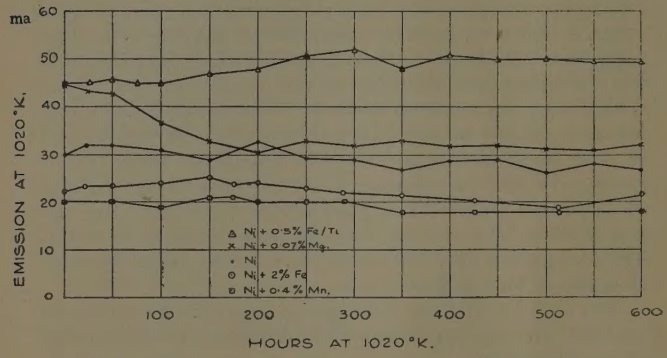

Effect of prolonged running at 1020° K. on emissions of alloy filaments.

Fig. 4.

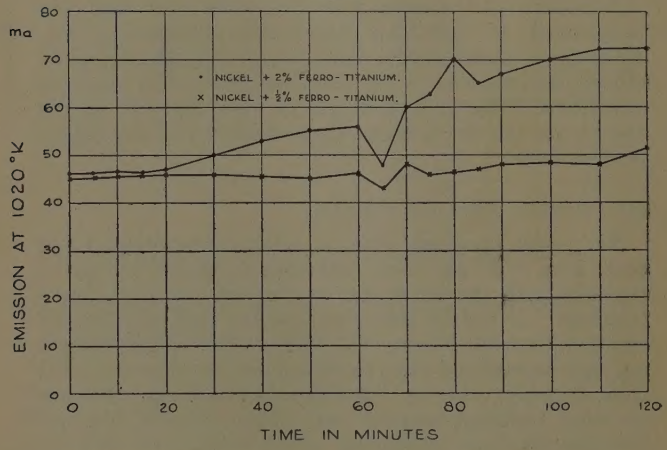

High-temperature ageing of nickel + 2 per cent. ferro-titanium and effect on emission.

persists until equilibrium is again restored at the higher temperature.

Discussion.

(a) *Summary of Results.*

Summarizing the results obtained, it appears that (*a*) titanium and magnesium increase the thermionic activity, and (*b*) iron and magnesium decrease the thermionic activity of oxide-coated nickel when these metals are present in small quantities in the nickel core-metal. The effect due to titanium is permanent over a long period of time, as are the effects due to manganese and iron. The magnesium exercises only a temporary influence; the emission falls in a relatively short time to a value of the order of that obtained from pure nickel.

(b) *Barium Concentration and Emission.*

The experimental evidence offered by many workers points to the fact that the active material in an oxide cathode is free barium metal. We need not, at this stage, concern ourselves with the exact mechanism of the emission, but need only deal with the fact that the amount of free barium produced can influence the activity of the cathode. Much work has been done on the methods by which the free metal is produced. Two main views exist: (*a*) under the action of an initially small emission current the coating is electrolyzed to form barium ions and oxygen ions—the former are liberated at the core-coating interface, and the latter at the surface of the coating; (*b*) under the initial heat treatment of the coating thermal dissociation of the oxide occurs with liberation of free barium; (*c*) the results of Lowry (*loc. cit.*), who activated cathodes by thermal treatment, only support the view of thermal dissociation and/or of possible reduction of the coating by the core-metal. These two effects, if they occur, cannot normally be distinguished.

However, as we shall proceed to show, the experimental results obtained can be explained by assuming that reduction of the coating by the core-metal does occur. In the experiments described, the amount of free barium formed by electrolysis or by thermal dissociation must be the same in each case, since all conditions of activation treatment were the same. The other method of producing barium, by the action of the core on the coating, may, however, be different, for the core-metals differ in nature

because of the different additives in the nickel. Let us suppose that, at the activation temperature of the filament, the additives in the core-metal can diffuse to the surface, and there reduce the oxide coating. Then, since the other methods of producing barium are the same, any differences in the reducing properties of the additives will result in differences in the barium concentrations in the coatings of the various filaments. If the heats of formation of the various metallic oxides are considered, we obtain the following order, considering only the monoxides :—

Metal oxide.	Heat of formation of a gram-molecule.
TiO_2	$218{\cdot}4 \times 10^3$ calories.
MgO	143·3 ,, ,,
SrO	141·0 ,, ,,
BaO	126·0 ,, ,,
MnO	90·8 ,, ,,
FeO.....	64·6 ,, ,,
NiO	57·9 ,, ,,

Thus we should expect the reducing power of the various core-wires to be in the following order : nickel and ferro-titanium, nickel and magnesium, nickel and manganese, and nickel and iron. We should also expect the thermionic activities of the coated wires to be in the same order. This is what does occur if we ignore for the moment the pure nickel filament. Thus we can attribute the enhanced activity of the magnesium and titanium alloy filaments to the fact that the additives, by their reducing action, result in an increased quantity of free barium metal in the coating. The activity from the pure nickel filament is, however, higher than the activities of the iron and manganese alloy filaments. It is not clear why this is so, for, from the values of the heats of formation, neither of the three metals will appreciably reduce barium oxide. It is possible to attribute the emission of the pure nickel cathode to the presence of the small traces of magnesium and aluminium, both powerful reducing agents, which are present, and the lower emissions of the manganese and iron alloy cathodes to the suppression, in some way, of the reducing action of the magnesium and aluminium by the very much larger quantities of manganese or iron. But against this there is, as we have seen, the fact that the presence of three times as much iron as titanium does not affect

the action of the titanium. If it were possible to obtain an absolutely pure nickel core-wire we should expect the emission from such a coated wire to be of the same order as that from the manganese and iron alloy cathodes. It has not, however, been possible to obtain such a core-wire. It is worth recording, however, that in the past it has been found that the thermionic emissions from a coated nickel wire, which from its electrical resistance must have been extremely pure, have been very low. It was not possible to obtain a sample of this nickel for experiment under the controlled conditions described in this paper.

The initial emission results obtained have, however, been explained generally in a satisfactory manner by the theory that the thermionic activity of a coated nickel wire is influenced by the reducing power of the additives present, the emissions being in the order of the reducing powers. The effect of the reducing action of the additives in the core results in a greater equilibrium concentration of barium metal, the active agent, in the coating.

The temporary nature of the enhanced emission of the magnesium alloy filaments, as shown by the high-temperature ageing, is explained by the fact that at the temperatures used magnesium is extremely volatile, and as the barium concentration falls, by evaporation from the surface, so the magnesium required to maintain the supply of barium metal also evaporates, and the emission falls to a value characteristic of a pure nickel cathode. The permanence of the enhanced emission due to the ferro-titanium can be attributed to a very slow rate of evaporation of titanium.

(c) *The Effect of Aluminium as an Additive.*

The results indicate that the magnitude of the effect on the emission of the cathode will be related to the reducing power of the additive. If we consider a list of possible metallic additives other than those already tried, we have :—

Metal oxide.	Heat of formation of gram-molecules.
La_2O_3	$447{\cdot}3 \times 10^3$ calories.
Al_2O_3	380·0 ,, ,,
ThO_2	326·0 ,, ,,
CeO_2	224·0 ,, ,,
ZrO_2	175·0 ,, ,,

Lanthanum and cerium occur together in the substance known as "misch-metal," and, with aluminium and thorium, are better reducing agents than titanium. Hence their addition to the core-metal should result in a still further increase in thermionic activity. Alloys were made with each of these metals. One of the alloys contained 0·19 per cent. thorium and another 2 per cent. aluminium, as determined by chemical analysis; the third alloy contained misch-metal, the actual amount of which was not estimated, but 2 per cent. of the substance was added to the nickel melt.

The wires made with these alloys were coated, and the thermionic activities compared with the pure nickel filaments in the manner described. The average emissions obtained are given in Table III.

TABLE III.

Emission Data of Nickel-Aluminium, Nickel-Thorium, and Nickel-Misch-Metal Cores.

Core-wire.	Average emission, ma. at 1020° K.	
	Alloy.	Nickel.
Nickel + 2 per cent. aluminium	50·0	30·0
Nickel + 0·19 per cent. thorium	34·0	
Nickel + 2 per cent. misch metal.....	20·0	

After activation, the various filaments were aged at 1100° K. and 1200° K., and the emission-time curves obtained are shown in fig. 5. The emission from the thorium alloy filament behaved very much like that from the pure nickel filament, although it seemed somewhat steadier at 1200° K. The emission from the misch-metal alloy filament tended to increase at first, and then it fell away again at 1200° K. The aluminium alloy filament, however, gave an emission which, initially greater than any previously obtained after activation, increased rapidly and became non-saturated. It reached a value of 70 ma., comparable with that of the 2 per cent. ferro-titanium alloy, but in a much shorter time, and its final value was over 80 ma.

Thus the presence of the aluminium has considerably increased the thermionic emission normally obtained from the nickel cathode, and this result is in striking support of the theory, expressed previously, that the activity can be considerably increased by addition of a suitable additive to the core-metal. The thorium and misch-metal emissions are lower than expected. That obtained from the misch-metal alloy is, indeed, very poor.

Fig. 5.

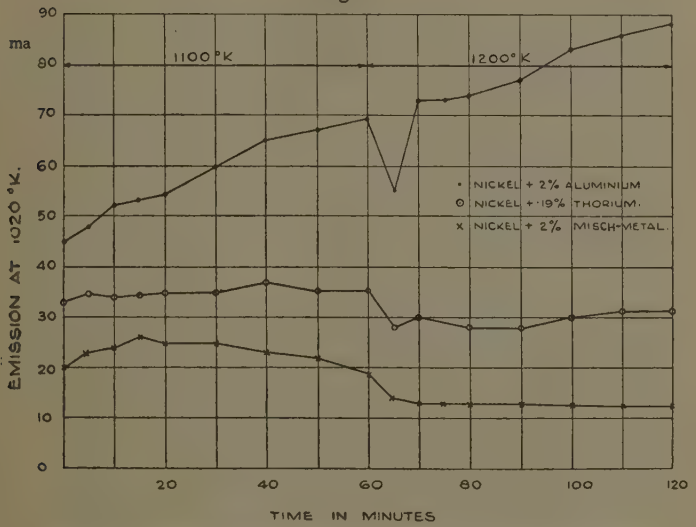

Effect of high-temperature ageing on nickel + 2 per cent. aluminium.

Since, however, thorium combines readily with hydrogen and nitrogen, and misch-metal combines readily with nitrogen, in each case very stable compounds being formed, it is possible that, during melting, the metals were attacked by the nitrogen and hydrogen used in the process.

Saturation of the Emissions at Low Temperature (600° K.).

It has been stated that the emissions from well activated nickel/aluminium and nickel/ferro-titanium alloy filaments

do not saturate at the normal measuring temperature, where the pure nickel, nickel-manganese, and nickel-iron alloy filaments do saturate. By saturation is meant a well-defined bending of the emission-current curve towards the voltage axis, for, as is well known, the saturation of the emission from oxide coatings is never as complete as in the case of the emissions from pure metals. This failure to saturate can be partly explained by an emission heating of the filament due to the very

Fig. 6.

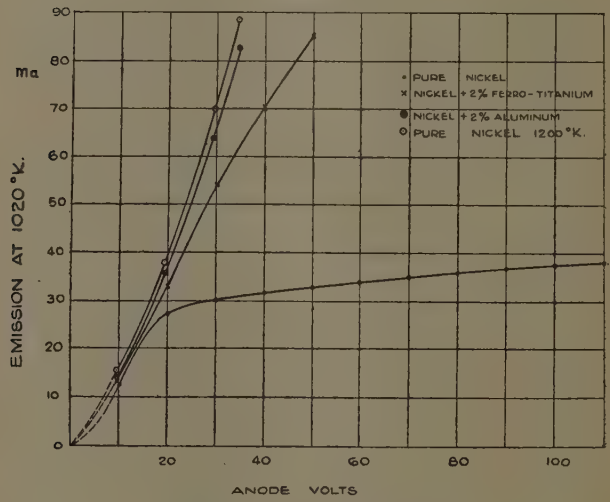

Emission-voltage curves at 1020° K.

large currents (70–80 ma. from a 90 ma. filament) returned to it. This explanation is supported by the fact that the emission of a pure nickel filament also fails to saturate when the emission is made sufficiently great, as when the temperature is raised. The emission-current voltage curves are shown in fig. 6, together with the curve for pure nickel at 1200° K.

It was thought advisable, however, to compare the emissions of the aluminium and ferro-titanium alloy filaments with that of the nickel filament at a temperature

where the emission heating effects would be negligible, and so to establish beyond doubt the existence of the enhanced activities. In fig. 7 are shown the emission-current voltage curves at a temperature which was not measured, but which was estimated to be in the neighbourhood of 600° K. In each case, it will be observed, the initial approach to saturation is well defined, the emission of the coated nickel-aluminium filament being

Fig. 7.

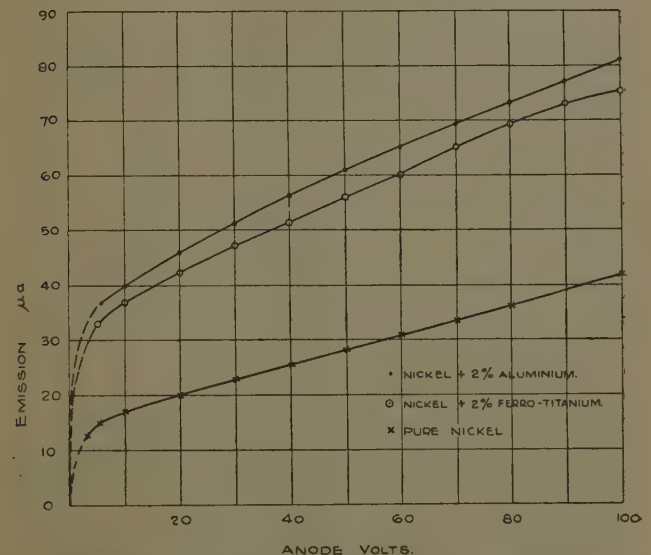

Emission-voltage curves (at 0·022 watts input to filaments).

about twice that of the coated nickel filament. A similar result is obtained with the ferro-titanium alloy filament, although its emission is not so great as that of the aluminium alloy filament.

Activation by Thermal Treatment only.

It has been stated by some authors that the oxide-coated cathode is only completely activated when current is drawn from the cathode. Lowry [3], however, has reported that both konel- and platinum-coated cathodes

can be completely activated by thermal treatment only, that is, by running the cathode at the activating temperature for some minutes without drawing current from it. It may well be that, if a reducing agent is present in the core, thermal treatment alone is sufficient for activation, whilst if it is absent activation can only be completed when sufficient barium is produced by drawing current from the coating, that is, by electrolysis. The emissions, however, may be different in the two cases, because of the difference in the final equilibrium concentration of the barium.

The various coated alloy filaments were assembled in the diode tubes described and, after treatment on the pump, the tubes were sealed off and activated by thermal treatment only. Each filament was flashed at 1250° K., snap-emission readings being made at 1020° K. at frequent intervals. Fig. 8 shows the rate of activation, with time of flashing, for typical filaments of each type. It will be seen that at the end of 10 minutes the aluminium, ferro-titanium, and magnesium alloy filaments are practically completely activated. The iron and manganese alloy filaments show very little activation. Prolonging the time of flashing results in a series of curves whose general shapes are similar to those in fig. 2.

The fact that activation occurs at all can only be attributed to the formation of free barium metal by the reducing action of the core and/or by any thermal dissociation of the coating itself. The latter factor, if appreciable, is the same for each filament, and thus the marked activation of the aluminium, ferro-titanium, and magnesium alloys can be attributed to the reducing action of the additive on the coating ; as is then to be expected, the manganese and iron alloy filaments show very little activation. The rapid decline of the magnesium alloy filament activity can be again attributed to the very rapid evaporation of the additive. The pure nickel filament behaves as in the previous experiments ; the activation is almost complete by thermal treatment only.

Finally, it is necessary to state that in no case were the emissions obtained by thermal treatment very stable at the measuring temperature. In general they fell away rapidly, but several hours' running of the tube

at this temperature, taking small currents, results in the emissions recovering to the original values, or sometimes to somewhat greater values, the emissions then being stable. This initial falling off may be due to an alteration in the equilibrium concentration of barium, due to the taking of emission current, with consequent electrolysis of the coating. Prolonged running will bring about a state of stable equilibrium.

The Mechanism of the Emission.

The experimental results have been explained by assuming that the additive in the core-metal can influence the actual concentration of free barium metal in the coating, the activity depending in some way on the barium concentration. It is, therefore, of interest to see how the explanation offered fits in with existing theories of emission mechanism.

The theory now seems to be fairly well established [12]. The experimental evidence of Reimann and Murgoci [6] and Becker and Sears [7], and the theoretical work of Wilson [8], [9], [10] and Fowler and Wilson [11] allow the oxide coating to be treated as an impurity semi-conductor, in which the necessary impurity is barium. On Wilson's theory the outermost electrons of the impurity atoms are at a discrete energy W_1 intermediate between the top of the last-filled band of allowable energies W_0 and the bottom of the first empty band W_2 in the oxide. Thermal agitation may result in electrons being excited from W_1 to W_2 under conditions where they cannot pass readily from W_0 to W_2, and the oxide will then have an electronic conductivity. The electrons in the normally unoccupied band (the conduction electrons) can now be further excited to the energy level W_v or beyond, where W_v is the potential energy of an electron in the vacuum, and so escape.

Now, as Reimann has outlined, by applying Wilson's expressions to this case the emission equation is obtained. If N_0 is the number of impurity atoms per unit volume and N_1 the number of electrons excited to W_2, then

$$N_1 = \text{const.}\ N_0^{1/2} T^{3/4} \epsilon^{-(W_2 - W_1)/2kT}. \quad . \quad . \quad . \quad (1)$$

Let N_2 be the number of electrons emitted. These are small in number, and, therefore, have a Maxwellian

velocity distribution. Consequently, treating them as Richardson did the supposedly free electrons of a metal, we obtain

$$eN_2 = i = \text{const.}\, T^{1/2} \epsilon^{-(W_v - W_2)/kT}. \quad . \quad . \quad . \quad (2)$$

On combining (1) and (2), we have the emission formula,

$$i = \text{const.}\, N_1^{1/2} T^{5/4} \epsilon^{-(W_v - \frac{1}{2}(W_1 + W_2))/kT}. \quad . \quad . \quad (3)$$

From (3) it will be seen that the magnitudes of the emissions will depend on the concentrations of barium in the coating. This is a possible explanation of the experimental results. In these the addition of aluminium was found to double the emission. This can be explained by supposing that the reduction of the oxide by the additive gives a fourfold increase in barium concentration. If, however, the adsorbed film of barium was not previously complete, the emission increase may in part be due to a decrease in W_v owing to an increased barium concentration.

Now, as Reimann [12] has pointed out, thermodynamical considerations necessarily lead to the same emission formula as that which applies to metals :

$$i = AT^2 \epsilon^{-\chi/kT}, \quad . \quad . \quad . \quad . \quad . \quad . \quad . \quad (4)$$

where $\chi = W_v - E_0$, E_0 being the Fermi critical energy of the free electrons in the core-metal. Equation (4) immediately follows from (3) by combining it with Wilson's expression for E_0 in the case where a metal is in equilibrium with the semi-conductor, viz.,

$$E_0 = \tfrac{1}{2}(W_1 + W_2) + kT \log \left\{ \frac{\alpha N_0^{1/2}}{(AT)^{3/4}} \right\}, \quad . \quad . \quad (5)$$

where α is a constant. We then obtain (4), where A is a constant (apart from any temperature variation in the mean transmission coefficient) and χ is equal to $W_v - E_0$. Thus we may regard the concentration of dissolved impurity as influencing not A but χ, as can be seen from (5).

It is important to note that the core-metal has no direct effect on the emission, for E_0 for the metal is completely determined by the conditions in the oxide and the impurity concentration, as is evident from (5).

The core-metal can only affect the emission indirectly by influencing the quantity of free barium in and on the coating, as, for example, by chemical reduction. This, as the experiments show, it apparently does do. Lowry's results with konel can be similarly explained. Since konel contains 2·5 per cent. titanium, the enhanced emission is to be expected.

Failure of Emission to Saturate at very low Temperatures.

During the course of measurements to find a suitable temperature for measurement of emission, a series of phenomena were observed which occurred with each type of filament, which was independent of the composition of the core-metal.

It was observed that :

(1) The emission at a sufficiently high temperature did not saturate.

(2) At low temperatures (600° K.) the emission saturated.

(3) At very low temperatures, about 500° K., in each case a temperature was found where, after the initial bend towards the voltage axis, the emission curve showed a distinct tendency to bend away from the voltage axis with increasing anode volts, the upward bending becoming apparent at about 50 volts.

(4) At temperatures lower than those in (3) the emission curves bend away from the axis, there being no sign of any approach to saturation except, possibly, at very low anode volts.

The temperatures at which these phenomena occur are, however, different for the different cores. The nickel, the iron alloy, manganese alloy and magnesium alloy filaments show these effects at very much the same temperature, but the aluminium alloy and ferro-titanium alloy filaments begin to show all these effects at much lower temperatures. (1) and (2) have been dealt with in a previous section.

The failure of the emission to saturate at the very low temperature is illustrated by the curves in figs. 7, 8, and 9, which are typical ones for the nickel and nickel-aluminium filaments. As has been described, the emissions from both filaments show a well-defined approach

to saturation at the temperature represented in fig. 7. In fig. 9 the temperature has been lowered, and it will be seen that the emission from the nickel-aluminium filament still saturates. The emission due to the pure nickel filament shows, however, a definite tendency to bend upwards and away from the voltage axis at about 50 volts.

On still further lowering the temperature to the values indicated in fig. 10. it is seen that now the aluminium-nickel emission (fig. 10, i) exhibits the same

Fig. 8.

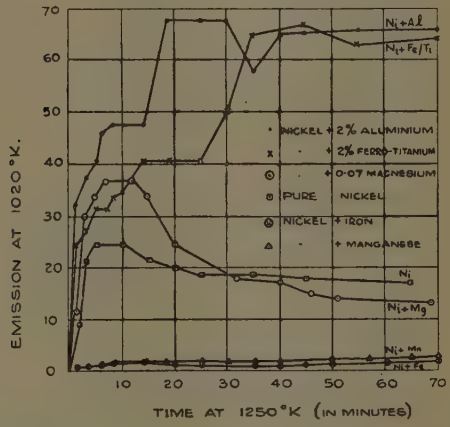

Activation of filaments by temperature treatment only.

tendency to bend away from the voltage axis as the pure nickel filament emission did at the higher temperature indicated in fig. 9. The nickel filament emission at this lowered temperature now shows no approach to saturation (fig. 10, ii). On reducing the temperature of the nickel-aluminium filament still further, the emission (fig. 10, iii) now exhibited the same failure to saturate as did the emission from the pure nickel filament at the immediately higher temperature. (The points on those curves which bend away from the voltage-axis are first-time readings, for it was not found possible to repeat exactly the readings, although on each occasion

the general shape of the curve remained the same.) The failure of the emission to saturate at very low temperatures has been observed by Reimann and Treloar [13] for pure nickel-oxide cathodes. They also found that

Fig. 9.

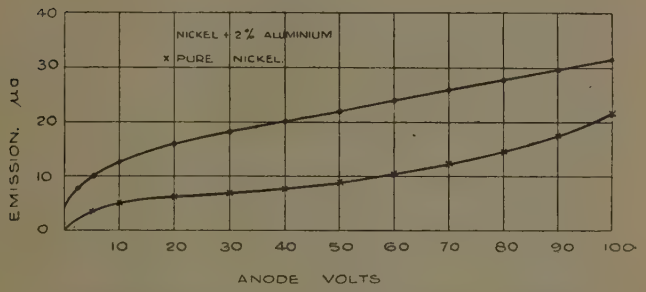

Emission-voltage curves (at 0·0185 watts input to filaments). Temp. ≠ 550° K.

Fig. 10.

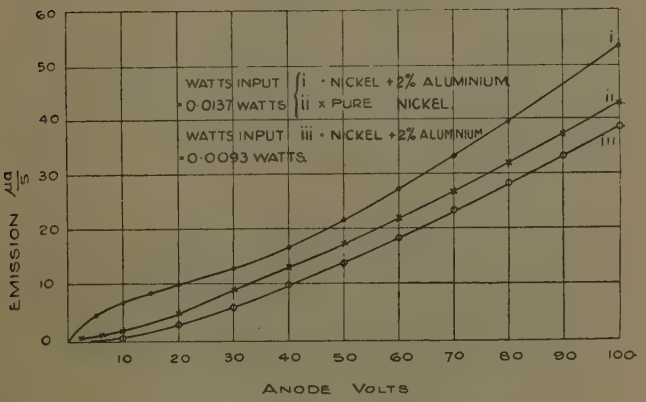
WATTS INPUT 0·0137 WATTS
i • NICKEL + 2% ALUMINIUM
ii x PURE NICKEL
WATTS INPUT 0·0093 WATTS
iii • NICKEL + 2% ALUMINIUM
EMISSION μa/in
ANODE VOLTS

Emission-voltage curves (at ≠ 500° K.).

the shape of the conductivity curve altered at the same time. Fowler and Wilson have reproduced these curves only by assuming that at low temperatures the conduction through the coating is now mainly electrolytic. Now the significant fact is that the emission fails to saturate

when the current changes from mainly an electronic one to mainly an electrolytic one. The temperature at which the electrolytic current becomes a significant part of the whole must depend on the concentration of the barium present in the coating, which is responsible for the electronic part of the current. The concentration of metallic barium in the nickel-aluminium and nickel-titanium cathodes has been shown to be about four times that in the pure nickel cathode, and thus one would expect the electrolytic current to become significant at a lower temperature in the more active filaments.

Additions of Impurities to the Coating.

The theory given indicates that a similar effect will be obtained by addition of a suitable reducing agent to the coating itself. This has been attempted, but without success. The difficulty has been to add the reducing agent direct to the oxide coating. The oxides, as such, are extremely unstable, and addition to the carbonates of a reducing agent merely results in the carbonates being decomposed more rapidly than usual. If the oxides can be obtained as such in a suitable solvent, the theory could be checked directly.

In conclusion, the author desires to tender his acknowledgements to the General Electric Company and the Marconiphone Company, on whose behalf the work was done which has led to this publication.

References.

(1) F. Deininger, *Ann. d. Physik*, viii. p. 230 (1908).
(2) C. J. Smithells, Brit. Pat. No. 26925/24 (1925).
(3) E. W. Lowry, Phys. Rev. xxxiv. p. 1367 (1930).
(4) C. E. Ransley and C. J. Smithells, Journ. Inst. Metals, xlix. p. 287 (1932).
(5) M. Benjamin and H. P. Rooksby, Phil. Mag. xv. p. 810 (1933).
(6) A. L. Reimann and R. Murgoci, Phil. Mag. ix. p. 440 (1930).
(7) J. A. Becker and H. Sears, Phys. Rev. xxxviii. pt. 2, p. 219 (1931).
(8) A. H. Wilson, Proc. Roy. Soc. A, cxxxiii. p. 458 (1931).
(9) A. H. Wilson, Proc. Roy. Soc. A, cxxxiv. p. 277 (1932).
(10) A. H. Wilson, Proc. Roy. Soc. A, cxxxvi. p. 487 (1932).
(11) A. H. Wilson and R. H. Fowler, Proc. Roy. Soc. A, cxxxvii. p. 503 (1932).
(12) A. L. Reimann, 'Thermionic Emission,' p. 229 (Chapman & Hall, Ltd., June 1934).
(13) A. L. Reimann and L. R. G. Treloar, Phil. Mag. xii. p. 1073 (1931).

II. *The Isotopes of the Radioactive Elements and their Disintegration.* *By* H. J. WALKE, *M.Sc., A.Inst.P., Demonstrator in Physics, Washington Singer Laboratories, University College, Exeter* *.

1. *Introduction.*

THE discovery by Fermi that β-radioactivity is a general nuclear property associated with certain isotopes of most elements suggests that a distinction can probably be drawn between the β- and α-radioactivity of the spontaneously radioactive elements. In the light of Fermi's discovery Aston's results possess a new significance, since the missing isotopes near the upper limit of the mass-range of any element may be regarded as β-radioactive synthesis links whereby each element evolved from the one preceding it in the periodic table, the general synthesis process for all the elements being neutron capture †. This is very well illustrated by the relationships existing between the isotopes of zirconium and niobium. The isotopes Zr_{40}^{93}, Zr_{40}^{95}, and Zr_{40}^{97} are missing, and, as niobium has a stable isotope Nb_{41}^{93}, it appears probable that during the cosmic synthesis of the elements Nb_{41}^{93} was evolved as a result of the β-radioactivity of Zr_{40}^{93}, viz. :—

$$Zr_{40}^{93} \rightarrow \beta \rightarrow Nb_{41}^{93}.$$

As, however, Aston has not detected any other niobium isotopes, Zr_{40}^{95} and Zr_{40}^{97}, formed when the stable isotopes Zr_{40}^{94} and Zr_{40}^{96} capture neutrons, give rise to molybdenum isotopes, thus :—

$$Zr_{40}^{95} \rightarrow \beta \rightarrow Nb_{41}^{95} \rightarrow \beta \rightarrow Mo_{42}^{95},$$

$$Zr_{40}^{97} \rightarrow \beta \rightarrow Nb_{41}^{97} \rightarrow \beta \rightarrow Mo_{42}^{97}.$$

In addition Nb_{41}^{94}, produced by the addition of a neutron to Nb_{41}^{93}, is β-radioactive, and as Nb_{41}^{95} and Nb_{41}^{97} are definitely missing, we conclude that all isotopes of niobium

* Communicated by Prof. F. H. Newman, D.Sc.

† Walke, Phil. Mag. xviii. p. 795 (1934); xix. p. 33 (1935); xix. p. 341 (1935).

with mass numbers higher than 93 are β-radioactive. As, however, Nb_{41}^{95}, though missing, corresponds to such stable isotopes as Cu_{29}^{65} and Ga_{31}^{71}, it appears likely that the period of this isotope would be relatively long * compared with the short life of the synthesis link Nb_{41}^{94}. Similarly as Zr_{40}^{96} is the heaviest stable zirconium isotope, and as Zr_{40}^{93}, Zr_{40}^{95}, and Zr_{40}^{97} are all β-radioactive, it is apparent that all zirconium isotopes with mass numbers greater than 96, *i. e.*, Zr_{40}^{97}, Zr_{40}^{98}, would give rise to two succeeding β-ray changes. Among the stable elements there are many isotopic configurations observed by Aston which suggest relations such as those discussed above. It must be concluded, therefore, that the production of several β-radioactive isotopes of a single element is a general possibility, as is the production of several isotopes of an element of even atomic number which give rise to two successive β-ray transformations. It is also noteworthy that the missing isotopes of an element of odd atomic number only give rise to single β-ray transformations, and that it appears probable that the expected heavier isotope of such elements which is often missing is a comparatively long-lived β-radioactive isotope.

It is thus apparent, in view of the observation of similar effects among the radioactive elements, *e. g.*,

$$UI_{92}^{238} \rightarrow \alpha \rightarrow UX_1\,{}_{90}^{234}\ ;\ UX_1\,{}_{90}^{234} \rightarrow \beta \rightarrow UX_2\,{}_{91}^{234} \rightarrow \beta \rightarrow UII_{92}^{234}$$

and

$$Th_{90}^{232} \rightarrow \alpha \rightarrow MsThI_{88}^{228}\ ;$$

$$MsThI_{88}^{228} \rightarrow \beta \rightarrow MsThII_{89}^{228} \rightarrow \beta \rightarrow RaTh_{90}^{228},$$

that the "characteristic instability" of the radioactive elements is α-ray instability, as most of the β-radioactive isotopes would similarly be β-radioactive even if the heavy elements were stable, since they would be "missing isotopes." It is therefore postulated that the radioactive elements differ from the stable elements only with respect to α-ray instability.

Making use of this hypothesis it is possible to indicate quite clearly those isotopes which would be detectable by means of a mass spectrograph if the radioactive elements were stable. It will be shown that the hypothesis will

* Walke, Phil. Mag. xix. p. 33 (1935).

account for all the effects *which have been observed experimentally.*

2. *Isotopes of Thorium, Protactinium, and Uranium.*

It is, however, first of all necessary to consider the isotopes of thorium, protactinium, and uranium. In a previous paper * an attempt was made to indicate how the radioactive elements were synthesized. Use was made of the synthesis process proposed for the stable elements, namely, neutron capture with β-radioactivity of missing isotopes. In this paper it was suggested that if the radioactive elements were considered as stable, the following isotopes would have existed with atomic numbers 92, 91, and 90:

Uranium	$z=92$	233, 234, 235, 236, 237, 238 (?),
Protactinium	$z=91$	233, 235,
Thorium	$z=90$	226, 227, 228, 229, 231, 232, 234,

synthesis from thorium to protactinium occurring as a result of the β-radioactivity of the missing Th_{90}^{233} and Th_{90}^{235}. Synthesis to uranium was thus due to β-ray emission from the missing Pa_{91}^{234} (UX_2).

In considering the experimental results referring to the disintegrations it now appears more probable that Th_{90}^{232} is the heaviest thorium isotope.

The following points are significant. $UY=Th_{90}^{231}$ is a very short-lived β-radioactive isotope, and as this is the characteristic of the "synthesis links," *e. g.*, N_7^{16} and Al_{13}^{28}, it appears more probable that the lighter protactinium isotope is Pa_{91}^{231}, due to the β-radioactivity of the "missing" Th_{90}^{231}. Thus, assuming that Th_{90}^{232} is the heaviest stable thorium isotope, the second isotope of protactinium, Pa_{91}^{233}, will arise as a result of the "missing" Th_{90}^{233}, and comparing with the results suggested by the stable elements, all heavier isotopes of thorium, viz., Th_{90}^{234}, Th_{90}^{235}, etc., should be short-lived β-radioactive substances. This hypothesis receives strong support from the fact that Th_{90}^{234} (UX_1) is β-radioactive with a half-period of 24·5 days. Hence it appears likely that the two most probable isotopes of protactinium are Pa_{91}^{231} and

* Walke, *loc. cit.*

Pa_{91}^{233}, and of these it is probable that Pa_{91}^{233} is a comparatively long-lived β-radioactive isotope (*cf.* I_{53}^{129}, Nb_{41}^{95}, Ac_{89}^{227}, etc.). Thus Pa_{91}^{231} is the more stable isotope of this element, and if the radioactive elements were "stable" it is mass number 231 which would be observed for element 91. It is significant that Pa_{91}^{231} is α-radioactive with a half-period of $1{\cdot}25 \times 10^4$ years.

Synthesis to uranium would then be due to the β-radioactivity of the short-lived Pa_{91}^{232} and Pa_{91}^{234} (UX_2) (which would be the "missing" isotopes of protactinium), so that the mass range of uranium would start at U_{92}^{232}. This isotope was most certainly a short-lived α-radioactive isotope which has disappeared.

In the light of this evidence it is therefore suggested that if the radioactive elements thorium, protactinium, and uranium were stable their isotopes would be :

Uranium	$z=92$	232, 233, 234, 235, 236, 237, 238 (?).
Protactinium	$z=91$	231.
Thorium	$z=90$	226, 227, 228, 229, 230, 232.

3. *The "Stable" (α-radioactive) Isotopes of the Elements $z=84$–92 and the Missing Series.*

As was shown previously * actinium probably consists of the two isotopes Ac_{89}^{225} and Ac_{89}^{227}. It is to be noted, however, that Ac_{89}^{227} is the heavier isotope of the two, and, moreover, that it is a long-lived β-radioactive isotope. It is thus apparent that if the radioactive elements were stable Ac_{89}^{227} would be missing (just as Nb_{41}^{95} is missing), and it must therefore be concluded that the synthesis of the elements heavier than bismuth is most completely understood if the following isotopes are considered as "stable" :—

Polonium.....	$z=84$	210, 211, 212, 213, 214, 215, 216, 218.
Eka-Iodine	$z=85$	217.
Emanation	$z=86$	218, 219, 220, 222.
Eka-Cæsium ...	$z=87$	221.
Radium	$z=88$	222, 223, 224, 226.
Actinium	$z=89$	225.
Thorium	$z=90$	226, 227, 228, 229, 230, 232.
Protactinium...	$z=91$	231.
Uranium.....	$z=92$	232, 232, 234, 235, 236, 237, 238 (?).

* Walke, *loc. cit.*

If the radioactive elements were "stable" these are the mass numbers which would be recorded on the mass spectrograph. The suggestion that Ac_{89}^{227} and Pa_{91}^{233}, the long-lived β-radioactive isotopes (*cf.* Nb_{41}^{95} etc.), would be missing, so that actinium and protactinium would be single elements with atomic weights about 225 and 231 respectively, is in accordance with the single isotopic configurations of scandium, yttrium, and lanthanum, which are homologues of actinium, and of vanadium, niobium, and tantalum, which are homologues of protactinium.

Hence if the hypothesis that the "stable" isotopes of the radioactive elements are α-radioactive, all the mass numbers in the above list should be α-radioactive.

This suggests that the missing radioactive series, probably headed by U_{92}^{237}, should disintegrate as below, and not as previously proposed *:

$$U_{92}^{237} \rightarrow \alpha \rightarrow Th_{90}^{233} \rightarrow \beta \rightarrow Pa_{91}^{233} \rightarrow \beta \rightarrow U_{92}^{233} \rightarrow \alpha \rightarrow Th_{90}^{229} \rightarrow \alpha$$
$$\rightarrow Ra_{88}^{225} \rightarrow \beta \rightarrow Ac_{89}^{225} \rightarrow \alpha \rightarrow EkaCs_{87}^{221} \rightarrow \alpha \rightarrow EkaI_{85}^{217} \rightarrow \alpha$$
$$\rightarrow Bi_{83}^{213} \rightarrow \beta \rightarrow Po_{84}^{213} \rightarrow \alpha \rightarrow Pb_{82}^{209} \rightarrow \beta \rightarrow Bi_{83}^{209},$$

the β-ray emission occurring at Ra_{88}^{225} rather than as previously suggested, since Ra_{88}^{225} is the "missing" synthesis link from radium to actinium (see list above). With this slight alteration it will be seen that all the isotopes in the above list are α-radioactive, the "missing" isotopes being the β-ray emitters.

It can therefore be concluded that this isotopic scheme will account very satisfactorily for the three known series and the two missing series headed by U_{92}^{237} and Th_{90}^{226} †. Thus at the beginning of the uranium and thorium series disintegration occurs as below:

$$U\,I_{92}^{238} \rightarrow \alpha \rightarrow UX_{90}^{234} \rightarrow \beta \rightarrow UX_{2\,91}^{234} \rightarrow \beta \rightarrow U\,II_{92}^{234},$$
$$Th_{90}^{232} \rightarrow \alpha \rightarrow MsTh\,I_{88}^{228} \rightarrow \beta \rightarrow MsTh\,II_{89}^{228} \rightarrow \beta \rightarrow RaTh_{90}^{228},$$

because the initial α-ray emission from U_{92}^{238} and Th_{90}^{232} produces the "missing" short-lived β-radioactive isotopes $UX_{1\,90}^{234}$ (Th_{90}^{234}) and $MsTh\,I_{88}^{228}$ (Ra_{88}^{228}) respectively. α-ray emission then occurs, the series of α-ray transformations

* Walke, *loc. cit.*
† Walke, *loc. cit.*

ending at RaB and ThB. It is noteworthy that all the isotopes produced in the α-ray series are "stable." The disintegration of the B products will receive attention later.

In the case of the actinium series headed by AcU_{92}^{235} (or more probably by PaU_{92}^{239} *), the α-ray emission from U_{92}^{235} produces the "missing" Th_{90}^{231} (UY) which is rapidly transformed to the "stable" Pa_{91}^{231}. The latter emits an α-particle and produces the heavier actinium isotope Ac_{89}^{227}, which is a long-lived β-radioactive isotope. The "stable" Th_{90}^{227} (RaAc) then emits an α-particle and gives rise to the rest of the series, α-ray emission occurring from the "stable" isotopes.

It must be concluded, therefore, that the proposed table of isotopes will account in a very satisfactory fashion for the three main series, and relates very definitely the radioactive and stable elements. It is apparent moreover that, except for the α-radioactivity, the elements from $z=82$ to $z=92$ obey the same rules as are suggested for the stable elements by Aston's table of isotopes when this is considered in the light of Fermi's discovery.

4. *The Disintegration of the* B, C, C′, *and* C″ *Bodies.*

In order to show the applicability of the hypothesis put forward let us consider the end portions of the three known series in relation to the isotopes Aston has detected for thallium, lead, and bismuth. The mass numbers which have been observed are:

Thallium.....	$z=81$	203, 205.
Lead	$z=82$	203, 204, 205, 206, 207, 208, 209 (?), 210 (?).
Bismuth	$z=83$	209.

According to the rules suggested in section 1 we should therefore expect all isotopes of thallium with mass numbers higher than 205 to be short-lived and β-radioactive. In addition any lead isotopes of mass greater than 210 should similarly be short-lived β-ray emitters and, further, bismuth isotopes with higher mass numbers than 209 should be β-radioactive, Bi_{83}^{211} being

* Walke, Phil. Mag. xviii. p. 259 (1934).

probably of comparatively long life. It is significant that RaC″, ThC″, and AcC″ (*i. e.*, Tl_{81}^{210}, Tl_{81}^{208}, and Tl_{81}^{207}), and RaB, ThB, and AcB (*i. e.*, Pb_{82}^{214}, Pb_{82}^{212}, and Pb_{82}^{211}), are short-lived β-radioactive isotopes. In addition, RaC and ThC (*i. e.*, Bi_{83}^{214} and Bi_{83}^{212}) disintegrate mainly by emitting β-radiation and RaE (Bi_{83}^{210}) is β-radioactive with a half-period of 5·0 days.

The three isotopes RaC, ThC, and AcC (Bi_{83}^{214}, Bi_{83}^{212}, and Bi_{83}^{211}) are very interesting, as they illustrate clearly the essential difference between the elements heavier than lead and those of lower atomic number. In the first place, if bismuth was a stable element, Bi_{83}^{210}, Bi_{83}^{212}, and Bi_{83}^{214} would be short-lived β-radioactive isotopes, Bi_{83}^{211}, missing from the mass spectrum, being comparatively long-lived. It must be remembered, however, that the elements heavier than lead are α-unstable. Moreover Gamow * has shown that the very short decay periods of RaC′, ThC_4', and AcC′ (which are all α-radioactive) can be accounted for by their positions on his α-particle stability curve. It thus seems plausible to assume that the isotopes of element 83 of corresponding mass numbers are also favourably placed for α-particle emission. In consequence in these nuclei we have two opposing tendencies, the "normal" tendency to β-ray emission and the additional tendency to α-ray emission, The branching of the C bodies is thus accounted for in a satisfactory manner.

Moreover it is to be expected that the missing or β-radioactive isotopes of an element will have shorter and shorter half-periods as the number of nuclear neutrons increases. This is indicated by the β-radioactive isotopes of thallium, viz.:

RaC″ (Tl_{81}^{210})	$40\alpha+p+49n$	1·32 min.,
ThC″ (Tl_{81}^{208})	$40\alpha+p+47n$	3·20 min.,
AcC″ (Tl_{81}^{207})	$40\alpha+p+46n$	4·76 min.,

so that if there were no tendency to α-particle emission from RaC, ThC, and AcC (Bi_{83}^{214}, Bi_{83}^{212}, and Bi_{83}^{211}), we should expect RaC to have a shorter life than ThC (the

* Gamow, International Conference on Physics (1934).

half-periods of these isotopes being small), whereas AcC, corresponding to a possible stable isotope of bismuth, would be comparatively long-lived. Hence, if the probability of α-ray emission from the three isotopes is relatively high, and is of the same order for all three isotopes, then, on account of their differences with respect to β-ray decay, we should expect to find when these atoms have decayed that a higher percentage of the RaC atoms compared with those of ThC will have emitted β-radiation. Moreover, on account of the long life of AcC with respect to β-ray emission, we should expect most of the AcC atoms to have emitted α-rays. This is exactly the state of affairs which is observed in practice, viz. :

RaC$\rightarrow\beta\rightarrow$RaC′ (99·97 p. c.) ;	RaC$\rightarrow\alpha\rightarrow$RaC″ (0·03 p. c.).
ThC$\rightarrow\beta\rightarrow$ThC′ (65 p. c.) ;	ThC$\rightarrow\alpha\rightarrow$ThC″ (35 p. c.).
AcC$\rightarrow\beta\rightarrow$AcC′ (0·3 p. c.) ;	AcC$\rightarrow\alpha\rightarrow$AcC″ (99·7 p. c.).

We conclude therefore that the hypothesis " missing isotopes are β-radioactive " is strongly supported by the observed disintegration of the spontaneously radioactive elements. In addition, the suggestion that the α-radioactive isotopes correspond to the stable isotopes of the normal elements clarifies the problem of the unstable elements and shows clearly the relationship existing between the elements of atomic number higher than 82 and those which are " stable."

III. *The Refractive Index of the Alkaline Chlorides at Low Concentrations. By* H. J. Walke, *M.Sc., A.Inst.P., Demonstrator in Physics, Washington Singer Laboratories, University College, Exeter* *.

I. *Introduction.*

THE refractive index of an electrolytic solution is not proportional to the concentration. This is in part due to the fact that when a salt is dissolved the contraction or expansion during solution per unit

* Communicated by Prof. F. H. Newman, D.Sc.

quantity of salt varies with the concentration of the solution.

In dilute solutions, however, where the degree of dissociation, is large, the increments of refractive index with changing concentration, if referred to molecular quantities of salt, show distinctly additive properties. The additive principal which is applicable to many properties of solutions depends upon the hypothesis of the practical independence of the constituents within the solution. Thus the additive effect mentioned above is to be expected if it is an ionic rather than molecular property.

The Lorentz expression is based on certain assumptions, and was derived strictly for a system consisting only of particles of the same kind, so that in any complicated system molecular refraction would not be expected to show strict additivity. Applied to ions in solution there must be some mutual action between any ion and the surrounding medium. There is, for example, the polarization of the ions in the electric field of the light waves and the deforming action of the ions in the absence of light. It is certain that the electrostatic interaction of the ions on one another, as well as on the surrounding dipole molecules of water, is accompanied by polarization phenomena. The cations exert attractive forces on the electron shells of the anions or on the water-molecules surrounding them, and deform them to some extent. In this way the ionic refraction is changed.

In addition, there is always a more or less uncertain correction for the effect of hydration.

The additive relationship should be most satisfactory at infinite dilution, but the difficulty of obtaining sufficiently accurate measurements makes the verification, as a rule, less satisfactory with very dilute solutions.

The present paper contains an account of an experimental investigation of the variation of refractive index of solutions of the chlorides of sodium, potassium, and lithium with concentrations within the range 0·002–0·0001 equivalent per 1000 gm. of water.

II. *Experimental Technique.*

The refractive indices were measured by means of a standard Hilger-Rayleigh Refractometer, using white

light to obtain the fringes. In view, however, of the low concentrations used, the relative retardation between the two beams of light caused by the difference in refractive index between the solutions and distilled water was very small, and in consequence very small fringe-shifts had to be measured. Certain special precautions were, therefore, taken in order to reduce all errors to the minimum.

In the first place it was found that the optically worked glass cell, although of constant thickness to within one wave-length of sodium light, showed sufficient inhomogeneity to cause appreciable errors if the cell was moved on the refractometer table, and inconsistent readings were obtained if the cell was shifted from the refractometer and replaced after filling with a fresh sample of the solution under test. Accordingly the cell was waxed firmly in position, and each section was filled with the cell fixed on the refractometer.

Separate pipettes were used for filling the two halves of the cell, one being kept for use with distilled water and the other for solutions. The latter was always carefully cleaned and washed out thoroughly many times with the particular sample being tested. Great care was also exercised in ensuring that no inaccuracies were introduced on account of small residues of samples of different concentration from the one under test being left in the part of the cell used to contain the solutions.

Both halves of the cell were, therefore, emptied at the end of each complete set of readings, when one half of the cell contained distilled water and the other the sample tested. The cell was then carefully washed out with distilled water, the part used to contain the solutions being thoroughly cleaned out at least twenty to thirty times. All traces of the solution having been removed in this manner, the distilled water was then emptied, and after further washing both were filled with distilled water from a special container which was filled at the beginning of each set of experiments, and which held sufficient for the one sample from the still to be used as a standard throughout. In consequence all the solutions were compared with distilled water of constant refractive index.

When the temperatures of both sides of the cell were constant, and equal, a set of drum-readings corresponding

to coincidences of both sets of fringes was taken, consisting of four sets of ten, and the mean value of the forty readings was used as the zero for this series of observations. On completing these measurements the distilled water was removed from the solution side of the cell, and the latter was washed out with some of the sample to be tested. This procedure was repeated many times, the half of the cell being completely emptied each time great care being taken to ensure that no drop of solution entered the other half of the cell, which was still filled with distilled water. After the concentration of the solution in the cell had been made equal to that of the sample under test, conditions were once more allowed to settle. (In general half an hour was allowed between filling the cell and taking the first reading.) The temperatures being constant, a series of readings of the coincidences of the two sets of fringes was taken for this sample. The mean of the forty readings was used as the reading corresponding to this sample. By subtracting from this the value used as zero, the relative retardation produced by filling one half of the cell with the sample under test instead of distilled water was found, and from this the value of $d\mu$, the difference between the refractive index of the solution and that of distilled water, was obtained. Thus for each sample used eighty readings were taken, as shown in Table I.

At least four samples were used at each concentration, so that each point on the curves obtained represents a minimum of three hundred and twenty separate observations.

The drum of the refractometer was standardized by means of the D-lines of sodium, readings of consecutive coincidences of the two sets of fringes being plotted against the number of the coincidence. The curve was accurately linear, and over the small range used eighteen drum-divisions are equivalent to a relative retardation of one wave-length of sodium light. In setting the drum to observe coincidence of the two sets of fringes it was ensured that the drum was always rotated in the same direction.

The refractometer and source of light were adjusted at the beginning of the experiments, and were fixed on a table, free from vibrations, set up on concrete pillars sunk to the foundations of the Laboratories, so that with the cell fixed in position the paths of the two interfering

beams remained constant, except for changes in the refractive index of the solution.

TABLE I.

Typical Set of Observations.

Distilled water.				·001 N NaCl.—Sample IV.			
60·0	60·1	60·0	60·0	63·3	63·6	63·5	63·5
59·9	59·9	59·9	60·0	63·5	63·7	63·7	63·5
59·9	60·0	60·0	60·0	63·3	63·6	63·4	63·3
59·9	60·0	60·0	59·9	63·5	63·5	63·6	63·5
60·0	60·1	59·9	60·0	63·5	63·6	63·5	63·6
60·0	59·9	59·9	59·9	63·5	63·5	63·3	63·7
60·0	60·0	60·0	59·9	63·4	63·4	63·3	63·5
60·0	59·9	60·0	59·9	63·3	63·5	63·5	63·6
60·0	60·0	59·9	60·1	63·6	63·5	63·6	63·5
60·0	59·9	60·0	60·0	62·5	63·6	63·5	63·3
59·97	59·98	59·96	59·97	63·44	63·55	63·46	63·50
Mean ..... 59·97				Mean ..... 63·49.			

Difference.... 3·52 drum-readings.

III. *Sources of Error.*

The main source of error in the measurements made, as in all experiments involving visual estimates of very small effects, lies in the personal equation of the observer. At the lower concentrations the fringe-shift is so small that great difficulty is experienced in making accurate measurements. The accuracy of the experiment depends entirely on these measurements, and these in turn depend very much on the physical state of the observer. In particular after a fairly long period of observation fatigue effects were found to play an important part, and fluctuating readings were obtained. It was, therefore, usual to finish the experiments when, after a period of constant observations, fluctuating readings were obtained.

It was also found that at the commencement of a period of observation a little time was required to attain the rhythm of best accuracy (corresponding to the minimum fluctuation in a given set of readings), so that

it was usual to discard observations until a sufficient number of preliminary readings had been taken to ensure that this condition was attained. In addition, when from some accidental cause a fluctuating set of observations was obtained in a series of otherwise consistent readings it was usual to reject this set and to take fresh readings later.

In spite of possible personal errors, however, it is apparent from the consistency of the readings obtained that the change in shape of the curve is a real effect, and, further, the fact that the shape at concentrations higher than ·0005 N is definitely parabolic, is in itself evidence against any *direct* influence of a personal equation on the form of the curve obtained.

IV. *Preparation of the Solutions.*

In making up the solutions distilled water from one still was prepared in large quantities, and all solutions were made up from the one sample. With all the salts experimented on accurate normal solution was prepared, chemically pure salt being used. It was ensured that the salt was free from moisture by prolonged heating prior to the weighing out of the salt and the making up of the solution.

From the accurate normal solution was prepared a solution of concentration ·01 N, which was used as a standard. All the other solutions were made from this standard solution, though ·001 N prepared from this standard was employed for making all the solutions of lower concentration. All measuring flasks and pipettes used were certified by the National Physical Laboratory, and great care was taken in preparing each solution to ensure that the more concentrated solution from which it was diluted was thoroughly mixed. The preparation of more dilute solutions was deferred until this solution too, was homogeneous. This was ensured by periodically shaking the solutions and allowing them to stand for an interval. This procedure was carried out for two, sometimes three, days, so that the actual preparation of the solutions took several weeks. Hence any error in concentration is due to error in the normal solution first prepared. It is probable that the relative concentrations are accurate to a high degree.

V. *Experimental Results.*

The refractive indices of the solutions were calculated from the observed mean difference dr between the drum-reading corresponding to coincidence of the two sets of fringes with distilled water in one half of the cell and the solution in the other, and that corresponding to coincidence of the two sets of fringes with distilled water in both halves of the cell by means of the formula

$$d\mu = \frac{dr}{t \times 18} \times 5893 \times 10^{-8},$$

where t = the thickness of the cell in cm. and 18 = the average difference between the drum-readings for consecutive coincidence of the fringes, using sodium light to illuminate the slit of the refractometer. In the actual instrument used $t = 1$ cm. and $\mu H_2O = 1{\cdot}3322112$ at 17° C.

The results obtained are shown in Tables II., III., and IV. and figs. 1, 2, and 3.

The significant feature of the curves showing the relationship between refractive index and concentration of the solution is the change in slope and shape which occurs with each salt at concentrations greater than 0·0005 N. Below this concentration all the curves are linear, and the values of μ for the separate solutions are so nearly equal that the linear portion is almost identical for each substance. At higher concentrations, however, there is a change in the form of the curve, this change being similar for all the salts used, and showing that the refractive indices are less than would be expected if the linear relation found at very low concentrations held over the whole range.

To determine the nature of this change of form of the curve fresh graphs were drawn showing the variation of refractive index with the square root of the concentration. It was found that the curves so obtained were again similar for each substance. These curves are shown in figs. 4, 5, and 6.

In these curves the parts corresponding to the non-linear parts of the first set of curves were found to be linear, showing that the equations of these sections of the curves are of the form

$$\mu = A + B\sqrt{c},$$

TABLE II.

Refractive Indices of NaCl Solutions 0·002 N–0·0001 N.

Concentration of solution.	Difference between zero (H_2O reading) and actual drum-reading for solution.	Relative retardation in λ 5893 Å.	$D\mu$.	Refractive index of solution at 17° C.
0·002 N	6·07	0·337	0·0000199	1·3322311
0·00134 N	4·53	0·252	0·0000149	1·3322261
0·001 N	3·51	0·195	0·0000105	1·3322217
0·00067 N	2·51	0·139	0·0000082	1·3322194
6·0005 N	2·01	0·112	0·0000065	1·3322177
0·0004 N	1·54	0·086	0·0000051	1·3322163
0·00025 N	1·00	0·051	0·0000031	1·3322143
0·000125 N	0·50	0·026	0·0000015	1·3322127
0·0001 N	0·42	0·023	0·0000014	1·3322126

Fig. 1.

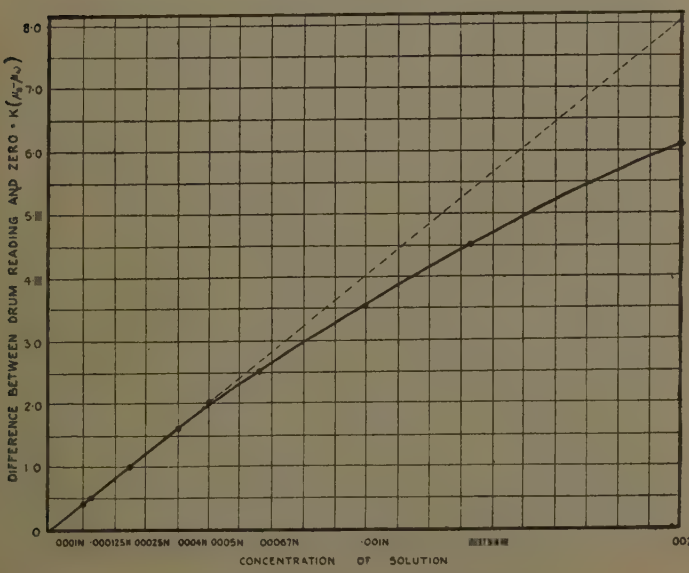

Curve showing relation between refractive index and concentration for sodium chloride.

TABLE III.

Refractive Indices of KCl Solutions 0·002 N–0·0001 N.

Concentration of solution.	Difference between zero (H_2O reading) and actual drum-reading for solution.	Relative retardation in λ 5893Å.	$D\mu$.	Refractive index of solution at 17° C.
0·002 N	6·83	0·379	0·0000223	1·3322345
0·00134 N	4·81	0·267	0·0000157	1·3322269
0·001 N	3·63	0·202	0·0000119	1·3322231
0·00067 N	2·52	0·140	0·0000083	1·3322195
0·0005 N	1·96	0·109	0·0000064	1·3322176
0·0004 N	1·61	0·089	0·0000052	1·3322164
0·00025 N	1·04	0·058	0·0000034	1·3322146
0·000125 N	0·51	0·028	0·0000016	1·3322128
0·0001 N	0·43	0·024	0·0000014	1·3322126

Fig. 2.

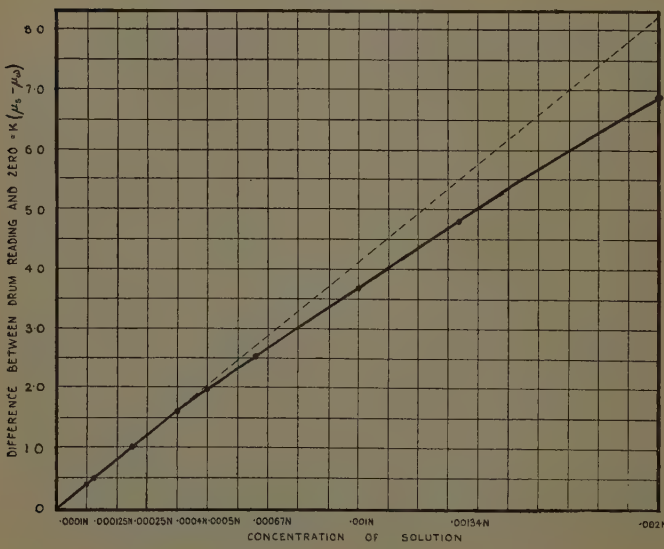

Curve showing relation between refractive index and concentration for potassium chloride.

TABLE IV.

Refractive Indices of LiCl Solutions 0·002 N–0·0001 N.

Concentration of solution.	Difference between zero (H_2O reading) and actual drum-reading for solution.	Relative retardation in λ 5893 Å.	$D\mu$.	Refractive index of solution at 17° C.
0·002 N	5·90	0·328	0·0000193	1·3322305
0·00134 N	4·27	0·237	0·0000139	1·3322251
0·001 N	3·43	0·191	0·0000113	1·3322225
0·00067 N	2·53	0·141	0·0000083	1·3322195
0·0005 N	1·94	0·108	0·0000064	1·3322176
0·0004 N	1·58	0·088	0·0000052	1·3322164
0·00025 N	0·99	0·056	0·0000033	1·3322145
0·000125 N	0·49	0·027	0·0000016	1·3322128

Fig. 3.

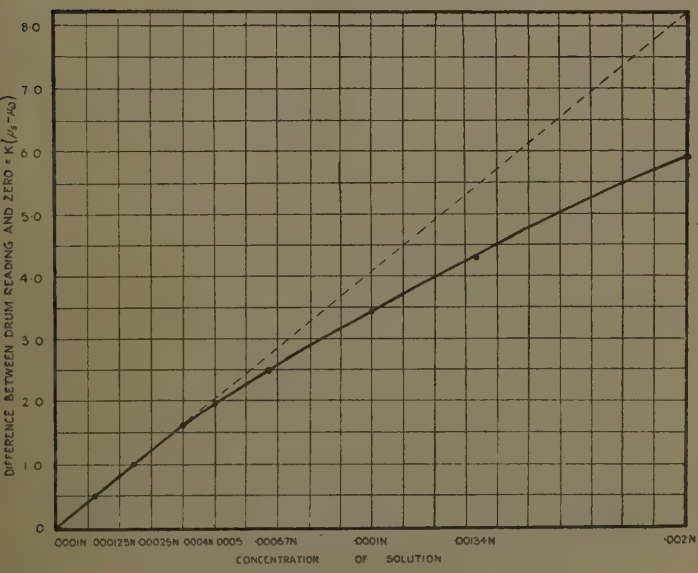

Curve showing relation between refractive index and concentration for lithium chloride.

Fig. 4.

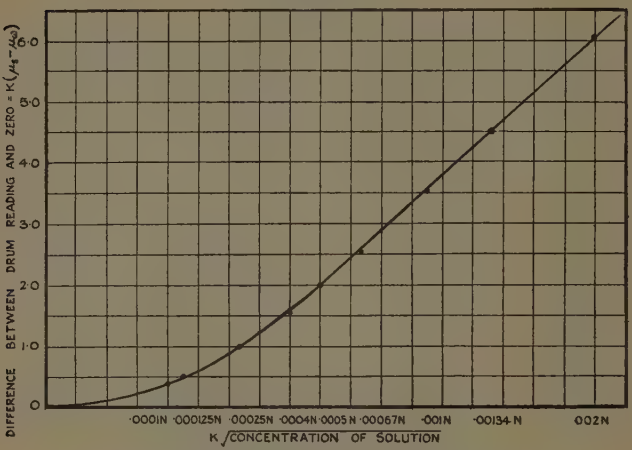

Curve showing relation between refractive index and concentration for sodium chloride.

Fig. 5.

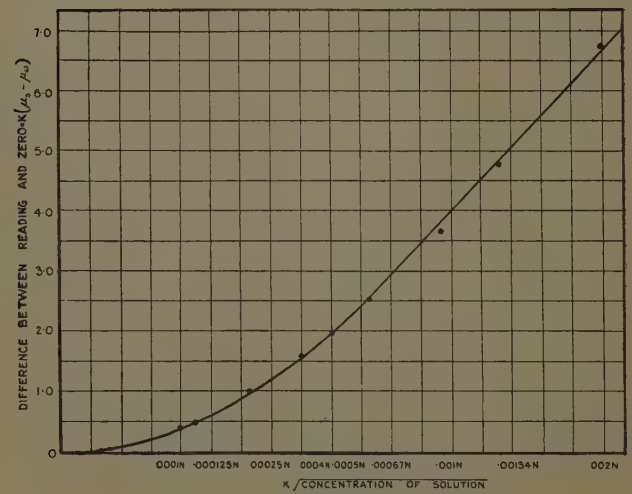

Curve showing relation between refractive index and concentration for potassium chloride.

Fig. 6.

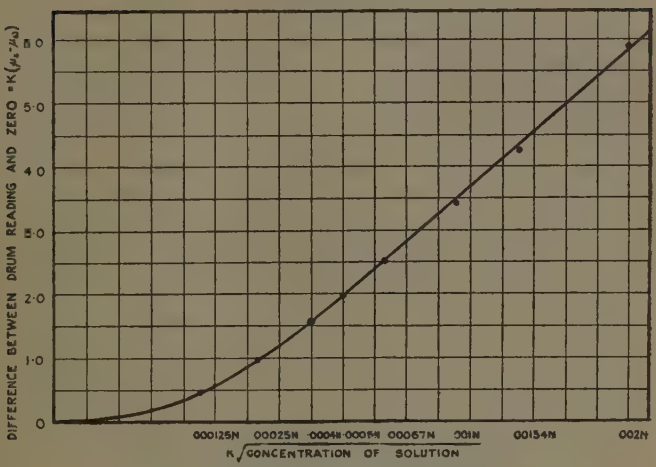

Curve showing relation between refractive index and concentration for lithium chloride.

where A can be written in the form

$$A=(\mu_0-K),$$

μ_0 being the refractive index of distilled water and c the concentration of the solution in gm. molecules per 1000 c.c.

The values of A and B for the three salts used are given in Table IV.

TABLE IV.

Values of A and B for Salts used.

Salt.	Value of A.	Value of B.
Sodium chloride	1·3321927	·000884
Potassium chloride	1·3321990	·000763
Lithium chloride.....	1·3322060	·000522

It is significant that similar relations have been found to represent the variation of viscosity and electrical conductivity of strong electrolytes with concentration. It must, therefore, be concluded that some relationship exists between these three properties of solutions of strong electrolytes.

The change in form of the curves below 0·0005 N may indicate that below this concentration the salt-molecules are completely ionized, and that at higher concentrations there exist in the solution some undissociated molecules as well as completely dissociated ions.

This seems evident when we consider the fact that below 0·0005 N the curve is linear, indicating that over this range the additive principle applies. As this principle depends on the hypothesis of the practical independence of the constituents within the solution, this linear section must be regarded as evidence in favour of the complete dissociation of the salt-molecules into constituent ions below 0·0005 N concentration.

At higher concentrations, however, this principle is clearly not applicable, so that it must be concluded that undissociated molecules exist in the solution as well as the dissociated ions. Thus the two sections of the curve suggest that for a certain range of concentrations there exist positive and negative ions within the solution, whereas for higher concentrations there exist undissociated molecules as well as positive and negative ions.

In conclusion I should like to express my gratitude to Prof. F. H. Newman for suggesting this problem to me, and for his unfailing interest and encouragement during the time that the experiments were performed.

I wish also to express my thanks to Colonel Ransom Pickard, C.B., C.M.G., F.R.G.S., for the gift of the Hilger-Rayleigh Refractometer, with which this research was carried out, and to the College for a Research Scholarship, without which the carrying out of the experiments would have been impossible.

IV. *Remarks on the Experimental Determination and Theoretical Calculation of Flame Temperatures and Explosion Pressures* [1]. *By* Bernard Lewis [2] *and* Guenther von Elbe [3] *.

Flame Temperatures.

RECENTLY David, Davies, and Jordan [4] have submitted measurements of the temperature of a fine platinum-rhodium wire heated by a moving flame by utilizing the change in its electric resistance.

* Communicated by the U.S. Bureau of Mines.

There is one fundamental difficulty with the measurement of flame temperature by this method, of which David and Jordan are aware. A solid body, such as a hot wire, is cooled much faster by radiating than a gas at the same temperature. If a wire is inserted in a flame it will become the source of considerable loss of heat on account of radiation, even though conduction to the outside leads is negligible, and a local temperature gradient will be set up rising from the surface of the wire to the gas. This difference in temperature between the main body of gas and the wire will become more marked the higher the temperature.

Hopkinson [5], who conducted similar experiments, estimated corrections for the radiation loss from the wire. He showed that differences of 100°–200° C. may be expected with a wire 0·001 inch in diameter at temperatures 1600°–1800° C.

Appreciating this fact other investigators compensated the radiation loss by heating the wire electrically [6]. In this method the temperature of the wire is determined as a function of the current, first, when it is placed within a flame, and second, in a vacuum. The point of intersection of the two curves marks the true flame temperature. The total energy dissipated is the same at this point, whether the wire is in the flame or in a vacuum. Since the only sources of energy loss in a vacuum are radiation and conduction along the leads, there can be no interchange of energy between the wire and the flame, that is, they are at the same temperature. In this way the methodical error in the wire method is eliminated.

The same was also accomplished without placing the wire in a vacuum by measuring directly the radiation from the wire as a function of its temperature determined by optical pyrometry.

The flame temperatures given by the electrically heated wire method were found to be in excellent agreement with the temperatures given by the line-reversal method [6], [7] in which the brightness temperature of alkali metal-coloured flames is measured. Thus the applicability of Kirchhoff's law to the alkali metal lines in flames was established.

Independent agreement with the line-reversal flame temperatures was found by the electric conductivity method [8] and the radiometric method [9]. In the

electric conductivity method the equilibrium between sodium atoms, sodium ions, and electrons in a sodium-coloured flame is measured experimentally, and the temperature corresponding to this equilibrium is found from the Saha equation. The radiometric method depends on the determination of the emissivity of a flame from total radiation measurements.

In the following discussion we shall deal with objections raised by David and Jordan to the line-reversal method and, simultaneously, with the methodical errors which, in our opinion, have entered into the values of experimental and theoretical flame temperatures published by David and coworkers. David and Jordan believe that the line-reversal method measures temperatures "higher than those corresponding to the mean molecular translational energy of the flame gases." The argument was based on the following :—(1) That lower temperatures are obtained with thallium-coloured flames than with alkali metal-coloured flames ; (2) that temperatures measured by Jones, Lewis, and Seaman [10] in weak methane-oxygenated air mixtures, by Jones Lewis, Friauf, and Perrott [11] in very rich hydrocarbon-air mixtures, and by Ellis and Morgan [12] in very rich CO-air mixtures, are higher than the theoretical flame temperatures calculated on the basis of normal heat capacities ; (3) that the temperatures measured by the wire method, as used by David and coworkers [4], are generally lower than those obtained by the line-reversal method.

No consideration was given by David and coworkers to the large amount of experimental material quoted above, by which the validity of the line-reversal method was proved. The question arises whether this material is to be considered disproved or whether the factual evidence cited by them may not lend itself to another interpretation.

The present authors take the view that the evidence in support of the line-reversal method is incontrovertible. Concerning the use of thallium, the low results reported by Jones, Lewis, Friauf, and Perrott are not in agreement with the results of Kohn [13]. The latter investigator found the same flame temperature with thallium salts as with alkali metal salts. We have traced the difference in the experimental results to the somewhat greater

difficulty of colouring the flame sufficiently with thallium in the experimental method used by Jones, Lewis, Friauf, and Perrott. These authors state "it was impossible to obtain a reversal and the point of extinction (of the green thallium line) was very indefinite." For this reason they discarded the use of thallium and performed all their experiments with sodium.

Concerning the high results in the weak methane-oxygenated air mixtures and very rich hydrocarbon or CO-air mixtures, evidence will be presented below which suggests that at least in the former mixtures the explanation is to be found in the so-called excitation lag effect. The effect has been verified [14] experimentally in CO_2, N_2O, O_2, N_2, CO, and Cl_2. Immediately after combustion the thermal energy liberated distributes itself at different rates among the degrees of freedom in the system. These rates are very fast for the translational and rotational, but not for the vibrational degrees of freedom of the above molecules. This means that the heat capacity of, say, the excess oxygen or nitrogen in the burned mixture becomes a function of time, increasing from that of an almost vibrationless diatomic molecule to normal vibrational excitation. Thus an air-fuel mixture may on combustion temporarily attain a temperature considerably in excess of its final normal temperature.

Concerning the temperature measurements by the wire method, we note that, although David and coworkers realized the existence of radiation loss from the wire, they believed it to be negligible for the purposes of their investigation and consequently they made no corrections. Thus for CO-air explosions their estimate of the radiation loss was $<40°$ with the wire at 1800° C. This is at variance with the careful estimates of Hopkinson [5], who found a difference of 200° for 0·001-inch platinum sire at 1800° C. This discrepancy cannot be accounted for by the fact that David and coworkers used 0·0005-inch wire, and indeed David, Davies, and Jordan find [15] only slightly higher temperatures with the 0·0005-inch wire than with the 0·001-inch wire in the same flame. A reconsideration of this correction seems to be advisable. A good method of approach would be to determine it experimentally by heating the wire electrically in the flame and in the vacuum as described above. It is given

by the difference between the temperature at the point of intersection of the two curves and the temperature of the wire in the flame for zero current. It appears most probable that with such precautions the results of previous investigators [6] will be confirmed, namely, that identical flame temperatures are obtained by line-reversal and wire methods.

David and coworkers compare their experimental temperatures with calculated ideal temperatures derived from theoretical heat capacities. However, in the light of the accurate data now available on heat capacities and dissociation equilibria [16], their calculated curves with dissociation allowed for must be revised. Actually they should be from 30 to 70° lower in the temperature range considered. Thus for both reasons, namely, failure to correct for radiation loss from the wire and the use of data which give unwarrantedly high calculated temperatures, the differences between the experimental and theoretical curves are exaggerated throughout their work [17]. We are, therefore, unable to accept the above comparisons between experimental and theoretical flame temperatures. We have prepared instead Table I., in which line-reversal flame-temperature measurements and accurate theoretical flame temperatures for a few selected mixtures are compared.

Before entering into a discussion of these data, however, we wish to clarify the status of an hypothesis proposed by David and coworkers to account for, (*a*) their large temperature differences mentioned above, (*b*) results of the line-reversal method as interpreted by them, (*c*) their luminosity experiments, and (*d*) their explosion pressures and temperatures in closed vessels. We refer to their hypothesis of "after-burning" or "latent energy" in the form of large amounts of long-lived abnormal molecules in the flame gases. From a strictly theoretical point of view we may perhaps conceive of such a phenomenon in the following way. Freshly formed products of reaction may temporarily carry large amounts of vibrational energy derived from the heat of reaction, and take time to reach equilibrium with the degrees of freedom of the system in analogy with the excitation lag effect. However, the life-time of such excited molecules would be short in contrast to the assumption of David and coworkers. Whether this idea

will prove to be fruitful for interpreting future experimental work remains to be seen. At present we are forced to confine ourselves to an appraisal of the evidence for this hypothesis put forward by these investigators.

As far as their evidence derived from differences between observed and calculated flame temperatures is concerned, Table I. shows to what extent these differences exist. They admit of no such interpretation. Their evidence derived from the interpretation of the line-reversal method was shown above to be invalid. The alleged evidence from pressure measurements in spherical vessels of different sizes [18] has been shown to be invalid [19]. Similarly, no support for this hypothesis can be derived from the measurements of wire temperatures and explosion pressures in a sphere and in a short cylindrical vessel reported by David and Davies [4].

Referring to spherical vessel explosions first: The present authors have shown [20] that in the mixtures under consideration, namely, H_2, O_2, and N_2, the agreement between the observed (by Pier and others, also David and Thorp, see below) and theoretical explosion pressures is very close, a fact which excludes all possibility of "afterburning" or "latent energy." This agreement was found for all the experimental material investigated, and applies also to the experimental material for an 18-inch vessel published by David, Brown, and El Din [18], a fact not mentioned in the quoted paper [20].

David and Davies placed thin wires near the centre and near the wall (1 inch from wall of 18-inch sphere). The time-temperature curve of the central wire corresponded simply to what is to be expected in the normal course of the explosion [21], [22], *i. e.*, at the moment of maximum pressure the temperature of the wire had risen above the temperature inferred from the pressure. However, the temperature of the wire near the wall at the same instant was between these. Analysis of the temperature along the radius [21], [22] at the moment of maximum pressure indicates that the temperature of the wire near the wall should be below that inferred from the pressure [23]. That such is the case was shown experimentally by Hopkinson [5], using the same wire method and coal gas-air mixtures. Since the explanation given by David and Davies, namely, unloading of "latent energy" from excited molecules on to the wire, is ruled

out by the above-mentioned evidence excluding the existence of "latent energy" in the burned gases, the explanation of the anomalous effects found by them must be sought elsewhere. The behaviour of the system after maximum pressure would seem to depend very much on the experimental arrangement, considering that convection currents are set up in the vessel both after maximum pressure and for slow-burning mixtures before maximum pressure.

Concerning their cylindrical vessel explosions, we suggest that the geometry of the vessel must influence the distribution of the isotherms in the burned gas. It would seem to be profitable to investigate this theoretically (assuming no disturbing influences of convection currents) in connexion with any conclusions to be drawn from explosions in such a vessel. Some thought which we have given the matter leads us to believe that this consideration with the superimposed effects of convection currents may account for the experimental results of these investigators.

Although the case for "afterburning" or "latent energy" has now been disposed of, it may be well to add a few words concerning David and Davies's luminosity experiments. The beautiful snapshots by Ellis and Wheeler [24], taken at different stages of the explosion process in a spherical vessel, show conclusively that the duration of luminosity is due to emission from the central core of burned gas. On account of the temperature gradient which is established in explosions in a spherical vessel with central ignition, the temperature of this core at maximum pressure is from 400° to 600° C. above the mean temperature inferred from the pressure [25]. Since "afterburning" was non-existent [19], [20], it was obvious that the photographs by Ellis and Wheeler could be interpreted readily by this temperature condition [19]. David and Davies, themselves, realize that the intensity and duration of the luminosity or afterglow depend only on the temperature of the inflamed gases, but they believe it to be the temperature radiation of *abnormal* molecules, formed during the combustion, which remain stable for a long time [26]. David supports his argument by the statement [26], "it is well known that gases like CO_2, H_2O, N_2, etc., in their normal condition when heated by external means to temperatures such as

inflamed gases have in these experiments, remain dark." A perusal of the literature [27] on the subject shows that this is not so well known. In fact, the experiments have yet to be performed. To our knowledge, nobody has ever heated CO_2, H_2O, H_2, N_2, etc., and mixtures of them externally to temperatures ranging from approximately 1800° to 3000° C., which are the temperatures of the central core at various stages of the liminosity, and made luminosity observations. The temperatures at which such observations have been made are those at which gases formed in flames also remain dark.

We shall now consider our comparisons of experimental and theoretical flame temperatures. The latter were calculated with the aid of accurate heat capacities and dissociation data provided by the analysis of band spectra. The method of calculation is given in the appendix to this paper. The experimental measurements of David and coworkers are excluded because of the unknown wire temperature correction. Measurements by the electrically heated wire method are too few, but considerable material is available from line-reversal measurements. In particular we shall confine our attention to measurements made in the laboratories of the U.S. Bureau of Mines [28] and the measurements of Ellis and Morgan on CO [29] because of their completeness and because the conditions under which the measurements were made are known.

The Bureau of Mines experiments had for their object solely the determination of the maximum flame temperatures attainable with a given fuel for industrial needs. It is needless to mention that there are temperature gradients within a stationary flame above a burner (Meker type). One of them decreases upward from the top of the cones along the central axis [30]. The operator followed the gradient along the central axis by focussing various points on the slit of the spectroscope. This could be accomplished with great sharpness, because the image of the flame was large compared with the dimensions of the slit. The region above the cones within which the maximum temperature remained sensibly constant varied with the type of combustible mixture and the gas flow.

Table I. contains the results of a few typical mixtures. The observed temperatures are not single observations,

Table I.

Comparison of Calculated and Observed Flame Temperatures.

Case.	Composition of mixture*, per cent.						Flame temperature, °C.		Experimenter.	Method.
	H_2.	CO.	CH_4.	O_2.	N_2.	H_2O.	Calculated.	Observed.		
1	31·12	—	—	13·81	52·31	2·76	2047	2045	Jones, Lewis, and Seaman	Sodium line-reversal.
2	—	34·23	—	13·17	49·84	2·76	2082	1955	Loomis and Perrott; Jones, Lewis, and Seaman.	do.
								1985	Ellis and Morgan.	do.
3	—	—	8·75	18·49	70·00	2·76	1844	1820	Jones, Lewis, and Seaman.	do.
4	—	—	8·75	20·50	67·99	2·76	1848	1935	Jones, Lewis, and Seaman.	do.

* In the publications from the Bureau of Mines laboratories the percentage composition was given on a dry basis. They are given here on a wet basis. The gases were saturated with water vapour at 23° C.

but are derived from previously published curves of flame temperature versus mixture composition which include many observations. In going over the original Bureau of Mines' notebooks we find the entry that in cases 1 and 3 the temperature remained rather constant for a distance of about 10 mm. above the cones (total height of flame 5 to 6 cm.). In case 2 the following observation is recorded : " The flame gave a good reversal ; for a distance of 10 mm. above the cones the flame was not very yellow, therefore the reading was always made above this region." In case 4 the notes read :— " A considerable temperature gradient exists in the flame directly above the burner ; the readings were taken 1 mm. above the burner."

As Table I. shows, excellent agreement is found in case 1. This is to be expected if radiation losses are negligible, as indeed David, Brown, and El Din's measurements show [18], and if the anomalous effect of the excitation lag in the nitrogen molecule is absent. Judging from our previous calculations [20] of Pier's nitrogen explosions we should expect a negligible excitation-lag effect in this case because the flame temperature is well above Tb_e, the temperature of the last burned portion of a similar mixture exploded in a spherical vessel (central ignition), in which region the excitation lag is believed to exert its influence on the pressure. Thus the agreement found may be considered to be an excellent confirmation of the results obtained in spherical vessels by various investigators.

In the methane flame, case 3, the observed value is 24° below the calculated. This difference may probably be explained by radiation loss which is known to occur in these flames. However, a very marked discrepancy appears in case 4, in which a small amount of the nitrogen of the case 3 mixture is replaced by oxygen. Since both mixtures are on the lean side the theoretical temperatures are nearly the same, the difference being due to the effect of the additional oxygen on dissociation. The observed temperature is surprisingly high, 87° above the calculated. A clue seems to be furnished by the observation in the notebook quoted above. Thus in case 3 the observations were made 10 mm. above the cones in a region where the temperature remained practically constant over some distance, whereas in case 4

the observations were made 1 mm. above the burner approximately at the beginning of a short and steep temperature gradient. This suggests the influence of the excitation lag effect ; that is, the nitrogen (and oxygen) emerge from the boundary of the flame front in a state of lower heat capacity [31] than they are in a short time later at a point farther removed from the cones. Whether a similar temperature gradient existed in the case 3 mixture cannot be said, for evidently it was confined to so narrow a region that it escaped the notice of the observer. It may be mentioned in this connexion that the flame speed of this mixture is slower than that of the case 4 mixture. It is unfortunate that in the methane-oxygenated air mixture, temperature readings were not recorded 10 mm. above the cones because agreement with the case 3 mixture should have been found here. David and Jordan [4], on investigating similar mixtures with their wire method, failed to observe a difference in temperature between the two mixtures. In the light of the above remarks this would be adequately accounted for by the short duration of the excitation lag effect which is comparable with the time required for the flame to heat the wire to its maximum temperature.

We believe that stationary flames should be given a more searching investigation, particularly with regard to determination of the isotherms under various conditions. It should prove to be a unique and simple way of studying the time function of the heat capacities. We regret that we are unable to undertake this work at the present time.

In case 2, that of CO in air, the calculated temperature is higher than the observed by 127° in the Bureau of Mines measurements and 97° in Ellis and Morgan's measurements. Concerning the reason for the different observed temperatures a clue is furnished by the notebook remarks quoted above and the specifications in Ellis and Morgan's paper. The latter authors succeeded in producing a flame in which the temperature remained constant over $3\frac{1}{2}$ mm. above the cone, and was appreciably lower above this zone. For this type of mixture they were able to measure temperatures in a hotter part of the flame (at the tip of the cone) than the Bureau of Mines investigators were able to do. Therefore greater weight is to be attached to their

measurement. Even so the difference between the calculated and observed temperatures appears rather large, the unaccounted energy amounting to approximately 5 per cent. [32]. Whether this difference can be accounted for quantitatively by radiation, which for CO is rather strong, cannot be stated definitely. It is conceivable that a strong emission takes place within the flame front where there is a high concentration of freshly formed CO_2 molecules. An investigation along such lines would be highly instructive and desirable.

Explosion Pressures.

In a recent publication entitled 'The Specific Heats of Gases at High Temperatures,' David and Leah [33] give the results of their thermodynamic calculations of explosions in spherical vessels made by them and Thorp [33]. They find discrepancies in the heat balance which they attribute to the "afterburning" effect. However, ample evidence has been cited in the first part of this paper against the validity of the "afterburning" hypothesis. One must therefore seek further for the explanation of these discrepancies.

Again we note that for their calculations the authors used inaccurate data on heat capacities and dissociation equilibria of the gases involved.

Our interest at present being centred around explosions of mixtures of hydrogen and oxygen with and without inert gases, we have selected at random some such explosions of David and Leah's and Thorp's and have carried out the calculations rigidly as described elsewhere [20]. The results are given in Table II.

$P'e_{(obs.)}$, the observed maximum pressure, corresponds to David and Leah's Pm. This is to be compared with $P'e_{(calc.)}$, the theoretical explosion pressure. The superscript prime is used to distinguish the actual explosion pressure from the pressure Pe, which would be obtained if the temperature were equalized throughout the vessel at the end of the explosion. In reality a temperature gradient exists rising inward from the wall to the centre, which results in $P'e < Pe$ [25]. The temperature corresponding to the equalized temperature state is Te. In calculating values of Pe and $P'e$ the increase in the number of molecules due to dissociation is included.

TABLE II.

Comparison of Observed and Calculated Explosion Pressures.

Experiments of David and Leah, and Thorp.

$T_i = 293°$ K.

No.	Experimenter.	Composition of mixture.				P_i, mm. Hg.	T_e, °K.	P_e calc., mm. Hg.	P'_e calc., mm. Hg.	P'_e obs., mm. Hg.	Percent. difference.
		H_2.	O_2.	N_2.	H_2O.						
1	Thorp.	90	10	—	—	760	2301	5392	5378	5328	−0·93
2	D. and L.*	51 60	10·18	38·22	—	2280	2309	16138	16102	15709	−2·44
3	Thorp.	20	80	—	—	760	2097	4513	4507	4502	−0·11
4	D. and L.*	54·00	9·54	35·89	0·57	2280	2203	15517	15487	15344	−0·92

* These are explosions in their 18″ vessel.

The comparison of the theoretical and observed pressure is convenient, because it allows an immediate appraisal of the deviations from experimental error.

The results of the calculation of these data are in substantial agreement with our previously published results [20]. On comparing explosions 1 and 2 with those in table ii. of our paper [20], explosion 3 with explosion 2·6 in table iv., and explosion 4 with those in the second sections of tables i. and iii., one observes that the experiments of David and Leah and Thorp harmonize with those of other investigators within the limits of experimental error. Therefore, their experiments are fully interpreted by the discussion already given [20].

David and Leah's and Thorp's experiments, and those of others with dry hydrogen-oxygen mixtures, confirm the water-vapour effect discovered by Wohl and von Elbe [34]. It is well to point out that the explanation proposed by the latter authors is only an hypothesis based on indirect evidence and that elucidation of the phenomenon must await further experimentation.

Explosion pressures of mixtures of hydrogen and oxygen diluted with argon or helium and small amounts of water-vapour agree very well [20] with theoretical pressures, leaving no energy unaccounted for. Reference was made by David and Leah to high-pressure explosions by Bone, Newitt and Townend [35], who found that $CO–O_2$ mixtures diluted with helium yielded maximum pressures appreciably lower than those yielded by similar mixtures diluted with argon. These results were quoted by David and Leah as indicating differences in the ability of these monatomic gases to deactivate the abnormal molecules (that is, within the picture of the "after-burning" hypotheses). A much simpler explanation is provided from a knowledge of the experimental facts. In the experiments of Bone, Newitt, and Townend the spark plug was located at the wall. The burning gases were in contact with the wall during the explosion, and heat losses were inevitably larger in the helium mixtures. That no difference is found when central ignition is employed has been verified by the present authors in the case of $H_2–O_2$ mixture diluted with identical amounts of helium or argon [19].

As for explosions of carbon monoxide and oxygen, the present authors have no material prepared at present.

However, evidence for any anomalous effects in carbon monoxide explosions, as in any other explosions, should be based on rigid calculations as above.

Appendix.

Calculation of Flame Temperatures.

In order to allow a simpler expression of the multiple dissociations the previously published[36] procedure will be modified.

1. *Mixtures of* H_2, O_2, N_2, *and* H_2O—*Excess* H_2.

Consider a unit volume of unburned mixture at the initial temperature T_u and pressure P (usually 1 atmosphere) at which combustion takes place.

Vi_{H_2}, Vi_{O_2}, etc., are defined as the " partial volumes " of the indicated components in the unburned mixture, so that

$$Vi_{H_2}+Vi_{O_2}+Vi_{H_2O}+Vi_{N_2}=1. \quad . \quad . \quad . \quad (1)$$

The values of Vi_{H_2}, Vi_{O_2}, etc., are given by the composition of the unburned mixture. It is customary to express the latter by m_{H_2}, m_{H_2O}, and m_{N_2}, which represent the number of mols of excess or inert gas per mol of H_2O formed if no dissociation occurs. Thus

$$Vi_{H_2}=\frac{1+m_{H_2}}{1{\cdot}5+\Sigma m}, \quad . \quad . \quad . \quad . \quad . \quad (2)$$

$$Vi_{O_2}=\frac{0{\cdot}5}{1{\cdot}5+\Sigma m}, \quad . \quad . \quad . \quad . \quad . \quad (3)$$

$$Vi_{H_2O,\,N_2}=\frac{m_{H_2O,\,N_2}}{1{\cdot}5+\Sigma m}. \quad . \quad . \quad . \quad . \quad . \quad (4)$$

After combustion is complete the mass of gas contained in the unit volume of unburned mixture has reached the flame temperature T_b and the volume ΣV, the pressure remaining at P. V_{H_2}, V_{O_2}, etc., are defined as the " partial volumes " of the indicated components in the burned mixture, so that

$$V_{H_2}+V_{O_2}+\text{etc.}=\Sigma V. \quad . \quad . \quad . \quad . \quad . \quad (5)$$

The following equilibria [37] will be considered :—

$$H_2+\tfrac{1}{2}O_2 \rightleftharpoons H_2O \qquad (H_2O \text{ dissociation I}),$$

$$\tfrac{1}{2}H_2+OH \rightleftharpoons H_2O \qquad (H_2O \text{ dissociation II}),$$

$$2H \rightleftharpoons H_2 \qquad (H_2 \text{ dissociation}),$$

$$\Sigma V = V_{H_2}+V_{O_2}+V_{H_2O}+V_{OH}+V_H+V_{N_2}. \quad . \quad (5a)$$

The partial pressure of each component in the burned mixture is related to the partial volume by

$$p_{H_2}, \text{ etc.} = \frac{V_{H_2}, \text{etc.}}{\Sigma V} P. \quad . \quad . \quad . \quad . \quad . \quad (6)$$

The equilibrium constants of the three reactions are, therefore, given by

$$K_{pI} = \frac{V_{H_2} V_{O_2}^{1/2}}{V_{H_2O}} \left(\frac{P}{\Sigma V}\right)^{1/2}, \quad . \quad . \quad . \quad . \quad (7)$$

$$K_{pII} = \frac{V_{H_2}^{1/2} V_{OH}}{V_{H_2O}} \left(\frac{P}{\Sigma V}\right)^{1/2}, \quad . \quad . \quad . \quad . \quad (8)$$

$$K_{pH_2} = \frac{V_H^2}{V_{H_2}} \frac{P}{\Sigma V} . \quad . \quad . \quad . \quad . \quad . \quad . \quad . \quad (9)$$

Taking into consideration the disappearance of H_2O and H_2 due to dissociation,

$$V_{H_2O} = \frac{T_b}{T_u} (V i_{H_2O} + 2V i_{O_2}) - 2V_{O_2} - V_{OH}, \quad . \quad . \quad . \quad (10)$$

$$V_{H_2} = \frac{T_b}{T} (V i_{H_2} - 2V i_{O_2}) + 2V_{O_2} + \tfrac{1}{2} V_{OH} - \tfrac{1}{2} V_H . \quad . \quad (11)$$

Further,

$$V_{N_2} = \frac{T_b}{T_u} V i_{N_2} . \quad . \quad . \quad . \quad . \quad . \quad . \quad . \quad . \quad . \quad . \quad (12)$$

The heat of combustion of 1 mol of H_2 at constant pressure and 296° K, is 57795 calories [38]. The energy equation then reads

$$57795 = (1+m_{H_2O})(\overset{\circ}{H}_{T_b} - \overset{\circ}{H}_{T_u})_{H_2O} + m_{H_2}(\overset{\circ}{H}_{T_b} - \overset{\circ}{H}_{T_u})_{H_2}$$
$$+ m_{N_2}(\overset{\circ}{H}_{T_b} - \overset{\circ}{H}_{T_u})_{N_2} + \Sigma(mD)(T_b - T_u). \quad (13)$$

$\overset{\circ}{H}_T$ in Lewis and Randall's system is the heat content of

the various components at the temperature T and is connected with the energy content $\overset{\circ}{E}_T$ by

$$\overset{\circ}{H}_T = \overset{\circ}{E}_T + RT. \quad . \quad . \quad . \quad . \quad . \quad . \quad (14)$$

The last term on the right-hand side of equation (13) is the contribution of the various dissociations to the heat balance,

$$\Sigma(mD) = \frac{1}{T_b - T_u} \frac{T_u}{T_b} \frac{1}{2Vi_{O_2}}$$

$$\times \left[2V_{O_2} \Delta \overset{\circ}{H}_{IT_b} + V_{OH} \Delta \overset{\circ}{H}_{IIT_b} + \tfrac{1}{2} V_H \Delta \overset{\circ}{H}_{H_2 T_b}\right], \quad (15)$$

where $\Delta \overset{\circ}{H}_{IT_b}$, $\Delta \overset{\circ}{H}_{IIT_b}$ are the heats of the dissociation reactions I and II at T_b per mol of H_2O; $\Delta \overset{\circ}{H}_{H_2 T_b}$ is the same for the H_2 dissociation per mol of H_2.

To calculate, assume a temperature T_b and find the corresponding values of the various equilibrium constants, heats of dissociation, and heat contents. The right-hand side of equation (13) may now be evaluated and must equal 57795. If it does not, assume a new temperature until agreement is found.

2. *Mixtures of* CO, O_2, N_2, H_2O—*Excess* CO.

For these mixtures,

$$Vi_{CO} = \frac{1 + m_{CO}}{1{\cdot}5 + \Sigma m}, \quad . \quad . \quad . \quad . \quad . \quad (16)$$

$$Vi_{O_2} = \frac{0{\cdot}5}{1{\cdot}5 + \Sigma m}, \quad . \quad . \quad . \quad . \quad . \quad (17)$$

$$Vi_{H_2O,\,N_2} = \frac{m_{H_2O,\,N_2}}{1{\cdot}5 + \Sigma m}. \quad . \quad . \quad . \quad . \quad . \quad (18)$$

The following equilibria will be considered :—

$CO + \frac{1}{2}O_2 \rightleftharpoons CO_2$ (CO_2 dissociation),

$H_2 + \frac{1}{2}O_2 \rightleftharpoons H_2O$,

or the alternative,

$CO + H_2O \rightleftharpoons CO_2 + H_2$ (Water gas equilibrium).

$\frac{1}{2}H_2 + OH \rightleftharpoons H_2O$,

$2H \rightleftharpoons H_2$;

$$\Sigma V = V_{CO_2} + V_{CO} + V_{H_2O} + V_{O_2} + V_{H_2} + V_H + V_{OH} + V_{N_2}. \quad (19)$$

The equilibrium constants are given by

$$K_{pCO_2} = \frac{V_{CO} V_{O_2}^{1/2}}{V_{CO_2}} \left(\frac{P}{\Sigma V}\right)^{1/2}, \quad . \quad . \quad . \quad . \quad (20)$$

$$K_{pI} = \frac{V_{H_2} V_{O_2}^{1/2}}{V_{H_2O}} \left(\frac{P}{\Sigma V}\right)^{1/2}, \quad . \quad . \quad . \quad . \quad (7)$$

or the alternative,

$$K_{wg.} = \frac{V_{CO} V_{H_2O}}{V_{CO_2} V_{H_2}} \quad . \quad . \quad . \quad . \quad . \quad . \quad . \quad (21)$$

$$K_{pII} = \frac{V_{H_2}^{1/2} V_{OH}}{V_{H_2O}} \left(\frac{P}{\Sigma V}\right)^{1/2}, \quad . \quad . \quad . \quad (8)$$

$$K_{pH_2} = \frac{V_H^2}{V_{H_2}} \frac{P}{\Sigma V} \quad . \quad . \quad . \quad . \quad . \quad . \quad . \quad (9)$$

Taking into consideration the changes in the components due to various dissociations,

$$V_{CO_2} = \frac{T_b}{T_u} V i_{CO} - V_{CO}, \quad . \quad . \quad . \quad . \quad . \quad . \quad . \quad . \quad (22)$$

$$V_{H_2O} = \frac{T_b}{T_u} V i_{H_2O} - V_{H_2} - \tfrac{1}{2} V_H - \tfrac{1}{2} V_{OH}, \quad . \quad . \quad . \quad (23)$$

$$V_{CO} = \frac{T_b}{T_u} (V i_{CO} - 2 V i_{O_2}) + 2 V_{O_2} + \tfrac{1}{2} V_{OH} - V_{H_2} - \tfrac{1}{2} V_H. \quad . \quad . \quad (24)$$

Equation (12) remains.

The heat of combustion of 1 mol of CO at constant pressure and 296° K. is 67628 calories [39].

$$67628 = (\overset{\circ}{H}_{T_b} - H_{T_u})_{CO_2} + m_{CO}(\overset{\circ}{H}_{T_b} - \overset{\circ}{H}_{T_u})_{CO} + m_{N_2}(\overset{\circ}{H}_{T_b} - \overset{\circ}{H}_{T_u})_{N_2} + m_{H_2O}(\overset{\circ}{H}_{T_b} - \overset{\circ}{H}_{T_u})_{H_2O} + \Sigma(mD)(T_b - T_u)], \quad . \quad . \quad . \quad . \quad . \quad . \quad . \quad (25)$$

$$\Sigma(mD) = \frac{1}{T_b - T_u} \frac{T_u}{T_b} \frac{1}{2 V i_{O_2}} \times [(2 V_{O_2} + \tfrac{1}{2} V_{OH} - V_{H_2} - \tfrac{1}{2} V_H) \Delta H_{CO_2 T_b} + (V_{H_2} + \tfrac{1}{2} V_H - \tfrac{1}{2} V_{OH}) \Delta \overset{\circ}{H}_{IT_b} + V_{OH} \Delta \overset{\circ}{H}_{IIT_b} + \tfrac{1}{2} V_H \Delta \overset{\circ}{H}_{H_2 T_b}]. \quad . \quad . \quad . \quad . \quad . \quad . \quad . \quad . \quad (26)$$

3. *Mixtures of* CH_4, O_2, N_2, H_2O—*Excess* O_2.

For these mixtures,

$$Vi_{CH_4}=\frac{1}{3+\Sigma m}, \quad . \quad . \quad . \quad . \quad . \quad (27)$$

$$Vi_{O_2}=\frac{2+m_{O_2}}{3+\Sigma m}, \quad . \quad . \quad . \quad . \quad . \quad (28)$$

$$Vi_{H_2O,\,N_2}=\frac{m_{H_2O,\,N_2}}{3+\Sigma m}, \quad . \quad . \quad . \quad . \quad . \quad (29)$$

where m_{O_2}, etc., are now the mols of indicated component per mol of CH_4 burned to CO_2 and $2H_2O$.

The same equilibria hold as in case 2 above for CO mixtures.

$$V_{CO_2}=\frac{T_b}{T_u}Vi_{CH_4}-V_{CO}, \quad . \quad . \quad . \quad . \quad . \quad . \quad . \quad . \quad . \quad (30)$$

$$V_{H_2O}=2\frac{T_b}{T_u}Vi_{CH_4}+\frac{T_b}{T_u}Vi_{H_2O}-V_{H_2}-\tfrac{1}{2}V_H-\tfrac{1}{2}V_{OH}, \quad . \quad (31)$$

$$V_{O_2}=\frac{T_b}{T_u}(Vi_{O_2}-2Vi_{CH_4})+\tfrac{1}{2}V_{CO}+\tfrac{1}{2}V_{H_2}+\tfrac{1}{4}V_H-\tfrac{1}{4}V_{OH}. \quad . \quad . \quad . \quad (32)$$

Equation (12) remains.

The heat of combustion of 1 mol of CH_4 to CO_2 and $2H_2O$ at constant pressure and 296° K. is taken as 189,700 calories [40].

$$189700=(H^{\circ}_{T_b}-H^{\circ}_{T_u})_{CO_2}+(2+m_{H_2O})(H^{\circ}_{T_b}-H^{\circ}_{T_u})_{H_2O}$$
$$+m_{O_2}(H^{\circ}_{T_b}-H^{\circ}_{T_u})_{O_2}+m_{N_2}(H^{\circ}_{T_b}-H^{\circ}_{T_u})_{N_2}$$
$$+\Sigma(mD)(T_b-T_u), \quad . \quad . \quad . \quad . \quad . \quad . \quad . \quad . \quad . \quad (33)$$

$$\Sigma(mD)=\frac{1}{T_b-T_u}\frac{T_u}{T_b}\frac{1}{Vi_{CH_4}}$$
$$\times\left[V_{CO}\Delta H^{\circ}_{CO_2T_b}+(V_{H_2}+\tfrac{1}{2}V_H-\tfrac{1}{2}V_{OH})\Delta H^{\circ}_{IT_b}\right.$$
$$\left.+V_{OH}\Delta H^{\circ}_{IIT_b}+\tfrac{1}{2}V_H\Delta H^{\circ}_{H\,T_b}\right]. \quad . \quad . \quad . \quad . \quad (34)$$

Summary.

Theoretical flame temperatures and explosion pressures may now be calculated accurately with the aid of exact band spectroscopic data on specific heats and thermal dissociation. It is shown that experimental and theoretical flame temperatures and explosion pressures agree very well in many instances. In some cases experimental values are somewhat higher and in other cases lower than the theoretical values. Various effects are discussed which are responsible for these anomalies, such as time dependency of specific heats and radiation losses. A method is given in an Appendix for rigid calculation of theoretical flame temperatures.

The works of David and coworkers are reviewed critically, and it is shown—

a. That their objections to the line-reversal method of measuring flame temperatures are invalid; that flame temperatures measured by their unheated wire method are at variance with the results of the electrically heated wire method, the electric conductivity method, and the radiometric method; and that, in addition, their estimated radiation losses from the wire disagree with those of Hopkinson.

b. That the conception of "afterburning" or "latent energy," that is, the existence of abnormal molecules of great stability in the flame gas carrying large amounts of energy, receives no support from experiments purported to prove it and is completely at variance with the known facts on flame temperatures and explosion pressures.

References.

(1) Published by permission of the Director, U.S. Bureau of Mines. (Not subject to copyright.)
(2) Physical Chemist, U.S. Bureau of Mines, Pittsburgh Experiment Station, Pittsburgh, Pa.
(3) Coal Research Laboratory, Carnegie Institute of Technology Pittsburgh, Pa.
(4) David and Davies, Phil. Mag. ix. p. 402 (1930); David, Davies, and Jordan, *ibid.* xii. p. 1034 (1931); David and Jordan, *ibid.* xvii. p. 172 (1934); xviii. p. 228 (1934).
(5) Hopkinson, Proc. Roy. Soc. A, lxxvii. p. 387 (1906).
(6) Schmidt, *Deut. Phys. Ges.* xi. p. 87 (1909); Kohn, *Ann. Phys,* xliv. p. 749 (1914); National Phys. Lab. 1926 Report, p. 63. Loomis and Perrott, Ind. Eng. Chem. xx. p. 1004 (1928); Griffiths and Awbery, Proc. Roy. Soc. A, cxxiii. p. 401 (1929).

(7) The line-reversal method has also been employed for stationary flames by Henning and Tingwalt, *Z. Phys.* xlviii. p. 805 (1928); Jones, Lewis, Friauf, and Perrott, J. Amer. Chem. Soc. liii. p. 869 (1931); Jones, Lewis, and Seaman, *ibid.* liii. p. 3992 (1931); liv. p. 2166 (1932); J. Franklin Inst. ccxv. p. 149 (1933); Ellis and Morgan, Trans. Far. Soc. xxviii. p. 826 (1932); and by Hershey, Ind. Eng. Chem. xxiv. p. 867 (1932); Univ. Ill. Eng. Exp. Station Bulletin No. 262 (1933).

(8) Barnes, Phys. Rev. xxiii. p. 178 (1924); Bennett, Phil. Mag. liii. p. 127 (1927); See also Noyes and Wilson, Astrophys. J. lvii. p. 20 (1923).

(9) Hershey, Ind. Eng. Chem. xxiv. p. 867 (1932).

(10) J. Amer. Chem. Soc. liii. p. 3992 (1931).

(11) Reference (7).

(12) Reference (7).

(13) Dissertation, Breslau (1913).

(14) Kneser, *Ann. Phys.* xi. pp. 761, 777 (1931), xvi. p. 377 (1933); *Phys. Z.* xxxii. p. 179 (1931); xxxv. p. 983 (194); *Z. Phys.* lxxvii. p. 649 (1932); 'Nature,' cxxix. p. 797 (1932); J. Acoust. Soc. Amer. v. p. 122 (1933); Zener, Phys. Rev. xxxviii. p. 277 (1931); Henry, 'Nature,' cxxix. p. 200 (1932); Eucken, Mücke, and Becker, *Naturwiss.* xx. p. 85 (1932); Wohl and Magat, *Z. Phys. Chem.* B, xix. p. 536 (1932); Lewis and von Elbe, J. Chem. Phys. iii. p. 63 (1935); Sharratt and Griffiths, Proc. Roy. Soc. A, cxlvii. p. 292 (1934); Eucken and Becker, *Z. Phys. Chem.* B. xxvii. pp. 219, 235 (1934).

(15) *Loc. cit.* p. 1046.

(16) It should be emphasized that the interpretation of results derived from Partington and Shilling's, Pier and Bjerrum's, and Goodeneough and Felbeck's heat capacity data is of questionable value. Even the Planck-Einstein functions for the harmonic oscillator are inadequate for precise work because of the anharmonicity of the vibrational and rotational levels. In the last four years heat capacity and equilibrium data, which are beyond reproach, have been derived from the band spectra of most of the common gases. It is essential that these accurate data be employed in future calculations. Accordingly we have gathered and arranged all the data in two concise tables (J. Amer. Chem. Soc., April, 1935).

(17) One striking disagreement given for CO-air mixtures on p. 1050 of David, Davies, and Jordan's paper, largely disappears in a later paper by David and Jordan (Phil. Mag. xvii. p. 176 (1934)), the reason apparently being ascribed to technical difficulties, consisting of cool currents of gas coming in contact with the spark electrodes and the wire leads themselves.

(18) David, Brown, and El Din, Phil. Mag. xiv. p. 764 (1932).

(19) Lewis and von Elbe, J. Chem. Phys. ii. p. 659 (1934).

(20) J. Chem. Phys. iii. p. 63 (1935),

(21) Lewis and von Elbe, J. Chem. Phys. ii. pp. 283, 665 (1934).

(22) Mache, 'Die Physik der Verbrennungserscheinungen,' 1918.

(23) We note that the maximum temperature in the 17 per cent. H_2-air mixture, reported in David and Davies's paper (fig. 8), is markedly lower, approximately 100°, than the temperature inferred from the pressure reported in David, Brown, and El Din's paper for the same mixture and in a vessel of the same size.

(24) J. Chem. Soc. p. 310 (1927).

(25) Lewis and von Elbe, J. Chem. Phys. ii. p. 665 (1934).

(26) See also David, 'The Engineer,' June 1, 1934, p. 558.

(27) See for example, Franck and Jordan, 'Anregung von Quantensprüngen durch Stösse,' Berlin, 1926, pp. 191–199.

(28) Reference (7); papers by Loomis and Perrott; Jones, Lewis, Friauf, and Perrott; Jones, Lewis, and Seaman.
(29) Reference (7), *loc. cit.*
(30) This accounts for the different results found by Griffiths and Awbery (*loc. cit.*) for identical mixtures of CO-air. The readings were taken at different points with respect to the cones. G. and A. interpret their experiments in this way.
(31) A rough calculation shows that the N_2 molecules possessed about 50 per cent. of their normal vibrational energy.
(32) This is in contrast to an estimate of about 20 per cent. made by David and Jordan, *loc. cit.* See also David, reference (26).
(33) Phil. Mag. xviii. p. 307 (1934).
(34) *Z. Phys. Chem.* B, v. p. 241 (1929).
(35) Proc. Roy. Soc. A, cx. p. 645 (1926); or 'Gaseous Combustion at High Pressures,' p. 209, Longmann's, 1929.
(36) Goodenough and Felbeck. Bull. Univ. Ill. Eng. Exp. Station No. 139 (1924); Jones, Lewis, Friauf, and Perrott. *loc. cit.*
(37) At very high temperatures the O_2 dissociation and the NO equilibrium should be considered.
(38) From Rossini, Bureau of Standards J. Res. vi. p. 1 (1931).
(39) From Rossini, Bureau of Standards J. Res. vi. p. 37 (1931).
(40) Int. Crit. Tables.

Physical Chemical Section,
Pittsburgh Experiment Station,
U.S. Bureau of Mines, Pittsburgh, Pa.
December 12, 1934.

V. *The Experimental Determination and Theoretical Calculation of Flame Temperatures and Explosion Pressures.* *By* Prof. W. T. David*.

DR. LEWIS and Dr. von Elbe, in their paper under the above title (of which they have been good enough to send me an advance copy) are mainly concerned to prove that actual flame temperatures are equal to the ideal calculated temperatures and that, therefore, flame gases cannot hold within them large amounts of latent energy as we believe.

Their proof is based upon two generalizations, viz. :—

(i.) That flame temperatures as measured by the sodium line reversal method are equal to the calculated temperatures; and

(ii.) that flame temperatures as measured by the sodium method are correct actual flame temperatures, because

* Communicated by the Author.

they agree with those measured by other methods, notably the electrically heated platinum wire method.

It is clear that if these generalizations are correct their deduction from them that actual flame temperatures are equal to the calculated temperature is correct, and latent energy consequently non-existent. But it is easily shown that the generalizations are incorrect, and the deduction in our view never correct.

In order to substantiate the first of their generalizations Dr. Lewis and Dr. von Elbe give in Table I. of their paper a " few selected mixtures " for which the sodium flame temperatures are nearly equal to the calculated. But had they made their selection upon a wider basis an entirely different perspective would have been attained. For example, the sodium temperatures for a " correct " CO-air mixture as measured by Loomis and Perrot, Ellis and Morgan, and Griffiths and Awbery are some hundreds of degrees C. *below* the calculated temperatures, and for a 52 per cent. mixture Ellis and Morgan, using a Smithell's separator, found a temperature some 200° C. *above* the calculated (far too great an excess to be explained in terms of excitation lag). And these results might be paralleled from the sodium measurements in hydrocarbon-air flames by Jones, Lewis, and Seaman. Indeed, a comprehensive examination of the sodium measurements recorded in scientific literature will show that so far from being in agreement with the calculated temperatures the sodium flame temperatures bear no obvious relationship to them *.

The second of their generalizations is also based upon an inadequate range of observations. Comparisons between measurements made by the sodium method and those made by the electrically heated wire method were not made over a wide range of conditions, but for single mixture strengths only. In certain exceptional cases our platinum wire temperatures are also much in agreement with the sodium temperatures ; for example, our temperature for a " correct " CO-air mixture is nearly as high as the sodium temperatures for the same mixture as measured by Loomis and Perrot and Ellis and Morgan, and considerably higher than that measured by Griffiths

* "The Sodium Line Reversal Method of determining Flame Temperatures," 'Engineering,' 2nd Nov. 1934, and 22nd Feb. 1935. See also 'Nature,' cxxxv. p. 470 (1935).

and Awbery *. But generally the sodium temperatures are much higher than the platinum temperatures (some 500° C. higher in the case of the Ellis and Morgan sodium temperature for the 52 per cent. CO-air mixture previously referred to).

The sodium temperatures when they are in agreement with the platinum temperatures, and the platinum temperatures always †, are many hundreds of degrees C. below the calculated. It is suggested that a careful examination be given to fig. 4 of our paper on "Flame Temperatures in Methane-air Mixtures" ‡. It will be seen that the platinum temperatures, while very much lower than the calculated temperatures, bear a rational relationship to them. The sodium temperatures obviously do not.

Much of the interesting speculation of Dr. Lewis and Dr. von Elbe requires reconsideration in the light of the above, but attention may be called to one other important point. The work of David, Brown, and El Din showing lower explosion pressures (after correcting for measured heat loss) in a 6-inch spherical vessel than in an 18-inch vessel has been confirmed by experiments with a 3-inch

* Our platinum wire temperatures are also in agreement with the sodium temperatures measured by Jones, Lewis, and Seaman in the case of ethylene-air mixtures on the weak side of the "correct."

The case of the "correct" CO-air mixture is interesting in that agreement occurs in this mixture in spite of the fact that here the largest radiation correction to the platinum wire temperature would be required. In framing their estimate of the radiation correction, Lewis and von Elbe refer to the work of David, Davies, and Jordan with ·0005 inch and ·001 inch wires. But this work related wholly to weak mixtures in which the temperatures were relatively low. Generalization to high temperatures is clearly illegitimate, and it may be of interest to point out that if the radiation correction suggested by Lewis and von Elbe were correct it would involve the raising of our platinum wire temperature for this mixture to a value which would be some 150° C. above the sodium temperature determined by Ellis and Morgan (the highest sodium temperature on record), and over 300° C. above the highest sodium temperature measured by Griffiths and Awbery. For this and many other reasons, which we have given in previous papers, it is obvious that a large radiation correction should not be applied to our measured temperatures.

† Except in the case of extremely weak mixtures of H_2 and air; but here it seems clear that the flame gases contain free H_2 and O_2 with the result that surface combustion takes place on the wire (Phil. Mag. xii. p. 1051 (1931)).

‡ Phil. Mag. xviii. p. 235 (1934). It may be pointed out that as the actual temperatures of the flame gases are below 2000° C., dissociation in them is small, and a fairer perspective is therefore obtained if comparisons are made with the calculated temperatures uncorrected for dissociation. See also 'The Engineer,' p. 230, March 1st, 1935.

vessel. Lewis and von Elbe state that their experiments with hydrogen mixtures in two vessels (one 12 inches and the other 18 inches in diameter) show equal pressures, but their vessels were not sufficiently different in size to produce a marked effect, and an oscillation, which has made itself felt in their pressure recording system *, suggests the desirability of repeating these experiments with improved pressure indicating arrangements.

VI. *Velocities of Positive Ions in the Corona Discharge.* *By* H. F. Boulind *M.A., B.Sc., Clare College, Cambridge* †.

1. The object of this communication is to summarize briefly the results for positive ion velocities obtained by various investigators using the method of the corona discharge, and to show how far these results agree with those obtained by Tyndall and his associates at Bristol, using a different method. The opportunity of correcting an error which appeared in a previous paper is also taken.

2. In a discharge between a wide outer cylinder and a narrow coaxial wire, the field-strength diminishes on passing from the inner to the outer electrode, and in most cases the discharge is confined to a small region surrounding the wire. Ions of sign similar to that of the charge on the wire drift through the region external to the discharge where the force is small, and give rise to a space-charge which tends to reduce the field-strength at the wire, so that, to increase the current, it is necessary to increase the potential between the electrodes. Townsend [1], on the assumption that the velocity of the ion is proportional to the field-strength, obtained an equation connecting the current in a corona discharge with the potential required to maintain it, and used the equation, together with experimental results, obtained by Watson [2], Schaffers [3], and himself to calculate the mobilities of positive and negative ions in air at atmospheric pressure, obtaining results in agreement with those of Langevin and Zeleny.

* See their explosion pressure record, J. Chem. Phys. ii. p. 662 (1934).

† Communicated by L. G. H. Huxley, M.A., D.Phil.

In 1928 Huxley [4] made experiments on corona discharges at low pressures in helium and neon, and used Townsend's equation to calculate the mobilities of positive ions in these gases for values of the ratio X/p, of the electric field-strength to the pressure, much greater than those used in previous direct determinations. Similar measurements were subsequently made by Huxley in nitrogen [5], by Bruce in hydrogen [6], and by myself in oxygen and air [7].

3. In no gas investigated was it possible to obtain negative coronas (*i.e.*, coronas in which the wire was at a negative potential), since the discharge became disruptive in every case. It appears that the negative ions move so rapidly that no appreciable space-charge is formed; this indicates that, at these values of X/p, the negative ions are free electrons—an assumption which is in agreement with the researches of Townsend [8] and of Tyndall and Powell [9].

4. In a previous communication [7] it was stated that, for the smaller values of X/p, the velocities W, of positive ions in oxygen, could be expressed by an equation,

$$W = 3180\, X/p,$$

W being in cm./sec., X in volts/cm., and p in mm. of mercury, and the results were also given in the form of a curve. The equation is correct, but, unfortunately, an arithmetical error was made in the calculation of the higher values of X/p, and the corrected curves for oxygen and air are shown in fig. 1 of this paper. The curve for hydrogen is not substantially different from that previously published.

The curve (fig. 1) is seen to consist of two parts, a linear portion, AB, representing the above equation, and another portion, BC, straight within the limits of experimental error. A similar curve was obtained by Huxley for helium. With the other gases—neon, hydrogen, and nitrogen—the results within the range of X/p investigated lie entirely on the portion of the curve corresponding to BC.

These curves may be interpreted as follows: the large values of the mobilities compared with those obtained in earlier researches with gases at higher pressures indicate that the positive ions are charged atoms or molecules, and neither clusters of molecules nor ions whose velocities

are controlled by exchange phenomena. The law, that W is proportional to X/p, holds up to a certain value of the latter quantity, but is no longer valid for greater values. The simplest interpretation is that the departure is caused by an increase in the mean free paths of the positive ions with increasing energy. This increase may be compared with that found for electrons by Ramsauer and by Townsend and Bailey, while Dempster [10] records

Fig. 1.

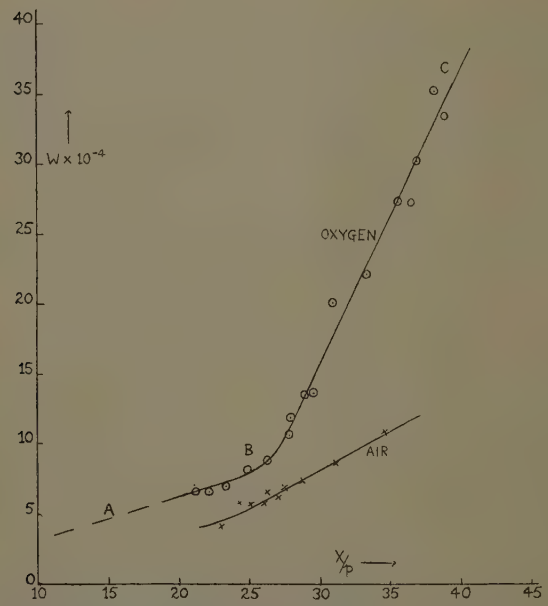

The velocities, W, of positive ions in oxygen, and in air, in the direction of the field X as a function of X/p. W in cm./sec, X in volts/cm., p in mm. of mercury.

an increase of up to seventeen times the kinetic theory value in the case of protons moving through helium with energies varying between 14 and 900 volts.

5. In the determination of mobilities by means of the corona discharge it is assumed that, at a given pressure, $W \propto X$. The mobility values obtained are average values

for the range of field-strengths existing between the wire and cylinder; but if the velocity W is proportional to the field-strength X, then the mobility $k(k=W/X)$ is independent of X, and no ambiguity arises. This is true for the portion AB of the curve; in addition, determinations of the mobilities made at one pressure, but with different field-strengths, give the same results, provided the pressure is not too low nor the field-strength too high *.

As the pressure is reduced and the potential increased, W first ceases to be proportional to X/p in the region near the wire. Were it possible to determine values of W when the ions move under constant field, the portion AB of the curve would be extended to higher values of X/p, and the upward bend at B would be sharper. The error is not so great as would appear at first sight on account of the space-charge effect, which tends to establish a uniform field behind wire and cylinder. The point to be emphasized, however, is that the corona-discharge experiments show that W is not proportional to X/p for the larger values of X/p. The point B in fig. 1 gives a lower limit for the value of X/p for which the law fails. It is seen also that the subsequent increase of W with X/p is very rapid.

6. Tyndall and Powell [11] also have concluded that positive ions in highly purified gases consist of single atoms or molecules. In their experiments, which were performed in air, nitrogen, and helium, they used uniform fields, and obtained more precise results than those given by the corona method. A similar conclusion was obtained from a further series of experiments [12] on alkali ions moving in argon, neon, and helium, and from the investigations of Powell and Brata [13] and of Brata [14]. Values of the mobility were found to diminish as the gas and apparatus were purified, and to increase again when the gas was allowed to stand in the apparatus and collect impurities. The clustering effect was found to diminish as p diminished and occasionally definite stages between clusters and single atoms were observed; thus Powell and Brata find 13·2 for the mobility, reduced to 760 mm., of the unclustered sodium ion, and 11·2 for a clustered ion, to which they ascribe the formula Na^+H_2O.

* See, for example, Phil. Mag. xviii. pp. 915–916 (1934).

Mitchell and Ridler [15] have found large increases in the mobility of positive ions (Li^+, Na^+, K^+, Rb^+, Cs^+, NH_3^+, $Na^+(NH_3)$) in nitrogen when X/p exceeds a critical value depending on the nature of the ion, the greater the smaller the mass. For the lighter ions the W against X/p curves obtained in these experiments—actually Mitchell and Ridler plot Wp/X against X/p—would be similar to that given for oxygen in fig. 1. The discontinuity is quite sharp, and both portions of the curve are straight within experimental error. Results were also obtained for nitrogen ions in nitrogen; again the graph is similar to fig. 1 Mitchell and Ridler conclude that the positive ion in nitrogen has the formula N_2^+, and that electron interchange takes place between ions and neutral molecules, this process resulting in a lowering of the mobility of the ion.

Thus measurements of the velocities of positive ions made by two very different methods indicate large increases when X/p exceeds a certain value.

7. The results of experiments on corona discharges are also of importance for the general theory of discharges, as positive ions may actually ionize molecules by collisions. This view has been criticized in two respects. Both criticisms are answered if the large velocities of the positive ions at the higher values of X/p are taken into account.

(*a*) Rogowski [16], Dunnington [17], and several others have measured the time-interval between the application to the electrodes of a potential greater than the starting potential and the occurrence of a spark. This time varies with the conditions, but it is of the order 10^{-7} of a second. It is objected that, while this time is ample for an electron to reach the anode, it is too short for the slower moving positive ion to cover any appreciable distance. Now, taking the case of the discharge in oxygen, fig. 1 shows that, for $X/p=40$ volts/cm. mm., the velocity of the positive ions is 370,000 cm./sec., a value much in excess of that calculated from mobility values determined at atmospheric pressures. In the intense field round the wire, X/p would be much greater than 40, and the positive-ion velocity is of the order 10^6–10^7 cm./sec. A positive ion could easily move through the space in which intense ionization occurs in 10^{-7} sec., an interval which is of the

same order as the probable time required for the initiation of a spark between coaxial cylinders. In hydrogen and other gases the positive-ion velocities are greater than in oxygen.

(*b*) Another objection, first raised by Holst and Oosterhuis [18], is that the chance of a positive ion acquiring sufficient energy to ionize a molecule by impact is too small for the process to exert a controlling influence.

In oxygen, at $X/p=40$, the velocity of the positive ions is about seven times what would be expected from mobility values determined at atmospheric pressure. However, part of this increase results from the fact that the oxygen ion is a charged single atom or molecule instead of a cluster. If the line AB is produced, it is seen that the velocity at $X/p=40$ is about three times the value it would have had if W had remained proportional to X/p, that is, the mean free path of the positive ion is about three times the kinetic theory value.

Taking $8{\cdot}7\times10^{-6}$ for the mean free path in oxygen at 760 mm., this gives $3\times8{\cdot}7\times10^{-4}$ for the mean free path of the positive ions at 7·6 mm. The average energy they acquire is

$$3\times8{\cdot}7\times10^{-4}\times7{\cdot}6\times40=0{\cdot}8 \text{ electron volt.}$$

The ionizing potential of oxygen is 13 volts, hence the chance of a positive ion reaching the ionizing potential is, roughly,

$$\epsilon^{-13/0{\cdot}8}=1/8900000.$$

If every positive ion possessing energy exceeding 13 volts produced a new pair of ions, the number produced per cm. path at 7·6 mm. pressure would be 0·00013, and at 760 mm. 0·013.

X/p near the wire for a corona discharge in oxygen would be much higher than 40 volts/cm. mm., and since W increases rapidly with X/p, the number of ion pairs produced per cm. may considerably exceed the above figures. In any case, the number is not impossibly small, as some previous investigators have stated.

Moreover, Townsend and Jones [19] have recently made a direct determination of the relative proportions in which electrons are produced in hydrogen by the two effects of positive ions, namely, formation of electrons by ionization of gas-molecules and formation of electrons

by impact of positive ions on the cathode. These experiments, and also those of Townsend and Yarnold [20] with helium, show that the ionization of gas-molecules by positive ions is an important process in the maintenance of discharges at pressures greater than that corresponding to the minimum sparking potential, in agreement with the conclusions which have been reached from experiments on corona discharges.

The opportunity is taken here of correcting an inaccuracy in my previous paper, to the effect that, according to Penning, the corona discharge in gases always occurs at a lower potential when the wire is negatively than when it is positively charged. Dr. Penning has drawn my attention to the fact that this statement refers to the noble gases, and in particular to neon, in a certain pressure-region.

Summary.

1. Reliable results for the velocities of positive ions in gases at low pressures can be obtained by the corona-discharge method provided that X/p is less than a certain value. The velocities exceed the values to be expected from mobility determinations at higher pressures, and this indicates that the positive ions in the corona discharge are single particles and not clusters. When the critical value of X/p is exceeded the method becomes inaccurate, but it shows that the velocity increases rapidly with X/p. This increase is attributed to an increase in the mean free path of the ions.

2. High values for the mobilities of positive ions in pure gases have been found by the more precise "four-gauze" method also, and similar large increases in the velocities of positive ions for the higher values of X/p are recorded by Mitchell and Ridler.

3. The increase in mean free path of the positive ions provides an answer to two criticisms of the theory that positive ions may produce appreciable numbers of new ion pairs by collision with gas-molecules.

References.

(1) Phil. Mag. xxviii. p. 83 (1914).
(2) 'The Electrician,' Feb. 11th, 1910.
(3) *Phys. Zeit.* xiv. p. 981 (1913); xv. p. 405 (1914).
(4) Phil. Mag. v. p. 721 (1928).

(5) Phil. Mag. x. p. 185 (1930).
(6) Phil. Mag. x. p. 476 (1930).
(7) Phil. Mag. xviii. p. 909 (1934).
(8) 'Motions of Electrons in Gases,' 1925.
(9) Proc. Roy. Soc. A, cxxix. p. 162 (1930).
(10) Phil. Mag. iii. p. 115 (1927).
(11) Proc. Roy. Soc. A, cxxix. p. 162 (1930); cxxxiv. p. 125 (1931).
(12) Proc. Roy. Soc. A, cxxxvi. p. 145 (1932).
(13) Proc. Roy. Soc. A, cxxxviii. p. 117 (1932).
(14) Proc. Roy. Soc. A, cxli. p. 454 (1933).
(15) Proc. Roy. Soc. A, cxlvi. p. 911 (1934).
(16) *Arch. f. Elektrotechnik*, xviii. p. 479 (1927).
(17) Phys. Rev. xxxviii. p. 1535 (1931).
(18) Phil. Mag. xlvi. p. 1117 (1923).
(19) Phil. Mag. xv. p. 282 (1933).
(20) Phil. Mag. xviii. p. 594 (1934).

VII. *On the Avoidance of Errors due to the "Leads" in Radio-frequency Measurements.* *By* R. M. Davies, *M.Sc., F.Inst.P., Lecturer in Physics, University College of Wales, Aberystwyth* *.

Contents.

Page
I. Introduction 75
II. Some Results from the Theory of Uniform Transmission Lines 77
III. Leads terminated by a Resistance 84
IV. Leads terminated by an Inductance 86
V. Leads terminated by a Capacitance 88
VI. Leads terminated by a Variable Condenser with a Linear Law 90
VII. Leads terminated by Capacitance and Resistance 95

I. Introduction.

RADIO-FREQUENCY measurements on a particular component of a circuit are often complicated, and may even become misleading, on account of the effect of the leads which are used to connect the component to the remainder of the circuit.

Referring to fig. 1, Z_r represents a circuit component with impedance Z_r between the terminals A and B; this component is connected to a circuit at the points C and D by means of the leads CA and DB. These leads will possess inductance, resistance, and capacitance, and, because of this, the impedance between the points C and D may differ appreciably from Z_r. It is in general

* Communicated by Vice-Principal Gwilym Owen, M.A., D.Sc.

impossible to calculate the effect of the leads in any specific practical case, since the electrical characteristics (inductance, etc.) of the leads will be distributed rather than concentrated, and, furthermore, these distributed characteristics will generally vary in an incalculable manner from point to point. To reduce the problem to a

Fig. 1.

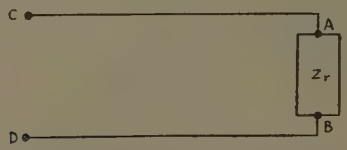

calculable form it is necessary to make some simplifying assumption. One possible assumption is to replace the distributed characteristics by "lumped" or concentrated characteristics, and this is the one usually made. If L′ and C′ be the total inductance and capacitance of the leads

Fig. 2 *a*.

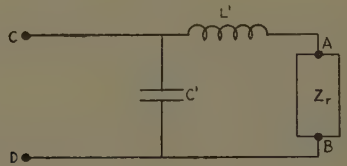

Fig. 2 *b*.

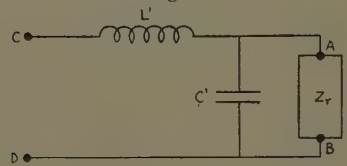

CA and DB of fig. 1, regarded as lumped characteristics, then one difficulty with regard to this method may be seen by referring to figs. 2 *a* and 2 *b*. These two figures represent two different ways in which these lumped characteristics may be arranged with reference to Z_r, the points A, B, C, and D in these figures having the

same significance as they have in fig. 1. The effective impedance between the points C and D may be termed the input impedance; let the input impedance of the arrangement of fig. 2*a* be Z′ and that of the arrangement of fig. 2*b* be Z″, Then, if the pulsatance of the current used be ω, and if $j=\sqrt{-1}$,

$$Z'=(Z_r+j\omega L')/(1-\omega^2 L'C'+j\omega C'Z_r) \quad . \quad . \quad (1.1)$$

$$Z''=(Z_r.\overline{1-\omega^2 L'C'}+j\,\omega L')/(1+j\,\omega Z_r C'.) \quad . \quad (1.2)$$

Thus, in general, $Z' \neq Z''$. In practice, however, $\omega^2 L'C'$ is small in comparison with unity unless the leads are very long and the frequency very high (v. Section II.); with this simplification, equations (1.1) and (1.2) give

$$Z'=Z''=(Z_r+j\,\omega L')/(1+j\,\omega Z_r C') \quad . \quad . \quad (1.3)$$

Another possible assumption as to the effects of the leads is justified in a number of practical cases; this assumption consists in assuming that the distributed characteristics of the leads are constant at all points. If this assumption is made, the connecting leads may be regarded as a uniform transmission line with distributed characteristics, and the results of the theory of transmission lines will be applicable. In the present paper the problem is regarded from this standpoint.

II. Some Results from the Theory of Uniform Transmission Lines.

The behaviour of a transmission line (assumed uniform) is determined by its resistance R, its leakance G, its inductance L, and its capacitance C, all reckoned per unit length of the line.

The propagation constant P of the line is defined by the equation

$$P^2=(R+j\omega L)(G+j\omega C) \quad . \quad . \quad . \quad . \quad (2.1)$$

and its characteristic impedance Z_0 by the equation

$$Z_0{}^2=(R+j\omega L)/(G+j\omega C). \quad . \quad . \quad . \quad (2.2)$$

When applying these results to leads such as are used in radio-frequency measurements, these equations can be simplified, since the insulation is usually good enough to allow the leakance G to be neglected in comparison

with the capacitative reactance ωC, and, also, since the resistance R is generally negligible in comparison with the inductive reactance ωL. To illustrate the latter point, suppose that $\omega = 10^6$, corresponding to a wave-length in air of about 1900 m.; let the leads be two parallel copper wires each 2·03 mm. in diameter (No. 14 S.W.G.), and let their separation be 4 cm. In this case $R = 1{\cdot}08 \times 10^{-4}$ ohm per cm., $L = 1{\cdot}571 \times 10^{-8}$ henry per cm., and $\omega L = 1{\cdot}571 \times 10^{-2}$ ohm per cm.; R can, therefore, be neglected in comparison with ωL.

With these assumptions, equations (2.1) and (2.2) become

$$P = j\omega\sqrt{LC} \quad Z_0 = \sqrt{\frac{L}{C}} \quad . \quad . \quad . \quad . \quad (2.3)$$

In dealing with connecting-leads it is more convenient to express results in terms of the *total* inductance L′ and *total* capacitance C′ of the leads rather than the inductance and capacitance per unit length. If the line be uniform, and if its length be l, $L' = lL$ and $C' = lC$, and equation (2.4) becomes

$$P = \frac{j\omega}{l}\sqrt{L'C'}; \quad Z_0 = \sqrt{\frac{L'}{C'}} \quad . \quad . \quad . \quad . \quad (2.4)$$

If a uniform line of characteristic impedance Z_0 and propagation-constant P is terminated by an impedance Z, then its input impedance Z_s is given by

$$\frac{Z_0}{Z_s} = \frac{\cosh Pl + \dfrac{Z_r}{Z_0}\sinh Pl}{\sinh Pl + \dfrac{Z_r}{Z_0}\cosh Pl} \quad . \quad . \quad . \quad . \quad (2.5)$$

(*v.* Mallett, E., 'Telegraphy and Telephony,' § 39. London, Chapman & Hall, 1929).

This expression may be reduced to a simpler form for cases which are likely to occur in practice. Assuming that the line is uniform, and that the surrounding dielectric is air, $\sqrt{LC} = 1/c$, where c is the velocity of electromagnetic waves *in vacuo*, giving

$$Pl = j\omega l/c = 2\pi jl/\lambda, \quad . \quad . \quad . \quad . \quad . \quad (2.6)$$

where λ is the wave-length (in air) corresponding to the pulsatance ω.

This equation shows that Pl will be small, since l is usually much smaller than λ. We may, therefore, write

$$\cosh Pl = 1 - 3\alpha/2 \; ; \quad \sinh Pl = j\omega\sqrt{L'C'}\,(1-\alpha/2),$$

where

$$\alpha = \frac{\omega^2}{3} L'C' = \frac{4\pi^2}{3} \cdot \frac{l^2}{\lambda^2} = 13{\cdot}16 \frac{l^2}{\lambda^2} \quad . \quad . \quad . \quad (2.7)$$

Remembering that α is small in comparison with unity, equation (2.5) becomes

$$Z_s = \frac{Z_r + j\omega L'(1+\alpha)}{1 - j\omega Z_r C'(1+\alpha)} \quad . \quad . \quad . \quad . \quad . \quad (2.8)$$

In most practical cases α is small and only occurs in terms involving C' and L', and hence it is generally permissible to replace $(1+\alpha)$ by unity. In order, for example that α should be 0·01, l must be about 5·5 m. for $\lambda = 200$ m.; for the same wave-length l must be about 1·7 m., in order that α should be 0·001. For small values of λ, α may, however, become important; if, for example, $\lambda = 20$ m., α is 0·01 if $l = 55$ cm., and $\alpha = 0{\cdot}001$ if $l = 17{\cdot}4$ cm

Referring back to the discussion of equations (1.1) and (1.2), it is seen that the statement as to the smallness of $\omega^2 L'C'$ is justified, and that, if α is neglected, equation (2.8) reduces to equation (1.3). In the case of uniform leads the usual procedure of replacing the distributed characteristics by lumped characteristics is thus justified, except in those cases where the length of leads becomes comparable with the wave-length used in the measurements. An alternative mode of expressing this result is obtained when it is remembered that, when l is small in comparison with λ, the current and potential difference is the same at all points of the leads ; when l, however, is comparable with λ, stationary waves may be formed on the leads and, consequently, the current and potential distribution may no longer be uniform.

An alternative method of deriving equation (2.8) is to replace the leads (regarded as a uniform line) by the equivalent Π and equivalent T. If Z_1 and Z_2 be the impedances constituting the equivalent Π as shown in fig. 3*a*, then (Mallett, *op. cit.* § 39)

$$Z_1 = Z_0 \sinh Pl \; ; \quad Z_2 = \frac{Z_0(\cosh Pl + 1)}{\sinh Pl}.$$

Substituting the values given in equation (2.7), we obtain

$$Z_1 = j\omega L'\left(1-\frac{\alpha}{2}\right);\quad Z_2 = \frac{2}{j\omega C'\left(1+\frac{\alpha}{4}\right)}. \quad . \quad (2.9)$$

The leads may therefore be replaced by the arrangement of inductance and capacitance shown in fig. 3*b*, the value of the inductance L_1 being $L'\left(1-\frac{\alpha}{2}\right)$ and that of the

Fig. 3 *a*.

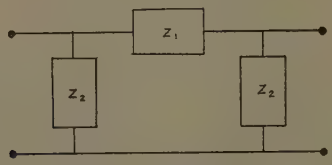

Equivalent Π of leads.

Fig. 3 *b*.

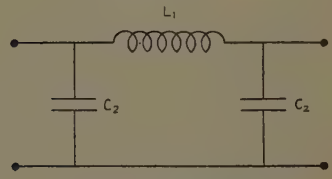

Equivalent Π of leads.
$L_1 = L'(1-\alpha/2)$; $C_2 = \frac{1}{2}C'(1+\alpha/4)$.

capacitances C_2 being $\frac{1}{2}C'\left(1+\frac{\alpha}{4}\right)$. Fig. 3*b* should be compared with figs. 2*a* and 2*b*.

If fig. 4*a* represents the equivalent T, composed of the impedances Z_1 and Z_2, as shown, then

$$Z_1 = \frac{Z_0(\cosh Pl - 1)}{\sinh Pl};\quad Z_2 = Z_0/\sinh Pl,$$

and these equations reduce to

$$Z_1 = \tfrac{1}{2}j\omega L'\left(1+\frac{\alpha}{2}\right);\quad Z_2 = \frac{1}{j\omega C'\left(1-\frac{\alpha}{2}\right)}. \quad (2.10)$$

An alternative equivalent circuit for the leads is thus that shown in fig. 4*b*, the value of the inductance L_1 being $\frac{1}{2}L'\left(1+\frac{\alpha}{2}\right)$ and that of the capacitance C_2 being $C'\left(1-\frac{\alpha}{2}\right)$. It is again interesting to compare this figure with figs. 2*a* and 2*b*.

Replacing the leads by either of these two equivalent circuits, it is easy to obtain equation (2.8) for the

Fig. 4*a*.

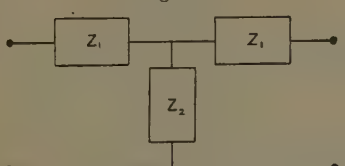

Equivalent T of leads.

Fig. 4*b*.

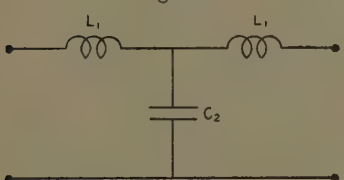

Equivalent T of leads.
$L_1=\frac{1}{2}L'(1+\alpha/2)$; $C_2=C'(1-\alpha/2)$.

input impedance when the leads are terminated by an impedance Z_r.

Two particular cases of equation (2.8) are of interest; they are the cases which correspond to open- and short-circuited leads, and the appropriate values of the input impedance in the two cases can be obtained from equation (2.8) by putting $Z_r=\infty$ and $Z_r=0$ respectively. If Z_{ss} be the effective impedance of the short-circuited leads, then

$$Z_{ss}=j\omega L'(1+\alpha), \quad . \quad . \quad . \quad . \quad (2.11)$$

showing that when α is small in comparison with unity,

the short-circuited leads behave as a concentrated inductance equal to the total distributed lead inductance; this result also shows that, in cases where α is small, L′ can be determined by finding the effective inductance of the leads when short-circuited.

If Z_{so} be the effective impedance of the leads on open circuit,

$$Z_{so}=1/(j\omega C'.\overline{1+\alpha}), \quad . \quad . \quad . \quad . \quad (2.12)$$

showing that, when α is negligible in comparison with unity, the leads behave on open circuit as though they

Fig. 5 *a*.

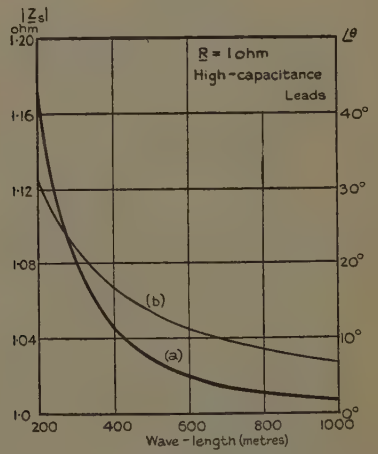

(*a*) Graph of $|Z_s|$ against wave-length.
(*b*) Graph of $\angle\theta$ against wave-length.

were a concentrated capacitance equal to the total lead-capacitance; this result also shows that in such cases it is legitimate to measure C′ by measuring the effective capacitance of the leads when on open circuit.

In the sequel, equation (2.8) will be used to find the effective impedance Z_s of various circuit components when used with connecting-leads. To demonstrate the effect of the leads it is desirable to illustrate the various cases by numerical examples, assuming for this purpose values for different circuit components which are likely to

occur in practice. As regards the leads, the calculations will be carried out with two typical sets, each 20 cm. long; the one set will represent leads of comparatively high capacitance, whilst the other set will be of comparatively high inductance. The high-capacitance leads consist of a wire of 1 mm. radius surrounded by a coaxal cylinder of 1 cm. internal diameter; for this system $C' = 6{\cdot}21_4$ e.s.u) $= 6{\cdot}90_4\ \mu\mu F$. and $L' = 7{\cdot}15_8 \times 10^{-20}$ e.s.u. $= 0{\cdot}0644_2\ \mu H$.

Fig. 5 *b*.

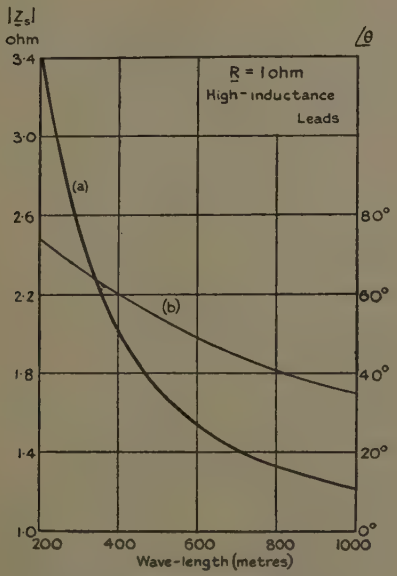

(*a*) Graph of $|Z_s|$ against wave-length.
(*b*) Graph of $\angle\theta$ against wave-length.

The high-inductance leads consist of two straight parallel wires, each 0·6 mm. in diameter and separated by a distance of 3 cm.; for this system $C' = 1{\cdot}08_6$ e.s.u. $= 1{\cdot}20_7\ \mu\mu F$. and $L' = 4{\cdot}09_4 \times 10^{-19}$ e.s.u. $= 0{\cdot}368_5\ \mu H$. These leads, 20 cm. long, give $\alpha = 1{\cdot}3 \times 10^{-5}$ at a wave-length of 200 m. and $\alpha = 5{\cdot}2 \times 10^{-7}$ at a wave-length of 1000 m.; in all cases α may, therefore, be neglected in comparison with unity.

III. Leads terminated by a Resistance.

Let the leads be terminated by a purely ohmic resistance R. Inserting $Z_r = R$ in equation (2.8), we obtain

$$Z_s = \frac{R + j\omega L'(1+\alpha)}{1 + j\omega C' R(1+\alpha)} = \frac{R\{1+3\alpha) + j\omega(L' - C'R^2)(1+\alpha)}{1 + \omega^2 C'^2 R^2 (1+2\alpha)} \quad . \quad . \quad . \quad (3.1)$$

Fig. 6 *a*.

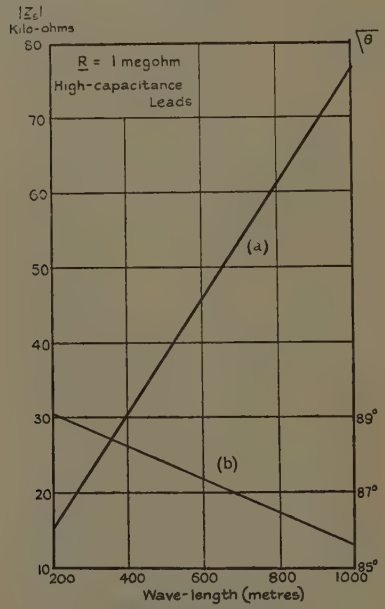

(*a*) Graph of $|Z_s|$ against wave-length.

(*b*) Graph of $\sqrt{\theta}$ against wave-length.

or

$$Z_s = \frac{R + j\omega(L' - C'R^2)}{1 + \omega^2 C'^2 R^2}, \quad . \quad . \quad . \quad . \quad . \quad (3.2)$$

neglecting α.

Figs. 5 *a* and 5 *b* show the variation of the effective impedance of a resistance of 1 ohm when used with the high-capacitance and high-inductance leads respectively. In both cases wave-lengths are plotted as abscissæ, whilst

the modulus $|Z_s|$ (or magnitude) and the phase-angle θ of the impedance Z_s are plotted as ordinates. In the present case the phase-angle θ is positive throughout and the impedance is, therefore, inductive.

Figs. 6*a* and 6*b* similarly show the variation of the modulus and phase-angle of Z_s with wave-length when

Fig. 6 *b*.

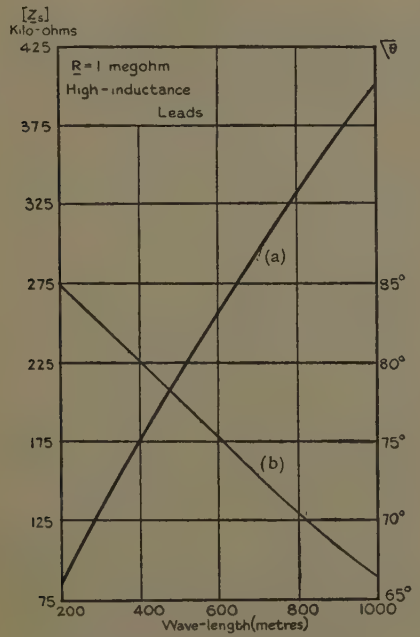

(*a*) Graph of $|Z_s|$ against wave-length.
(*b*) Graph of $\angle\theta$ against wave-length.

the resistance R=1 megohm. In this case the phase-angle θ is negative throughout, and the impedance is, therefore, capacitative.

These figures show very definitely that the leads can produce a very pronounced effect on the value of a resistance when connected in a radio-frequency circuit. The effect of the leads is two-fold: there is a change in the numerical value of the impedance as shown by the

change in the value of the modulus of Z_s, and there is also a change in the phase-angle, a pure resistance with zero phase-angle being converted into an impedance with a positive or negative phase-angle. In the case of the 1 ohm resistance the change is mainly due to the *inductance* of the leads, whilst in the case of the megohm resistance the change is due mainly to the *capacitance* of the leads.

When, therefore, it is desired to introduce a known resistance of small value into a circuit, leads of high capacitance should be used to diminish the disturbing effects of the leads; similarly, leads of high inductance should be used with high resistances.

IV. Leads terminated by an Inductance.

Let the leads be terminated by a coil of inductance L and resistance R. Then $Z_r = R + j\omega L$, which, on substitution in equation (2.8), gives

$$Z_s = \frac{R(1+3\alpha)+j\omega[\{L+L'(1+\alpha)\} \times\{1-\omega^2LC'(1+\alpha)\}-R^2C'(1+\alpha)]}{[1-\omega^2LC'(1+\alpha)]^2+\omega^2R^2C'^2(1+2\alpha)}. \quad (4.1)$$

Neglecting α in comparison with unity, this becomes

$$Z_s = \frac{R+j\omega[(L+L')(1-\omega^2LC')-R^2C']}{(1-\omega^2LC')^2+\omega^2R^2C'^2}. \quad (4.2)$$

This equation can generally be simplified further, since R^2C' is small in comparison with $(L+L')(1-\omega^2LC')$ and since $\omega RC'$ is small in comparison with $(1-\omega^2LC')$. Under these conditions

$$Z_s = \frac{R}{(1-\omega^2LC')^2}+\frac{j\omega(L+L')}{1-\omega^2LC'}. \quad (4.3)$$

For calculations to illustrate the effect of the leads two coils have been chosen. Coil I. is a comparatively low inductance coil; its inductance is $1{\cdot}5\times10^{-16}$ e.s.u. or 0·135 mH. and its resistance 3 ohm. Coil II. is a comparatively high inductance coil, with an inductance of $2{\cdot}222\times10^{-15}$ e.s.u. or 2 mH. and a resistance of 15 ohm. At a wave-length of 200 m. the impedance Z_r of coil I. is

$$3+1{\cdot}27_3\times10^3\,j \equiv 1{\cdot}27_3\times10^3\,\angle 89{\cdot}9^\circ \text{ ohm},$$

whilst at a wave-length of 1000 m. it is

$$3+2{\cdot}54_6\times10^2 j \equiv 2{\cdot}54_6\times10^2 \,/\, \underline{89{\cdot}3^\circ} \text{ ohm.}$$

For coil II., at a wave-length of 200 m., Z_r is

$$15+1{\cdot}88_5\times10^4 j \equiv 1{\cdot}88_4\times10^4 \,/\, \underline{89{\cdot}9_5^\circ} \text{ ohm,}$$

whilst at a wave-length of 1000 m. it is

$$15+3{\cdot}77_0\times10^3 j \equiv 3{\cdot}77_0\times10^3 \,/\, \underline{89{\cdot}8^\circ} \text{ ohm.}$$

The values of the effective impedance Z_s of these coils when used with the high-capacitance and high-inductance

TABLE I.

(a) *High-capacitance Leads.*

Wave-length (m).	Coil.	Z_s (ohms).	L_s (mH).
200	I.	$3{\cdot}56_1+1{\cdot}38_8\times10^3 j \equiv 1{\cdot}38_8\times10^3 \,/\, \underline{89{\cdot}9^\circ}$	$0{\cdot}147_2$
1000	I.	$3{\cdot}01_9+2{\cdot}55_4\times10^2 j \equiv 2{\cdot}55_4\times10^2 \,/\, \underline{89{\cdot}3^\circ}$	$0{\cdot}135_5$
200	II.	$291{\cdot}2 \quad -8{\cdot}30_5\times10^5 j \equiv 8{\cdot}30_5\times10^5 \,/\, \underline{89{\cdot}9_5^\circ}$	$-88{\cdot}1$
1000	II.	$16{\cdot}5_9 \quad +3{\cdot}96_5\times10^3 j \equiv 3{\cdot}96_5\times10^3 \,/\, \underline{89{\cdot}8^\circ}$	$2{\cdot}10_3$

(b) *High-inductance Leads.*

200	I.	$3{\cdot}08_9+1{\cdot}29_4\times10^3 j \equiv 1{\cdot}29_4\times10^3 \,/\, \underline{89{\cdot}9^\circ}$	$0{\cdot}137_3$
1000	I.	$3{\cdot}00_2+2{\cdot}55_3\times10^2 j \equiv 2{\cdot}55_3\times10^2 \,/\, \underline{89{\cdot}3^\circ}$	$0{\cdot}135_4$
200	II.	$24{\cdot}3_1 \quad +2{\cdot}40_0\times10^4 j \equiv 2{\cdot}40_0\times10^4 \,/\, \underline{89{\cdot}9_5^\circ}$	$2{\cdot}54_6$
1000	II.	$15{\cdot}2_6 \quad +3{\cdot}80_5\times10^3 j \equiv 3{\cdot}80_5\times10^3 \,/\, \underline{89{\cdot}8^\circ}$	$2{\cdot}01_8$

leads at wave-lengths of 200 and 1000 m. are given in Table I. in the third column; the fourth column gives L_s, the effective inductance of the leads and coils, in mH.

Before discussing these figures it is convenient to examine whether it is justifiable to neglect $\omega RC'$ in comparison with $(1-\omega^2 LC')$ and R^2C' in comparison with $(L+L')(1-\omega^2 LC')$. Considering $\omega RC'$, it is seen that its value is greatest for coil II. at a wave-length of 200 m. with the high-capacitance leads; for this case

$$\omega RC' = 3{\cdot}08\times10^{-4} \text{ e.s.u.,}$$

whereas $\quad (1-\omega^2 LC') = 2{\cdot}27\times10^{-1}$ e.s.u.

Considering R^2C', this term has its greatest value for coil I. and coil II. with the high-capacitance leads; for this case the value of R^2C' is $6{\cdot}91\times10^{-23}$ e.s.u. for coil I. and $1{\cdot}72\times10^{-21}$ e.s.u. for coil II. The least value of $(L+L')(1-\omega^2LC')$ occurs for both coils at 200 m. with the high-capacitance leads; under these conditions the value of $(L+L')(1-\omega^2LC')$ is $1{\cdot}38\times10^{-16}$ e.s.u. for coil I. and $-5{\cdot}04\times10^{-16}$ e.s.u. for coil II. It is thus clear that both assumptions are justified.

Examining the figures given in Table I., the first point of interest is the behaviour of coil II. at 200 m. with the high-capacitance leads; the coil behaves as a resistance in series with a condenser. The reason for this behaviour is the fact that any circuit, consisting of inductance, capacitance, and resistance in series, behaves as a condenser for wave-lengths less than the resonant wave-length; this is the case here, since the resonant wave-length of the circuit is 221·6 m.

The second point of interest is the fact, evident from equation (4.3), that the leads to a given coil always produce an *increase* in the effective resistance and inductance of the coil. As far as the leads are concerned this increase is mainly due to their capacitance; in equation (4.3) L′ appears in the numerator of the imaginary part as an addition to L, and since L′ is generally much smaller than L, the effect of L′ is very small.

When, therefore, it is required to introduce a known inductance into a circuit, it is necessary to keep the capacitance *of the leads as small as possible; neglect of this precaution can produce considerable increase in the effective constant of the coil, as the above figures show.*

V. Leads terminated by a Capacitance.

Let the capacitance of the condenser be C and its equivalent shunt resistance infinite; then $Z_{p}=-j/\omega C$, and, on substitution in equation (2.8), we obtain

$$Z_s=\frac{1}{j\omega C}\cdot\frac{1-\omega^2CL'(1+\alpha)}{1+\frac{C'}{C}(1+\alpha)}, \quad . \quad . \quad . \quad (5.1)$$

or, if C_s denotes the effective capacitance of the system,

$$C_s = \frac{C+C'(1+\alpha)}{1-\omega^2 L'C(1+\alpha)}$$

or

$$C_s = (C+C')/(1-\omega^2 L'C), \quad . \quad . \quad . \quad (5.2)$$

when α is neglected.

To illustrate the effect of the leads, calculations on two condensers are shown in Table II. Condenser I. is a comparatively small condenser with a capacitance of 50 $\mu\mu$F. or 45 e.s.u., whilst condenser II. is a compara-

TABLE II.

Wave-length (m.)	Condenser.	Effective capacitance C_s (in $\mu\mu$F.).
(a) *High-capacitance Leads.*		
200	I.	56·92
1000	I.	56·90
200	II.	1520
1000	II.	1507
(b) *High-inductance Leads.*		
200	I.	51·30
1000	I.	51·21
200	II.	1579
1000	II.	1504

tively large condenser with a capacitance of 1500 $\mu\mu$F. or 1350 e.s.u.

It is clear from equation (5.2) that L′ and C′ both tend to bring about an increase in capacitance. In the case of the high-capacitance leads the effect of the inductance of the leads is slight, amounting only to about 2 in 1000 in the case of condenser II. at a wave-length of 200 m., where this effect is greatest; the main part of the increase in capacitance is due to the capacitance of the leads. In the case of the high-inductance leads, the effect of L′ is naturally greater than in the former case, especially for a wave-length of 200 m.; it amounts to 2 in 1000 for condenser I. and to about 5 per cent. for condenser II.

For the same leads at a wave-length of 1000 m. the effect of L′ is much smaller, amounting to less than 1 in 10,000 in the case of condenser I. and to 2 in 1000 for condenser II.

We may, therefore, conclude that it is essential to use leads of small capacitance if it be desired to introduce a capacitance of definite value into a radio-frequency circuit.

VI. Leads terminated by a Variable Condenser with a Linear Law.

One particular case of the above is of considerable practical importance—that in which the capacitance in question is a variable air condenser with a linear law connecting capacitance C and angular scale-reading θ. For a considerable portion of its scale a condenser of this type obeys the relation $C=a+b\theta$, where a and b are constants.

Inserting this value of C in equation (5.2), we obtain

$$C_s=\frac{a+C'+b\theta}{1-\omega^2L'(a+b\theta)} \quad . \quad . \quad . \quad . \quad (6.1)$$

If $\Delta C=C_s-C$ be the apparent increase in capacitance due to the leads, we find

$$\Delta C=C_s-C=\frac{C'+\omega^2L'(a+b\theta)^2}{1-\omega^2L'(a+b\theta)} \quad . \quad . \quad . \quad (6.2)$$

In practice, in many cases, the function of a variable condenser is to produce an accurately known *change* in the capacitance of a circuit. In such a case an increase in the value of the capacitance corresponding to zero scale-reading is of no importance, provided that the law of the condenser remains unchanged; this will be the case if ΔC is constant for all values of θ. If, however, ΔC varies with θ, then, in addition to a change in capacitance at zero scale-reading, the law of the condenser will be altered, and the calibration curve, with and without leads, may differ appreciably.

An alternative way of regarding the problem is to calculate the effective slope b_s (*i. e.*, the change in effective capacitance per degree rotation) of the combination of condenser and leads. From equation (6.1) we obtain

$$b_s=\frac{dC_s}{d\theta}=\frac{b}{[1-\omega^2L'(a+b\theta)]^2}, \quad . \quad . \quad . \quad (6.3)$$

if we neglect 3α in comparison with unity. It is clear that the presence of leads always increases the slope of the condenser, this increase depending on the values of ω, L′, and $(a+b\theta)$. For fixed leads and a given wave-length the increase will be greater at the upper end of the condenser scale than at the lower end.

Fig. 7.

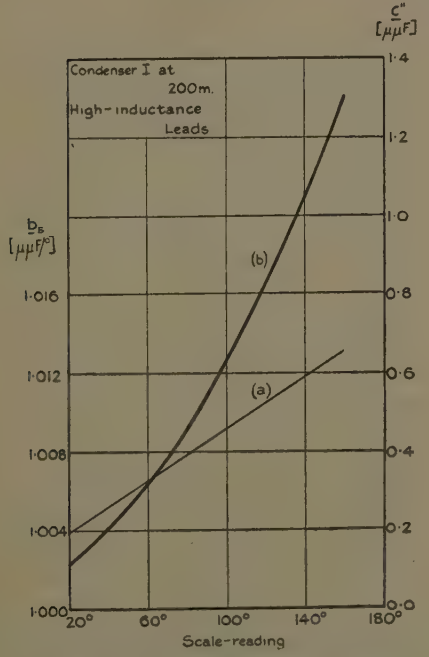

(*a*) Graph of b_s against angular scale-reading.
(*b*) Graph of C″ against angular scale-reading.

It is clear from equation (6.2) that ΔC is constant and equal to C′ if L′ is zero; variation in ΔC with θ is thus due to the *inductance* of the leads. Similarly, equation (6.3) shows that, if L′ is zero, then $b_s=b$, a constant; variation in b_s with θ and λ is, therefore, also attributable to the *inductance* of the leads.

To provide numerical illustration of the effect of the leads it is convenient to consider two condensers, designated as condenser I. and condenser II. respectively. Condenser I. will be a short-range condenser such as would be used at a wave-length of 200 m.; for this condenser we shall assume $a=40\,\mu\mu$F. and $b=1\,\mu\mu$F./degree, and calculation for this condenser will be carried out for a wave-length of 200 m. Condenser II. will be a long-range

Fig. 8.

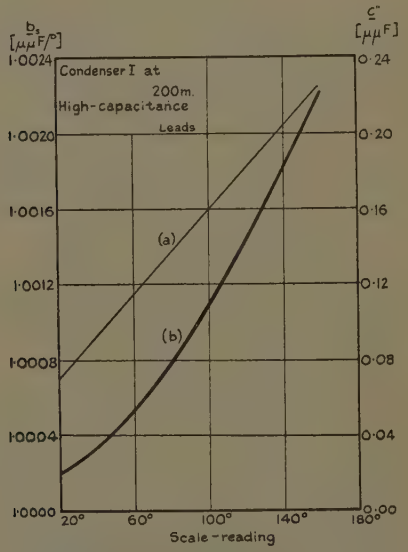

(*a*) Graph of b_s against angular scale-reading.
(*b*) Graph of C″ against angular scale-reading.

condenser such as would be used at a wave-length of 1000 m.; for this condenser we shall assume $a=40\,\mu\mu$F. and $b=7\,\mu\mu$F. per degree, and for this condenser calculations will be carried out for a wave-length of 1000 m. Assuming that the law of these condensers is linear between 20° and 160°, the useful range of condenser I. will be from $60\,\mu\mu$F. to $200\,\mu\mu$F., whilst that of condenser II. will be from $180\,\mu\mu$F. to $1160\,\mu\mu$F.

Figs. 7, 8, 9, and 10 show the results of such calculations. In each case angular scale-readings are taken as abscissæ; curve (*a*) in each figure shows the variation of the effective slope b_s with θ, whilst curve (*b*) shows the variation of $C''=(\Delta C-C')$ with θ. In curve (*b*) $\Delta C-C'$ has been chosen as ordinate rather than ΔC, since the former quantity is the one which is important when a variable condenser is used for producing a known *change* in the capacitance in a circuit; in this case the lead capacitance

Fig. 9.

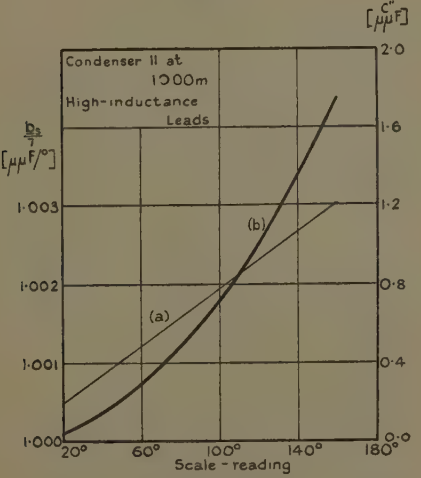

(*a*) Graph of b_s against angular scale-reading.
(*b*) Graph of C'' against angular scale-reading.

C′ acts simply as a permanent addition to the capacitance, affecting only the capacitance corresponding to zero scale-reading. Since $\Delta C-C'$ vanishes when L′ is zero, and depends mainly on L′, this quantity may be termed C″, the increase in capacitance due to the inductance of the leads. Referring to figs. 7 and 8, which relate to condenser I. at a wave-length of 200 m. with the high-inductance and high-capacitance leads respectively, it is clear that the variation of b_s and C″ with θ is greatest in the case of the high-inductance leads. The same remark applies to figs. 9 and 10, which relate to condenser II. at

a wave-length of 1000 m. when used with the high-inductance and high-capacitance leads respectively.

The error which would be introduced if the effect of the inductance of the leads were neglected can be seen by comparing the change in capacitance due to a rotation from 20° to 160°, (1) when the effect of the inductance of the leads is taken into account, (2) when the effect of the lead-inductance is neglected. For condenser I., without leads, the above rotation produces a change of capacitance of 140 $\mu\mu$F.; for condenser II. the change in capacitance

Fig. 10.

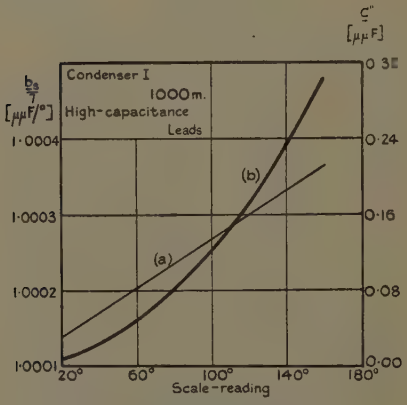

(*a*) Graph of b_s against angular scale-reading.
(*b*) Graph of C'' against angular scale-reading.

is 980 $\mu\mu$F. When condenser I. is used with the high-inductance leads this rotation produces a change of capacitance of 141·19 $\mu\mu$F., an increase of nearly 1 per cent. When the same condenser is used with the high-capacitance leads, the change in capacitance due to the rotation is 140·20 $\mu\mu$F., an increase of about $1\frac{1}{2}$ in 1000. With condenser II., when used with the high-inductance leads, the change in capacitance due to the rotation is 981·72 $\mu\mu$F., an increase of about 2 in 1000; when used with the high-capacitance leads the capacitance change is 980·30 $\mu\mu$F., an increase of about 1 in 3000.

These figures serve to show that the neglect of the effect of the inductance of the leads can lead to serious error unless suitable precautions are taken; the simplest way of avoiding the difficulty is to use short leads of high capacitance per unit length. This procedure will make the inductance L′ *of the leads, and, consequently, the correction* C″ *small.*

Another important practical point relates to the calibration of a variable condenser by the "step-by-step" method (*v.* Moullin, 'Radio-frequency Measurements," p. 311. London: C. Griffin, 1931). In this method a small auxiliary condenser is used to divide the scale of the variable condenser into a number of equal capacitance steps. If the condenser to be calibrated is connected to the remainder of the circuit by leads of finite length, then it is clear from the above discussion that the condenser used for calibration should be connected at the input end of the leads rather than at the variable-condenser end. If, in addition, the condenser to be calibrated is to be used for the measurement of capacitance by the substitution method (Moullin, *op. cit.* p. 307) then the calibrating condenser should be connected to the circuit at the points used in the substitution measurement for connecting the unknown capacitance; by adopting this procedure the effects of the inductance of the leads will be included in the calibration. If the effect of the inductance of the leads is appreciable in any particular case, then the wavelength used for calibration should be kept constant, and different calibrations will be required for different wavelengths.

VII. Leads terminated by Capacitance and Resistance.

Let the leads be terminated by a condenser of capacitance C, whose equivalent shunt resistance is R. Then $Z_r=R/(1+j\omega RC)$, which, on substitution in equation (2.8), gives

$$\frac{1}{Z_s}=\frac{1+j\omega R[C+C'(1+\alpha)]}{R[1-\omega^2L'C(1+\alpha)]+j\omega L'(1+\alpha)} \quad . \quad . \quad . \quad (7{\cdot}1)$$

If C_s and R_s denote the effective capacitance and shunt

resistance of the system, then, neglecting α in comparison with unity, we obtain

$$C_s = \frac{(C+C')(1-\omega^2L'C) - \dfrac{L'}{R^2}}{(1-\omega^2L'C)^2 + \dfrac{\omega^2L'^2}{R^2}}; \quad R_s = R[1-\omega^2L'C]^2 + \frac{\omega^2L'^2}{R^2}. \quad . \quad . \quad . \quad (7.2)$$

The main interest of the case under discussion lies in its application to the measurement of the dielectric constants of liquids at radio-frequencies. If the dielectric-constant of the liquid medium be ϵ and its conductivity be κ (ohm. cm.)$^{-1}$, and if the conditions are such that the medium can be considered to be of infinite extent, then R can be calculated in terms of C, ϵ, κ by the well-known relation $RC = 8{\cdot}84 \times 10^{-14}\, \epsilon/\kappa$, provided that R and C are expressed in a consistent system of units.

Since the terms involving R become important in equation (7.2) when ω and L′ are large and R small, an upper limit to the values of these terms may be obtained by considering the high-inductance leads at a wave-length of 200 m., and assuming the highest value of κ and the lowest value of ϵ likely to occur in practice. For this purpose liquids fall naturally into two classes—pure organic liquids and aqueous solutions. For pure organic liquids κ is usually of the order of 10^{-7} (ohm. cm.)$^{-1}$, and as an upper limit we may assume $\kappa = 5 \times 10^{-7}$ (ohm. cm.)$^{-1}$, whilst the lowest value of ϵ will be assumed to be 2. With aqueous solutions the usual resonant circuit methods fail for highly conducting solutions, and the upper limit of κ likely to occur in practice will be taken as 10^{-3} (ohm. cm.)$^{-1}$, whilst ϵ will be taken to be 80. For the purpose of illustration C will be taken to be 200 $\mu\mu$F., which gives $(1-\omega^2L'C) = 0{\cdot}9935$ and $(1-\omega^2L'C)^2 = 0{\cdot}987$, and $(C+C')(1-\omega^2L'C) = 199{\cdot}9\ \mu\mu$F.

For the organic liquid R = 1768 ohm, $(\omega^2L'^2/R^2) = 3{\cdot}86 \times 10^{-6}$, and $L'/R^2 = 1{\cdot}18 \times 10^{-13}$ F. $= 0{\cdot}118\ \mu\mu$F. It follows, therefore, that in the expression for C_s the denominator may be taken to be $(1-\omega^2L'C)^2$, and that the L'/R^2 term in the numerator is to be retained; in the expression for R_s, $\omega^2L'^2/R^2$ is negligible in comparison with $R(1-\omega^2L'C)^2$. Comparing equations (5.2) and (7.2), it is seen that the effect of the finite conductivity of the dielectric on the effective capacitance is represented in

the present case by the L'/R^2 term in the numerator of equation (7.2), and that its effect amounts to about 1 in 2000 here.

Taking the case of the aqueous solution, it is found that $R=35{\cdot}36$ ohm, giving $(\omega^2L'^2)/R^2=9{\cdot}65\times10^{-3}$, and $L'/R^2=294{\cdot}8\ \mu\mu F.$, which exceeds $(C+C')(1-\omega^2L'C)$, showing that in this case the high inductance of the leads, together with the low shunt resistance of the condenser make the system behave as an inductance rather than a capacitance.

These figures serve to point out the extreme importance of using leads of low inductance and of correcting for their effect when measuring the dielectric constant of aqueous solutions or other partially conducting substances.

It is to be feared that neglect of these precautions in some past determinations of dielectric constants detracts from the values of the results obtained. In some experiments which are now being carried out in this laboratory on dielectric constants this point is being borne in mind.

In conclusion, the author desires to express his sincerest thanks to Vice-Principal Gwilym Owen for his unfailing and constant encouragement and help.

March 1935.

VIII. *The Limaçoidal Heat Conductivity Distribution Function.* *By* W. S. Kimball, *Ph.D., Michigan State College, East Lansing, Michigan* *.

§ 1. *Introduction.*

DISTRIBUTION functions for viscosity and heat conduction have been derived by Chapman † and Enskog ‡, using successive approximations in solving the transport equation and Boltzmann's equation. The present paper employs the geometrical weight § method

* Communicated by the Author.
† S. Chapman, Phil. Trans. Roy. Soc. A, ccxvi. (1916).
‡ Enskog, Inaugural Dissertation, Upsala (1917).
§ W. S. Kimball, Journ. Phys. Chem. xxxv. p. 611 (1931).

that relies on stresses and strains in velocity and ordinary space. Hence the conclusions all rest on Newtonian mechanics and elasticity theory, and probability is just incidental.

We here treat the case of heat conduction through ideal gas at *uniform* pressure. The accuracy is of the same order as the gas law and Maxwell's velocity distribution. Refinements such as the Pauli exclusion principle, van der Waals's equation, the new statistics, and the nature of collisions and gravity are not considered, and large-scale elastic stresses replace any particular law of force between molecules.

New contributions, however, are made in that, first, the present distribution is an exact solution of Boltzmann's continuity equation. The method of solution is the new one first employed in treating the ellipsoidal viscosity distribution *, *i. e.*, it is assumed that the time-rates of change represented by the collision term are exclusively due to "collision forces," whose amount per unit mass replaces the accelerations. Accordingly, when the correct distribution function is fitted into Boltzmann's equation, the latter must reduce to those elementary force equations of Newtonian mechanics applicable to the case in hand. And the test of their applicability is that, when applied to the unstrained Maxwell distribution, it is these very forces that are calculated to distort it so as to maintain the strained distribution. Thus in the case of viscosity eq. (49) † emerging from Boltzmann's equation is the same as (2) †, which is the collision force that shears the unstrained Maxwell distribution over into the ellipsoidal viscosity distribution. Likewise here Boltzmann's equation reduces to (31) and (32), which are aspects of the elementary force expression due to temperature gradient (44) that is calculated to maintain the present limaçoidal distribution.

Secondly, like the new viscosity distribution †, the present one is entirely different *before* impact from what it is *after* impact, the latter involving, in the present case, half the strain of the former. As before, impacts refer to equivalent impacts of negligible time duration, so that velocities *before* impact have zero time and space

* W. S. Kimball, Phil. Mag. xvi. p. 1 (1933).
† Kimball, *loc. cit.* eqs. (2) and (49).

interval intervening *previous* to the next impact, and *vice versa* for velocities *after* impact.

Thirdly, neither mean free paths, on the one hand, nor the intermolecular force factors of Chapman and Enskog, appear in the formulas which depend instead upon the impact strain constant "a" due to temperature gradient, such as is characteristic of the geometrical weight method.

§ 2. *The limaçoidal heat conductivity distribution is the simplest one possible where a temperature gradient exists.*

This distribution is introduced here at the outset, and, starting with the most elementary requirements, it will be shown, step by step, to fit the case in hand. We consider ideal gas in a steady state at uniform pressure with a negative temperature gradient in the positive X direction, but no mass flow. We use polar coordinates in velocity space, measuring the polar angle θ from the x axis, which is the polar axis. Then

$$dn = nf(c,\theta)\, d\omega\, d\rho = nf\, c^2 dc \sin\theta\, d\theta\, d\phi\, d\rho,$$

where

$$nf(c,\theta) = \frac{n}{\alpha^3\pi^{3/2}b(1+\sigma\cos\theta)^4} \exp\left(\frac{-c^2}{\alpha^2(1+\sigma\cos\theta)^2}\right). \quad (1)$$

Eq. (1) gives the number per c.c. of molecules in volume element $d\omega = c^2 dc \sin\theta\, d\theta\, d\phi$ of velocity space that have pursued the ρ-fraction of their free paths (between ρ and $\rho+d\rho$). Here α is the most probable velocity of the unstrained Maxwell distribution at the same temperature T, given by the familiar

$$\tfrac{1}{2}m\alpha^2 = k\mathrm{T}, \quad . \quad . \quad . \quad . \quad . \quad . \quad (2)$$

where k is Boltzmann's constant. The b and σ appearing in (1) are the normalization constant (10) and strain constant (9) discussed below.

Eq. (1) is limaçoidal in that the exponents, when set equal to $-c'^2/\alpha^2$, represent "limaçoids" whose trace in each meridian plane ϕ = constant is the limaçon shown in fig. 1. These surfaces are evidently quartic surfaces

of revolution given in terms of cartesian and polar velocity coordinates by

$$\left.\begin{aligned} c &= c'(1+\sigma\cos\theta), \\ u^2+v^2+w^2 &= c'(\sqrt{u^2+v^2+w^2}+\sigma u), \end{aligned}\right\} \quad . \quad . \quad . \quad (3)$$

where

$$u = c\cos\theta \quad \text{and} \quad c^2 = u^2+v^2+w^2.$$

The parameter c' appearing in (3) and fig. 1 is the radius of the spheres of the unstrained Maxwell distribution.

Note two reasons why the departures from Spherical Symmetry represented by (3) and fig. 1 are seemingly

Fig. 1.

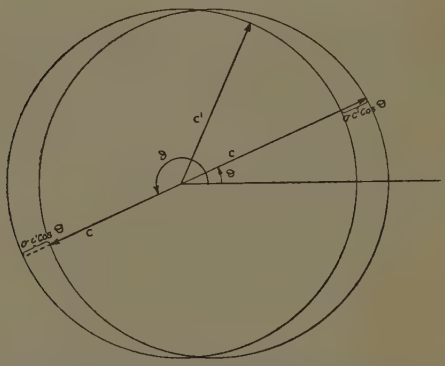

Meridian sections of the strain limaçoids and the unstrained spheres $c'=$const. of the Maxwell distribution.

the simplest possible that are consistent with the obvious facts of a temperature gradient: (*a*) the corrections in the case of velocities coming from hotter or colder parts of the gas than at the plane $x=$constant where (3) and fig. 1 hold must be corrections to velocity magnitudes, since temperature is a scalar quantity independent of agitation velocity direction; (*b*) secondly, these corrections must by symmetry be independent of the meridian angle ϕ, and will depend most simply on $\cos\theta$, with its reversal of sign for opposite directions and zero value for $\theta=\pi/2$. What, then, could be simpler than setting these temperature strains proportional to $\cos\theta$

as in (3), $(c-c')/c' = \sigma \cos\theta$? The limaçoids (3) represent heterogeneous strain, since homogeneous strain implies *linear* relations between the strain displacements and position coordinates, and hence yields a strain ellipsoid or quadric surface instead of the quartic (3). Fig. 2 shows a graph of the number of molecules per unit solid angle as a function of θ and c according to (1), indicating the most probable limaçon, $\beta = \alpha(1+\sigma\cos\theta)$.

Fig. 2.

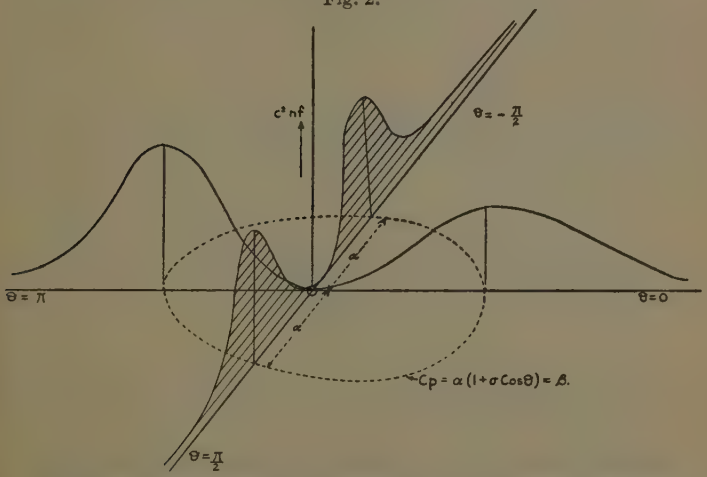

The velocity distribution as a function of c and θ for any meridian angle ϕ, showing maxima on the most probable limaçon β. The ordinates are $c^2\ nf$, the number of molecules per unit solid angle and unit dc are plotted against velocity magnitudes c for different angles θ and with the direction $\theta = 0$ of temperature gradient.

§ 3. *The Five Elementary Requirements.*

These are (*a*) Normal Law, (*b*) Symmetry, (*c*) Normalization, (*d*) Mass Flow is Zero, (*e*) Momentum Flux is the Pressure.

(*a*) Since c appears only in the exponent, and raised to the second power, condition (*a*) is satisfied, and (1) is a solution of equilibrium eqs. (31) of Theorem I.*, taking

$$A(\theta, \phi) = 1/\alpha^3\pi^{3/2}b(1+\sigma\cos\theta)^4$$

and

$$\lambda(\theta, \phi) = \frac{-W}{\frac{1}{2}m\alpha^2(1+\sigma\cos\theta)^2},$$

* W. S. Kimball, *loc. cit.* § 12, p. 24.

so that these equations indicate the elastic modulus,

$$kT(1+\sigma\cos\theta)^2=\tfrac{1}{2}m\alpha^2(1+\sigma\cos\theta)^2$$
$$=\frac{mc_1dc_1}{dr_1/r_1}=\frac{mc_2dc_2}{dr_2/r_2}=\ldots=\frac{mc_\kappa dc_\kappa}{dr_\kappa/r_\kappa}, \quad (4)$$

connecting stress and strain in velocity space. Here the range is the reciprocal of $nf(c)$ given by (1), and eqs. (4) determine the conditional maximum of the geometrical expression for weight,

$$W=n^\kappa(r_1r_2\ldots r_\kappa), \text{ where } r=\frac{1}{nf(c)}=\text{the range.} \quad (5)$$

(*b*) Since the x-direction is that of the polar axis, as well as that of the temperature gradient, (1) must be independent of the meridian angle ϕ, as indicated.

(*c*) When (1) is divided by n, the number of molecules per c.c., we have a probability whose integral must be unity. Integration with respect to c from 0 to ∞ and for ϕ, the meridian angle from 0 to 2π gives

$$\frac{\Delta n}{n}=\frac{\sin\theta\,d\theta\,d\rho}{2b(1+\sigma\cos\theta)} \quad . \quad . \quad . \quad . \quad . \quad (6)$$

for the joint probability of a molecule's having pursued the ρ-fraction of its free path and its inclusion in the solid angle $2\pi\sin\theta d\theta$.

Integrate out the polar angle θ ranging from 0 to π. Thus

$$\frac{\Delta' n}{n}=\frac{1}{2b\sigma}\log\left(\frac{1+\sigma}{1-\sigma}\right)d\rho=\frac{b_\sigma}{b}d\rho \quad . \quad . \quad . \quad (7)$$

is the probability of a molecule's having pursued the ρ fraction of its free path (between ρ and $\rho+d\rho$). Here

$$b_\sigma=\frac{1}{2\sigma}\log\left(\frac{1+\sigma}{1-\sigma}\right)=\frac{\tanh^{-1}\sigma}{\sigma}=1+\frac{\sigma^2}{3}+\frac{\sigma^4}{5}+\frac{\sigma^6}{7}+\ldots \quad (8)$$

To integrate (7) again we set

$$\sigma=a(1+\rho) \quad \text{or} \quad d\sigma=a\,d\rho. \quad . \quad . \quad . \quad . \quad . \quad (9)$$

This assumes two things : first, that the strain constant varies *linearly* with the fraction of the free path pursued, and second, that it is twice as big before impact ($\rho=1$) as after ($\rho=0$).

This latter assumption is required for this distribution by persistence of velocities and the mechanics of collisions, as shown in § 14 below. The *linearity* of the relation (9) between ρ and σ is indicated here as in the case of viscosity *, because distortions $d\sigma$ due to free path shifts of position of molecules at *constant* speeds are calculated to be *proportional* to the fraction $d\rho$ of the path traversed. With the help of (9) we calculate the normalization constant b by integrating (7),

$$b=\int_0^1 b_\sigma d\rho=1+\frac{7a^2}{9}+\frac{31a^4}{25}+\frac{127a^6}{49}+\ldots\frac{(2^{2n-1}-1)a^{2n-2}}{(2n-1)^2}+\ldots. \quad (10)$$

This b is evidently the average of (b_σ), and is expressed in terms of the constant impact strain "a" (see (33), § 9, below), and differs from unity by corrections of the order of 10^{-12} (see (59) below). Eqs. (6)–(10) fulfil requirement (c) above that the quadruple integral of (1) must equal n, the number of molecules per c.c.

(d) The velocity components in the x, y and z directions are given in terms of polar coordinates by

$$\left.\begin{aligned} u&=c\cos\theta,\\ v&=c\sin\theta\cos\phi,\\ w&=c\sin\theta\sin\phi \end{aligned}\right\}\ldots\ldots \quad (11)$$

The product of (1) by each of these will, upon integration, be the corresponding component of mass flow, which turns out to be zero in each case. Thus postulate (d) is satisfied by the integrals (12), which are easily checked.

$$\int uf\,d\omega=\int vf\,d\omega=\int wf\,d\omega=0. \quad \ldots \quad (12)$$

(e) The pressure in the x, y and z directions is given by the corresponding momentum flux. For each of the three directions we have, using (11) and (1),

$$p=\int nmu^2f\,d\omega=\int nmv^2f\,d\omega=\int nmw^2f\,d\omega=\frac{1}{2}\frac{nm\alpha^2}{b}=\frac{nkT}{b}. \quad (13)$$

By dropping $d\rho$ from (12) and (13) we consider all n-molecules per c.c. instead of the number $nd\rho$ having

* W. S. Kimball, *loc. cit.* § 20, p. 36.

pursued at a given time the ρ fractional part of their free paths. Since σ disappears from both (12) and (13) when integrating out the velocity variables, the result is the same as if we retained $d\rho$ and integrated it from 0 to 1, which would merely amount to substituting unity in place of it.

Note by (6) the fact that more molecules travel from cold to hot gas ($\cos\theta$ is minus) than from hot to cold gas ($\cos\theta$ is plus), which is to be expected (see fig. 5) where uniform pressure prevails together with differences in temperature, and hence, also, in molecular density. On the other hand, if we divide (1) by the Δn of (6), we have

$$\frac{dn}{\Delta n} = \frac{2c^3\,dc\,d\phi}{\alpha^3\pi^{3/2}(1+\sigma\cos\theta)^3}\exp\left(\frac{-c^2}{\alpha^2(1+\sigma\cos\theta)^2}\right) = \frac{2c'^2\,dc'\,d\phi}{\alpha^3\pi^{3/2}}\exp\left(\frac{-c'^2}{\alpha^2}\right), \quad . \quad (14)$$

where the right member comes from the left under transformations (3) for c and dc. According to (14) the probability or fraction of Δn included in $d\omega = c^2 dc \sin\theta\, d\theta\, d\phi$ is constant so long as c and dc vary according to (3), keeping c' and dc' constant. Thus the limaçoids (3) are equal probability limaçoids, as well as strain loci.

Eq. (7) involves a significant result in that, for a given $d\rho$, $\Delta n'$ increases with σ. Hence by (9) there is greater molecular concentration at the latter ends of the free paths than at the beginnings, where σ is smaller.

§ 4. *Energy Density.*

One half of each of the integrals (13) gives one component, so that the total *kinetic* energy density for monatomic gas is

$$\mathrm{E} = \int \frac{1}{2} mc^2\, dn = \frac{3}{4}\frac{n\, m\alpha^2}{b} = \frac{3n\,k\mathrm{T}}{2b} = \frac{3p}{2}. \quad . \quad (15)$$

That (15) is independent of ρ and σ, and hence the same before, after, and between impacts, is to be expected under conservation of energy and flux of momentum.

We note the striking fact that (15) is smaller ($b>1$) than the corresponding energy density $\frac{3}{2}nk\mathrm{T}$ of the Maxwell distribution at the *same* temperature.

This is because (1) can be thought of as obtained from such a Maxwell distribution under operation of internal temperature gradient forces (47) discussed below, which will accordingly store a corresponding internal potential energy whose measure is the difference between (15) and $\frac{3}{2}nk\mathrm{T}$, since by the geometrical weight method it is such forces that completely account for the new distribution. Thus the total and the potential internal energy density are given by

$$\left.\begin{aligned} \mathrm{U} &= \frac{3}{2}\,n\,k\mathrm{T} = \mathrm{P}+\mathrm{E} = b\mathrm{E}, \\ \mathrm{P} &= \mathrm{E}(b-1) = \frac{3}{2}\,n\,k\mathrm{T}\left(1-\frac{1}{b}\right) \end{aligned}\right\} \quad . \quad . \quad . \quad . \quad (16)$$

§5. *Energy Flux.*

Energy flux is given by the integral

$$q = \int dn\ \tfrac{1}{2}mc^2u = \int \tfrac{1}{2}mc^3\cos\theta\, dn$$

$$= \frac{4nm\alpha^3\sigma}{3\sqrt{\pi}b} = \frac{8}{3\sqrt{\pi}}p\alpha\sigma, \quad . \quad . \quad . \quad (17)$$

using (1) to replace dn and integrating first with respect to c, then θ, then ϕ, and taking $d\rho$=unity instead of integrating out the σ, *i. e.*, we consider the energy flux of n molecules when they have pursued the ρ fractional part of their several free paths. Also the pressure p given by (13) is introduced into the right member.

If we set $\rho=1$, and hence $\sigma=2a$, referring to the distribution immediately *before* impact, this will include *all* of the heat transfer effects due to extra velocity increments in the x direction, including (*a*) those arising from position shifts of free path extent under temperature gradient conditions, and (*b*) those persisting after the last previous impacts. Thus for $\sigma=2a$ and $\sigma=a$ we have

$$\mathrm{Q} = \frac{16}{3\sqrt{\pi}}p\,a\alpha \quad \text{(before impact)} \quad . \quad . \quad . \quad (18)$$

and

$$\frac{\mathrm{Q}}{2} = \frac{8}{3\sqrt{\pi}}p\,a\alpha \quad \text{(after impact)} \quad . \quad . \quad . \quad (19)$$

Continuity of the energy stream requires these latter quantities to be constants independent of x along the

heat stream, and since we here treat the pressure as uniform, we have

$$a\alpha = \text{constant}; \quad . \quad . \quad . \quad . \quad . \quad (20)$$

also from (17), if ρ is kept constant,

$$\alpha\sigma = a\alpha(1+\rho) = \text{constant}. \quad . \quad . \quad . \quad (21)$$

§ 6. *Entropy.*

To get entropy we use momentum range instead of range in velocity space. Thus each r of (5) is to be multiplied by m^3, and hence we note from (2) that the $\alpha^3\pi^{3/2}$ of (1) is to be replaced by $(m\alpha\sqrt{\pi})^3 = (2\pi mk\mathrm{T})^{3/2}$. Then, using (1) to replace the ranges of (5), we substitute W in Boltzmann's entropy equation,

$$\mathrm{S} = k \log \mathrm{W} = k\Sigma \log (2\pi mk\mathrm{T})^{3/2} b(1+\sigma\cos\theta)^4 + k\Sigma \frac{c^2}{\alpha^2(1+\sigma\cos\theta)^2}. \quad (22)$$

We may evaluate (22). Replace each summation Σ by (1) and integrate, using N instead of n so as to get entropy per mole. When the velocity variables are integrated out there remains, using $\mathrm{R} = \mathrm{N}k$ and $\mathrm{U} = \frac{3}{2}\mathrm{N}k\mathrm{T}$ and (8),

$$d\mathrm{S} = \left[\frac{\mathrm{U}}{\mathrm{T}} + \mathrm{R} \log (2\pi mk\mathrm{T})^{3/2} + \log b + \frac{2b\sigma}{b} \log (1-\sigma^2)\right] d\rho. \quad (23)$$

The only term that varies with ρ is the last one, which is negative (since $\log(1-\sigma^2)$ is minus and other factors plus), and is largest for maximum $\sigma = 2a$ when $\rho = 1$, referring to the distribution just before impact. This continuous decrease in entropy with increasing ρ is the entropy change taking place *between* impacts that compensates the sudden increase of entropy (strain) upon impact. The integration of (23) from $\rho = 0$ to 1, with the help of (8,) (9), and (10), gives

$$\mathrm{S} = \frac{\mathrm{U}}{\mathrm{T}} + \mathrm{R} \log (2\pi mk\mathrm{T})^{3/2} - \mathrm{R}\left(\frac{7}{3}a^2 + a^4(\ ) + \ldots\right). \quad (24)$$

The first two terms of (24) are well known as the entropy for equilibrium conditions and a Maxwell distribution. The last term is accordingly the reduction

in entropy due to temperature gradient distortions. Using $a=10^{-6}$ (see (59)) and R for a mole, we have an entropy reduction of the order of 10^{-5} C.G.S. units.

§ 7. *Temperature.*

The first law of thermodynamics, $dQ=T\,dS=dU+p\,dV$, gives the relation between temperature, entropy, and internal energy U (including both kinetic and potential). Taking $dV=0$, the partial derivative of (24) with respect to U is seen to be $1/T$, so that our T introduced by (2) becomes absolute temperature according to thermodynamics:

$$\frac{\partial S}{\partial U}=\frac{1}{T}. \quad . \quad . \quad . \quad . \quad . \quad . \quad . \quad (25)$$

Note also that eqs. (4) may be given a thermodynamic interpretation:

$$T_\theta=\frac{\partial U}{\partial S}=\frac{b\,mc\,dc}{k\,dr/r}=\frac{bm\alpha^2}{2k}(1+\sigma\cos\theta)^2. \quad . \quad (26)$$

Here the constant b is introduced into (4) so as to give total internal energy differences, for, according to (16), $dU=bdE$; and since θ is kept constant in (4), the ratio is a statistical constant, T_θ, like temperature for a given direction. The average (multiply by dn/n from (1) and integrate) value of (26) is the temperature T given by (2) and (25). Thus absolute temperature introduced by (2) is defined thermodynamically by (25) and checked by the integration of (26).

§ 8. *The limaçoidal distribution is an exact solution of Boltzmann's equation.*

We here employ the new method * of solving Boltzmann's equation †,

$$\frac{d(nf)}{dt}=\Big(X\frac{\partial}{\partial u}+Y\frac{\partial}{\partial v}+Z\frac{\partial}{\partial w}$$
$$+u\frac{\partial}{\partial x}+v\frac{\partial}{\partial y}+w\frac{\partial}{\partial z}\Big)n-\Big(\frac{dnf}{dt}\Big)_{coll}, \quad (27)$$

* W. S. Kimball, *loc. cit.*

† Jeans, 'Dynamical Theory of Gases, eq. (513), p. 208; the negative sign in front of the collision term makes it refer to collision forces (44) rather than the equal and opposite rate of change *between* impact given by (47).

in that we attribute the collision term to collision *forces* whereby (27) reduces, when operating on (1), to the force equations of Newtonian mechanics that are the basis of the present theory. Dropping the zero value terms (we treat a steady state with no force field between impacts, and (1) is independent of y and z), we specialize (27), indicating the rate of change in velocities due to collisions :

$$u\frac{\partial nf}{\partial x}-\left(\frac{\partial nf}{\partial c}\frac{dc}{dt}+\frac{\partial nf}{\partial \theta}\frac{d\theta}{dt}\right)_{\text{coll}}=0. \quad . \quad . \quad (28)$$

Now use (13) to replace n in (1), and rewrite it:

$$nf=\frac{2p\exp\left(\frac{-c^2}{(\alpha+\alpha\sigma\cos\theta)^2}\right)}{m\pi^{3/2}\alpha(\alpha+\alpha\sigma\cos\theta)^4}. \quad . \quad . \quad . \quad (29)$$

Since p is constant by (13) and $\alpha\sigma$=constant by (21), the dependence of (29) on x rests *solely* on the three α's that appear alone in (29).

Now operate on (29) by (28) and get

$$nf\frac{u}{\alpha}\frac{\partial\alpha}{\partial x}\left(\frac{2c^2}{\alpha^2(1+\sigma\cos\theta)^3}-1-\frac{4}{(1+\sigma\cos\theta)}\right)$$

$$=-nf\left[\frac{2c\frac{\partial c}{\partial t}}{\alpha^2(1+\sigma\cos\theta)^2}+\frac{\partial\theta}{dt}\left(\frac{2c^2\sigma\sin\theta}{\alpha^2(1+\sigma\cos\theta)^3}-\frac{4\sigma\sin\theta}{(1+\sigma\cos\theta)}\right)\right],$$

where the right member is the so-called collision term. Factor out nf and introduce $u=c\cos\theta$

$$\frac{c\cos\theta}{\alpha}\frac{\partial\alpha}{\partial x}\left(1-\frac{2c^2}{\alpha^2(1+\sigma\cos\theta)^3}+\frac{4}{1+\sigma\cos\theta}\right)$$

$$=\frac{2c\frac{\partial c}{\partial t}}{\alpha^2(1+\sigma\cos\theta)^2}+\sigma\sin\theta\frac{\partial\theta}{\partial t}\left(\frac{2c^2}{\alpha^2(1+\sigma\cos\theta)^3}\right.$$

$$\left.-\frac{4}{1+\sigma\cos\theta}\right). \quad (30)$$

If we equate the first term of each member we have

$$\frac{dc}{dt}=\frac{\alpha^2}{2}(1+\sigma\cos\theta)^2\cos\theta\frac{d}{dx}\log\alpha. \quad . \quad . \quad (31)$$

$$\theta=\text{constant}.$$

If we equate the last two terms of each member and multiply each by c' we have

$$\frac{dc}{dt} = -c'\sigma \sin\theta \frac{d\theta}{dt} = +cc' \cos\theta \frac{d}{dx}\log\alpha, \quad . \quad (32)$$

$$c' = \text{constant},$$

where the left member of (32) is introduced with the help of (3). Eqs. (31) and (32), be it emphasized, are the so-called "collision forces" per unit mass that depend on temperature gradient as indicated, since α is related to temperature by (2). The way they emerge from Boltzmann's equation under operation of this new method of solution shows how they maintain continuity for the distribution (1). We shall now show them to be aspects of the very force calculated by elementary mechanics to maintain those distortions of a Maxwell distribution at temperature T that are represented by (1).

§ 9. *The Impact Laws of Heat Conduction*: (a) *The impact* strains *due to temperature gradient are the same at a given place for all velocities*; (b) *the various impact* displacements, *in velocity space* due *to temperature gradient, are constants independent of velocity direction and of position along the heat stream.*

Divide (32) by $cc' \cos\theta = c'u = c'\frac{dx}{dt}$:

$$\frac{1}{c'}\frac{dc}{dx} = \frac{d}{dx}\log\alpha = -\frac{a}{\lambda}, \quad . \quad . \quad . \quad . \quad (33)$$

where

$$a = -\lambda \frac{d}{dx}\log\alpha = \frac{\Delta s}{c'}. \quad \text{(The Strain Law.)}$$

The left member is the temperature gradient strain in velocity space dc/c' per unit distance in the x direction, and is shown, by its indicated expression in terms of α, to be independent of the magnitude and direction of the velocities at this place. We write $1/\lambda$ for the number of impacts per unit distance travelled (independent of speed and direction by elementary theory). Then a, the strain per impact (by (9)) due to temperature gradient will fit by definition into (33) as indicated, and be also independent of speed and direction according to the

above impact law (a), which we thus see emerges from Boltzmann's equation.

Multiply (31) by $m\,dx \sec\theta$, introduce $c=\dfrac{dx}{dt}\sec\theta$ and divide by the logarithmic derivative. Then (31) becomes

$$\tfrac{1}{2}m\alpha^2(1+\sigma\cos\theta)^2=\frac{mc\,dc}{d\alpha/\alpha}=\frac{mc_1dc_1}{dc_1/c_1'}=\frac{mc_\kappa dc_\kappa}{dc_\kappa/c_\kappa'}, \quad . \quad (34)$$

which is the same as (4) except that the differentials refer to the extra temperature gradient changes involved

Fig. 3.

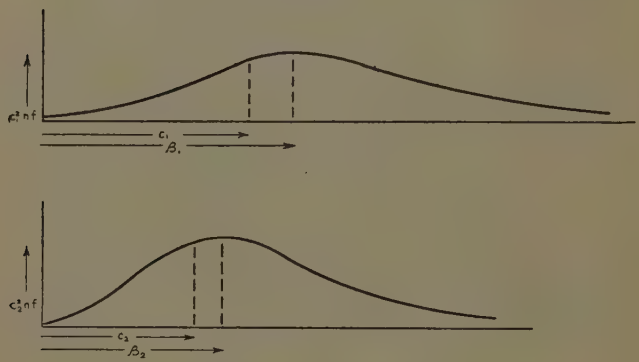

The velocity distribution for a given direction at two successive positions along the heat stream.

in collisions. The right members are introduced with the help of (33), and the equality of the denominators shows how the strain law (33) is required by (31) and (34) as well as (32), and how neatly it fits into the equation (4), giving the stress strain relations that maintain the limaçoidal distribution (1).

The impact changes of (33) may be shown graphically. Thus fig. 3 shows graphs of (1) at two successive positions x_1 and x_2 along the heat stream, plotted against velocity magnitudes.

The ordinates are c^2nf, the number of molecules per unit dc per unit solid angle $d\omega=\sin\theta\,d\theta\,d\phi$ in any meridian plane $\phi=$constant and making angle θ with the polar axis

or x direction. The most probable velocity, $\beta=\alpha(1+\sigma\cos\theta)$, is easily shown to determine the maximum of c^2nf.

Consider only pairs of velocities c_1 and c_2 that satisfy the proportion

$$\frac{c_1}{\beta_1}=\frac{c_2}{\beta_2}=\frac{c_1'}{\alpha_1}=\frac{c_2'}{\alpha_2}, \quad . \quad . \quad . \quad . \quad . \quad (35)$$

where the two right members come from dividing out $(1+\sigma_1\cos\theta)$ and $(1+\sigma_2\cos\theta)$ from the first two members. If we multiply numerator and denominator of the third and fourth members by a_1 and a_2 respectively, the strain constants at x_1 and x_2, we get

$$\frac{c_1'a_1}{\alpha_1 a_1}=\frac{c_2'a_2}{\alpha_2 a_2}. \quad . \quad . \quad . \quad . \quad . \quad (36)$$

But these denominators are equal by (20). Hence for the numerators

$$\Delta s=c_1'a_1=c_2'a_2', \quad \text{or} \quad c'a=\text{constant},$$
$$\text{(The Displacement Law.)} \quad (37)$$

provided the c''s vary according to (35) and fig. 3. Then, also, for a given fraction ρ of free paths traversed,

$$c'\sigma=c'a(1+\rho)=\text{constant}. \quad . \quad . \quad . \quad . \quad (38)$$

Hence, from (38) and (3),

$$\frac{dc}{dx}=\frac{dc'}{dx}. \quad \text{(Subject to (35).)} \quad . \quad . \quad . \quad (39)$$

Now, let $c_2'=c'$ and $c_1'=c'+dc'$, etc. Then from (35) we have

$$\frac{dc'}{c'}=\frac{c_1'-c_2'}{c_2'}=\frac{\alpha_1-\alpha_2}{\alpha_2}=\frac{d\alpha}{\alpha};$$

or, dividing by $dx=x_2-x_1$, and taking account of (39), we have

$$\left.\begin{aligned}\frac{1}{c'}\frac{dc}{dx}&=\frac{dc'}{c'dx}=\frac{d}{dx}\log\alpha=-\frac{a}{\lambda},\\ \text{or}\qquad \frac{dc}{dx}&=\frac{dc'}{dx}=-\frac{ac'}{\lambda}=-\frac{\Delta s}{\lambda}.\end{aligned}\right\} \quad . \quad . \quad . \quad (40)$$

Since (40) is identical with (33), and since the argument can be reversed, the changes indicated by (35) and fig. 2 are identified with the temperature gradient changes

(33) required by Boltzmann's equation. Thus (40) defines, according to these requirements, the space gradient of a velocity magnitude *due* to *temperature gradient*, and the velocity impact displacement $\Delta s = ac'$ is constant by (37) along the heat stream, according to the impact law (*b*) entitling this section.

We thus see, as pointed out in § 1, that (31), (32), and (33) emerging from Boltzmann's equation check eqs. (4), which are the very stress-strain relations required by mechanics to maintain the distribution (1). Furthermore, they, together with Boltzmann's equation, are the foundation on which rests the proof herein of the above :

Fig. 4.

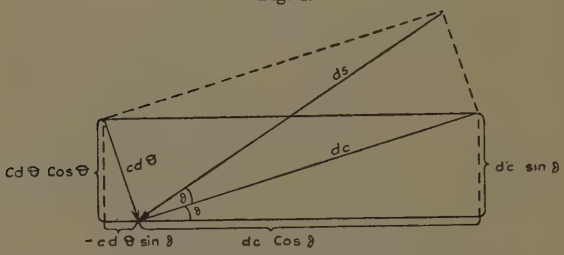

The counterbalancing rates of shear for dc and $c\,d\theta$ arising from collisions.

(*a*) strain law (33), and (*b*) displacement law (37) for velocity changes under temperature gradient conditions at uniform pressure.

§ 10. *Equilibrium of torques requires the collision force to make twice the angle that the velocity does with the direction of temperature gradient.*

The components of dc are shown in the right half of fig. 4, along ($dc \cos\theta$) and across ($dc \sin\theta$), the x direction, which is that of the temperature gradient. If we divide by dx we get the two components of (40); $\frac{dc}{dx}\cos\theta$ is the time-rate of squeeze and $\frac{dc}{dx}\sin\theta$ is the time-rate of shear, which latter we see involves a *counter clockwise*

torque. Since each plane, $x=$const., represents an isothermal velocity distribution, there will be no temperature force to counterbalance this shear within this plane, which, consequently, must be balanced by a change in velocity *direction*, such as indicated by fig. 4 on the left and given by the equality

$$\frac{c\,d\theta}{dx}\cos\theta=\frac{dc}{dx}\sin\theta. \quad . \quad . \quad . \quad . \quad (41)$$

The left member of (41) evidently represents a *clockwise* rate of shear that balances the right member. We see from (41) and fig. 4 that $ds(=\sqrt{dc^2+c^2d\theta^2})$ makes twice the angle that c does with the x direction. Accordingly this will be true for the collision force per unit mass :

$$\mathrm{F}=\frac{ds}{dt}=\frac{ds}{dx}\frac{dx}{dt}=c_1\frac{dc}{dx}\frac{dx}{dt}+\theta_1\frac{c\,d\theta}{dx}\frac{dx}{dt}$$

$$=-\frac{cc'a}{\lambda}(c_1\cos\theta+\theta_1\sin\theta), \quad . \quad . \quad . \quad . \quad (42)$$

where (40) and (41) are used to replace $\frac{dc}{dx}$ and $\frac{c\,d\theta}{dx}$, and c_1 and θ_1 are unit vectors along c and normal to it given in terms of the constant unit vectors i and j by

$$\left.\begin{aligned} c_1&= \ \ i\cos\theta+j\sin\theta,\\ \theta_1&=-i\sin\theta+j\cos\theta.\end{aligned}\right\} \quad . \quad . \quad . \quad . \quad (43)$$

Now substitute (43) in (42) and get

$$\mathrm{F}=-\frac{cc'a}{\lambda}(i\cos 2\theta+j\sin 2\theta)$$

$$=cc'\frac{d}{dx}\log\alpha(i\cos 2\theta+j\sin 2\theta). \quad . \quad . \quad . \quad . \quad . \quad (44)$$

Note from fig. 4 that $dc=ds\cos\theta$. Accordingly we multiply (44) or (42) by $\cos\theta$ to get the vector magnitude (32) ; or multiply both sides of (32) by $\sec\theta$ to get (44). Since Boltzmann's equation is a continuity equation, it can of course supply us only with the force *magnitude*, and so we see that the rates of change (40) to (44) are various aspects of the very same rates of change (31) and (32) emerging from Boltzmann's equation.

Note also from (42) that the constant strain per impact given by (33) has components

$$\left.\begin{aligned} a\cos\theta &= \text{impact squeeze due to temperature,} \\ a\sin\theta &= \text{impact shear due to temperature.} \end{aligned}\right\}. \quad (45)$$

So that the loss in stretch (negative squeeze) from taking $\rho=1$ and $\rho=0$ in (3) and subtracting is

$$\frac{\Delta c}{c'} = \frac{c_1 - c_0}{c'} = a\cos\theta, \quad . \quad . \quad . \quad . \quad (46)$$

whereby (42) checks (3) and (9).

§ 11. *The collision forces are equal and opposite to the corresponding rates of velocity change between impact.*

Where a steady state prevails involving no change in the distribution, say, before impact, then the distortions

Fig. 5.

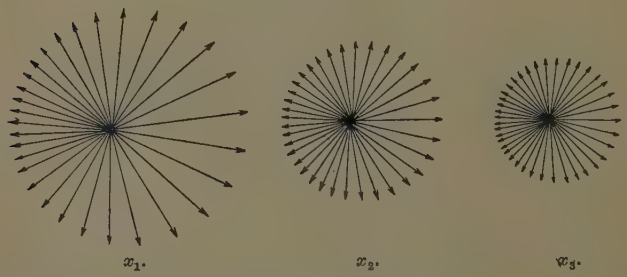

Neighbouring limaçoidal distributions at different temperatures, showing symmetry about the direction of temperature gradient and greater angular spacing as well as greater magnitudes for velocities with positive x components. Note also the increased number of vectors at the lower temperatures where the vectors are small.

of and departures from that distribution *upon* impact indicated by fig. 3 and the collision force (44) will have to be exactly compensated by the occurrences *between* * impacts. We can readily see qualitatively how (44) is compensated by an examination of fig. 5, showing velocity

* This is the "third way" referred to by Maxwell in which changes in a phase element may occur. See his 'Scientific Papers,' ii. p. 681, and section 7, p. 696.

magnitudes and directions at a hot place, x_1, at an intermediate place, x_2, and at a cold place, x_3, along the temperature gradient. The velocity vectors at x_1, which are pointing to the right, will carry molecules down the heat-stream (in absence of impacts) to where x_2 is the abscissa, and those pointing to the left at the cold place, x_3, will take them up stream towards x_2 (in absence of impacts). Thus the effect of free paths (impact absences) upon the distribution at x_2 will be high velocities for molecules coming from the hot side and low velocities for those coming from the cold side. The effect will be maximum just before molecular impact, for at such time the entire free path has been traversed, and hence the kinematical effect of the position change involved in the free trip will be greatest.

A further fact to be noted is that hot, high velocity molecules coming to x_2 from x_1 have greater *angular* spacing in velocity space than those at x_2, because of a smaller number of molecules per c.c. at x_1 than at x_2. This, of course, results from uniformity of pressure, together with temperature differences, making "n" decrease with increase of temperature. Likewise those coming to x_2, from the colder place, x_3, will have *less* solid angular spacing than at x_2.

Thus, mathematically, the velocity shifts at x_2 due to *constant* molecular velocities operating through free paths will involve positive dc and $d\theta$ where θ is acute and molecules come from x_1, and this, we note, is *qualitatively* opposite to the *impact* changes due to temperature gradient shown in fig. 4, involving a negative dc and $d\theta$. That these kinematical shifts are also *quantitatively* opposite to the reactions involved in (44) and shown in fig. 4 follows immediately from the continuity of the steady state as noted at the outset of this section. Accordingly the continuity force or rate of change incident to continuity and due to kinematic shifts of position *between* impacts is a force equal and opposite to (44):

$$\mathrm{F}' = -c\,c'\frac{d}{dx}\log\alpha(i\cos 2\theta + j\sin 2\theta). \quad . \quad . \quad (47)$$

Although (47) refers to changes representable by a graph showing vectors equal and opposite to those shown in fig. 4, yet it does not obviate the necessity for the equality (41) to maintain equilibrium of torques. This

is because the $-\frac{dc}{dx}\sin\theta$ of (47) is a *counter clockwise* torque, which equals the also counter clockwise $\frac{dc}{dx}\sin\theta$ of (40) and (44) shown in fig. 4, and forms with it a couple that can only be compensated by the equal *clockwise* couple made up of the $\frac{cd\theta}{dx}\cos\theta$ and $-\frac{c\,d\theta}{dx}\cos\theta$ of (44) and (47), which represent equal clockwise torques.

§12. *The Field of Force in Velocity Space.*

By elementary theory (41) shows that ψ, the angle between the radius vector c and the curve whose differential equation is (41), is equal to the polar angle itself:

$$\frac{c\,d\theta}{dc}=\tan\psi=\tan\theta, \quad . \quad . \quad . \quad . \quad . \quad (48)$$

and by integration

$$c=\mathrm{D}\sin\theta=\frac{c'}{\sin\theta'}\sin\theta. \quad . \quad . \quad . \quad . \quad (49)$$

Here the constant of integration D is expressed in terms of the coordinates (c', θ') of a point on the unstrained sphere $c'=$const. of a Maxwell distribution. The new strained position (c, θ) comes from displacements along the circular paths (49), which are loci characterized by having their direction make twice as great an angle (2θ) as the radius vector c does with the polar axis or x direction. The forces (44) and (47) act back and forth along these circular paths, which are the *lines* of *force* in velocity space. The diameter of each circular path is evidently $\mathrm{D}=c'/\sin\theta'$, and their ensemble (for each meridian plane $\phi=$const.) constitutes a one-parameter family of circles (D=the parameter), which is the *field* of force in velocity space due to (44) and (47). The smaller circles of fig. 6 are the circular paths (49) for the indicated (c', θ') or for any other pair of velocity coordinates giving the same $\mathrm{D}=c'/\sin\theta'$, and fig. 7 shows part of the family of circles (49) for the same c' but a series of D's. The part shown is that which is included *between* the two limaçoids (3) taking $\rho=1$ or 0 referring to the strain before and after impact. So far as temperature gradient changes are concerned (*i. e.*, when c' is constant), each molecule

or point in velocity space pursues the paths of fig. 7 back and forth from one to the other of the limaçoids (3) along the paths (49). By keeping c' constant, we restrict attention to temperature gradient strains and rule out random jumps. The arrows with points on the after

Fig. 6.

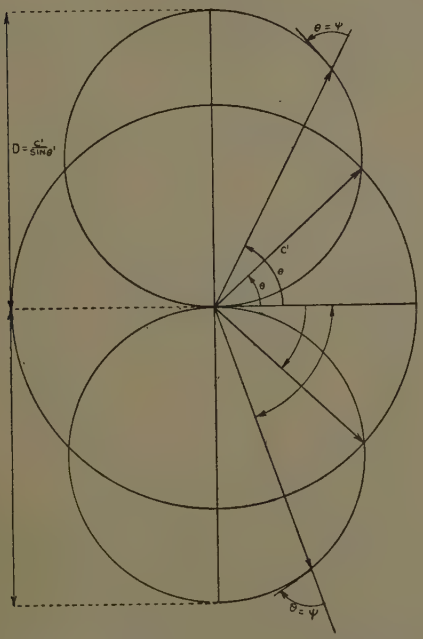

The circular force path (49) in velocity space.

impact limaçoid of strain "a" indicate the molecular shifts of position under (44), representing the excess collision force due to temperature gradient, and the arrows with points on the before impact limaçoid of strain $2a$ indicate the equal and opposite shifts involved in the redistribution incident to free trips at constant speed *between* impacts from hotter and colder places

more or less distant, being the time rates of change referred to by (47).

§ 13. *The Transformation of Phase Volume Element under Temperature Gradient Forces.*

Eliminate the c''s from (49) by using (3). Then

$$\frac{\sin\theta}{1+\sigma\cos\theta}=\sin\theta' \quad . \quad . \quad . \quad . \quad . \quad (50)$$

is the angular shift of position under temperature forces, which we see depends on σ, and hence ρ, the fraction of

Fig. 7.

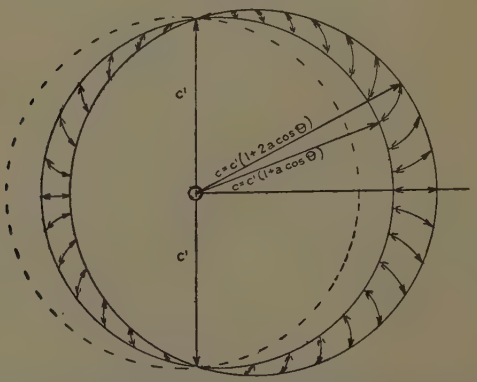

The field of force in velocity space traversed by molecules under temperature gradient forces (c'=const.) along the circular paths (49) between the before and after impact limaçoids for various values of θ.

the free path traversed. Accordingly the probability of a molecule's inclusion in solid angle $2\pi\sin\theta\,d\theta$ will be tied up with the fraction of the free paths traversed, and we have

$$\frac{\sin\theta\,d\theta\,d\rho}{2b(1+\sigma\cos\theta)}=\frac{\sin\theta'\,d\theta'\,d\rho'}{2}=\frac{\Delta n}{n} \quad . \quad . \quad (51)$$

for the fraction (or probability) of molecules included in such a solid angle, and having traversed the ρ or ρ' fractional part of their free paths, where b is the normalization constant (10) above. The left member checks (6)

above, and since (49), (50), and (51) specify the force field and angular shifts of position, due to forces (44) and (47), we see that (1) and (6) (which is (51)), also represent this force field.

Note that (51) also gives the transformation of a fixed fraction out of n molecules of an unstrained Maxwell distribution to the new solid angular position and $d\rho$ under the distribution (1) as a one-to-one correspondence reached under operation of forces (44) and (47) along lines of force (49). We have seen by (46) that (3) gives the velocity magnitude shifts due to these forces, so that (3), when combined with (51), taking $\phi=\phi'$ by symmetry, gives the transformation of volume elements due to (44):

$$\frac{c^2 \sin\theta\, dc\, d\theta\, d\phi\, d\rho}{b(1+\sigma\cos\theta)^4} = c'^2 \sin\theta'\, dc'\, d\theta'\, d\phi'\, d\rho'. \quad . \quad (52)$$

It is readily seen that a Maxwell distribution at temperature T given by (2) transforms under (3) and (52) into (1). Now (3) and (52) are the very transformations caused by the mechanical operation of forces (44) and (47), which in turn check the forces (31) and (32) arising from Boltzmann's continuity equation. Thus mechanics and continuity check one another in confirming the correctness of (1).

§14. *The Mechanics of Collisions.*

By symmetry the integral of the components of (44) across the heat stream is zero. In the x direction, however, we get a temperature gradient stress. The sum of the x components of this collision force for all molecules in unit volume needs to be divided by $1/\lambda$, the number of impacts per unit length, to give the ensemble effect or unit face of unit cube. Thus, to get the temperature gradient stress, first multiply (44) by $m\cos 2\theta$ to get the x component of force per molecule, then *divide* by $1/\lambda$ and integrate, using (1):

$$\left.\begin{aligned} f = -\int mcc'a\cos 2\theta\, dn = -ma\int \frac{c^2\cos^2\theta\, dn}{(1+\sigma\cos\theta)} \\ +ma\int \frac{c^2\sin^2\theta\, dn}{(1+\sigma\cos\theta)} \\ = -pa+2pa = f_c+f_\theta = pa, \end{aligned}\right\} \quad (53)$$

where $f_c=-pa$ and $f_\theta=2pa$.

Comparison of the integrand of (53) with (42) shows how the first integral gives the impact stress due to changes in velocity magnitude dc as indicated by the subscript, whereas the second one refers to impact changes in velocity direction $d\theta$ due to temperature gradient. f_c and f_θ are sums of the stretch and shear components respectively of the arrows with points on the after impact limaçoid of strain "a," shown in fig. 7, which makes plain why the ensemble of the former is negative and of the latter positive.

This stress (53) is of course balanced by an equal and opposite stress due to (47) (the arrows with points on the before impact limaçoid of strain $2a$ of fig. 7) that represents those rates of change involved in kinematical shifts of molecular position resulting from free trips under temperature gradient conditions, according to fig. 5. Also note the striking fact that the elastic modulus for (53) is again the pressure, as shown in so many cases * where the geometrical weight method has been applied.

To find the time-rate of doing work by these stresses multiply the integrand of each by the speed c and integrate:

$$W_c = -\int \frac{am\,c^3 \cos^2\theta\, dn}{(1+\sigma\cos\theta)} = -\frac{8}{3\sqrt{\pi}} p\,a\alpha = -\frac{Q}{2}, \qquad (54)$$

$$W_\theta = \int \frac{am\,c^3 \sin^2\theta\, dn}{(1+\sigma\cos\theta)} = \frac{16}{3\sqrt{\pi}} p\,a\alpha = Q. \quad . \quad . \quad . \quad (55)$$

(a) *Conservation of Energy.*—The rate of energy supply before impacts is given by (18) above (it equals (55)), and the rate of discharge after impact is given by (19) above. Their difference will be the rate of consumption of energy in doing the work of impacts represented by the arrow shifts of fig. 7 which work, in turn, is the sum of (54) and (55):

$$Q - \frac{Q}{2} = W_c + W_\theta = \frac{Q}{2}. \quad . \quad . \quad . \quad . \quad (56)$$

(b) *Action and Reaction.*—The consequence of impacts on (1) is a reduction, $-a\cos\theta$, in the strain of (3) as σ

* W. S. Kimball, *loc. cit.*, item 4, section 26.

changes from $2a$ to a, according to (9). Another consequence of impacts is the special *after* impact case of (1), where $\sigma=a$, representing a strain $+a\cos\theta$ in (3) at any place (c, θ, ϕ) in velocity space. That these strains are equal and opposite is a case of action and reaction, the one being a departure from what (1) was *before* impact when $\sigma=2a$, and the other an equal and opposite departure, from the equilibrium distribution of Maxwell, applicable in case of no disturbance such as excess collision reactions. The former effect is summed into (54) and the latter into (19). Thus, for action and reaction we have their sum equal to zero:

$$W_c+\frac{Q}{2}=0. \quad . \quad . \quad . \quad . \quad . \quad . \quad (57)$$

(c) *Equilibrium of torques requires equipartition of energy.*

We have seen by (42) that the integral (55), $W_\theta=\int f_\theta c\,dn$, refers to forces normal to c and required by equilibrium of torques as shown in fig. 4, whereas (54) refers to forces in direction c. The fact that (55) is twice (54) is a case of equipartition, since the former gives the rate of energy supply to the two angular degrees of freedom and the latter to the radial degree of freedom. And since (55) springs directly from (41), the torque equilibrium equation, we see how the latter causes equipartition for the case in hand. The same conclusion comes from considering the degrees of freedom for cartesian coordinates. Thus $c'am$ is by (37) the momentum increment per impact due to temperature gradient, whose components in the x, y, and z directions are given when multiplied by $\cos\theta$, $\sin\theta\cos\phi$, $\sin\theta\sin\phi$, and the corresponding force components per molecule (molecular flux of momentum) are given when each again is multiplied respectively by u, v, or w according to (11). And the corresponding rates of energy supply per degree of freedom emerge when each is multiplied by the time-rate of molecular arrival, c, and the integration performed. Thus, using (11), we may write (54) and (55),

$$\left.\begin{aligned} -W_c=W_x=\int am\,c'u^2\,du=\frac{Q}{2}, \\ W_\theta=W_y+W_z=\int am\,c'(v^2+w^2)dn=Q, \end{aligned}\right\} \quad . \quad . \quad (58)$$

which show the equipartition of energy supply rate as it is required by equilibrium of torques.

(*d*) *Persistence of Velocities**.—Note that, as the strain σ of (3) drops upon impact from $2a$ to a, the velocity excesses are exactly halved according to Jeans's persistence of velocities, which results in (19) being half of (18).

§ 15. *The Conductivity Coefficient and the Experimental Check.*

From (33) and (2) we have

$$a=-\frac{\lambda}{2}\frac{1}{T}\frac{dT}{dx}=-\frac{1}{6}10^{-7}\frac{dT}{dx}. \quad . \quad . \quad . \quad . \quad (59)$$

taking $\lambda=10^{-5}$ and $T=300°$. Thus it appears that the strain a is ordinarily about one-millionth in order of magnitude as given here for a gradient of 60° per cm. Thus second and higher power terms in expansions like (10) are highly negligible, and b is almost unity.

We may replace p and a in (18) by (13) and (59), and the remaining α can be replaced by $\bar{c}$, using

$$\bar{c}=\frac{1}{n}\int c\,dn=\frac{2\alpha}{\sqrt{\pi}b}. \quad . \quad . \quad . \quad . \quad . \quad (60)$$

Then in place of (18) we get

$$Q=-\frac{4}{3}n\lambda\bar{c}k\frac{dT}{dx}. \quad . \quad . \quad . \quad . \quad . \quad . \quad (61)$$

Hence the conductivity coefficient is

$$K=\frac{4}{3}n\lambda\bar{c}k=\frac{8}{9}n\lambda m\bar{c}C_v, \quad . \quad . \quad . \quad . \quad (62)$$

where $mC_v=3k/2$ is the specific heat per molecule.

To get the "crucial ratio" used to check these theories, divide (62) by the product of C_v and $\eta=\frac{\pi}{8}n\lambda m\bar{c}$, the viscosity coefficient given† by the geometrical weight method.

$$\epsilon=\frac{K}{\eta C_v}=\frac{64}{9\pi}=2{\cdot}263+\ldots\ldots \quad . \quad . \quad (63)$$

* Jeans, *loc. cit.* sec. 371, p. 275.
† Kimball, *loc. cit.*

This ratio, smaller than the 2·5+ given by Chapman and Enskog, seems to check reliable data for monatomic gas within the limits of experimental error, especially at low temperatures *. These data indicate uncertainty of the order of magnitude of the difference between (63) and the 2·5+ of Chapman and Enskog. If this is attributed to a very likely cause, such as leakage in heat-conduction measurements, then the indication is that the smaller values of ϵ like (63) are the more accurate.

§16. *Uniqueness of the Limaçoidal Distribution.*

Not only does (1) fulfil the five elementary requirements (*a*) to (*e*) of §3, but it is an exact solution of Boltzmann's continuity equation, whereby it yields a collision-force expression (44) which is the very one required by Newtonian mechanics to distort an unstrained Maxwell distribution into the strained distribution (1), according to the transformations (3), (50) and (52). This is a very exacting requirement, whereby Newtonian mechanics checks continuity. Not only this, but (1) also meets the requirements (*a*) to (*d*) of the mechanics of collisions as shown in § 14, and which are :—

Conservation of Energy, Action and Reaction, Equilibrium of Torques, Equipartition of Energy, and Persistence of Velocities.

It is of interest to note what happens when we choose a different strain constant instead of (9), *i. e.*, $\sigma = a(1{\cdot}2+\rho)$ so as to increase (18) to 1·1 Q. This latter results since now the *after* impact strain $\sigma_1 = 2{\cdot}2\,a$, instead of $2\,a$, though still keeping $a = \sigma_1 - \sigma_0 = 2{\cdot}2\,a - 1{\cdot}2\,a$ as the impact strain or difference between σ before and after impact. This also makes (61), (62), and (63) larger by the same 10 per cent. factor. This would bring the crucial ratio (63) up to the value 2·5+ derived by Chapman and Enskog. Such a change would not affect the five elementary requirements discussed in §3, nor would it impair the exactness of our solution of Boltzmann's equation nor interfere with any formulas except (18) and (19) and those dependent on them. Since the impact strain $\sigma_1 - \sigma_0 = a$ would be the same as before, the force equations and rate of doing work expressions (54), (55),

* Jeans, *loc. cit.* sec. 402, p. 300.

and (58) would be the same. Even the conservation of energy expression (56) would still hold, since

$$1{\cdot}1\,\mathrm{Q}-\frac{1{\cdot}2\,\mathrm{Q}}{2}=\frac{\mathrm{Q}}{2}$$

as before. But Action and Reaction given by (57) would be upset since

$$\mathrm{W}_c+1{\cdot}2\left(\frac{\mathrm{Q}}{2}\right)\neq 0.$$

In other words, the *after* impact distribution ($\sigma=1{\cdot}2a$ and $\rho=0$) would have a velocity increment $+c'a\,(1{\cdot}2)\cos\theta$ *not* equal and opposite to the reduction in velocity $-c'a\cos\theta$ due to impacts, and it is, seemingly, required by action and reaction that these two after effects of impacts shall be equal and opposite. For this reason the crucial ratio is required by action and reaction to be (63) instead of the 2·5 given by Chapman and Enskog, which latter is too large, since it leads to the inequalities

$$\left.\begin{aligned}\mathrm{W}_c+1{\cdot}2\,\frac{\mathrm{Q}}{2}\neq 0,\\ -ac'\cos\theta+1.2ac'\cos\theta\neq 0\end{aligned}\right\}\quad\ldots\quad(64)$$

instead of (57).

In this connexion note from the last paragraph the striking fact that (1) is not uniquely determined unless we rely on Action and Reaction given by (57), which requires the strain σ given by (9) to range from a to $2a$. That is, it is not enough that a distribution shall satisfy the five elementary requirements (*a*) to (*e*) of § 3, even though, in addition, it is an exact solution of Boltzmann's equation, and meets the exacting requirements of conservation of energy and is derived from Newtonian forces arising out of Boltzmann's equation. Besides all this, it will not be unique unless it provides a distribution *before* impact differing from that *after* impact in such a way as to meet the requirements of action and reaction involved in the dynamics of collisions. For all the above requirements save the latter are met by *any* strain constant so chosen to make σ have values before and after impact that differ by the impact strain $a=\sigma_1-\sigma_0$, while the latter requires that $\sigma_1=2a$ and $\sigma_0=a$.

As a further aspect of this action and reaction requirement (*b*) that determines the range of σ, note that the

shearing forces causing (55) are always at right-angles to the forces of (54) that cause stretch and squeezing strains. The reactions to these must then be independent, and hence they represent independent sources of energy supply. Accordingly we note from (55) that W_θ equals the entire heat energy supply from the left or hot direction, whereas (54) represents in magnitude the independent quantity coming negatively in the opposite direction from the right. Furthermore, the left members of these two equations are unchanged so long as the difference between the before and after impact strain is $a=\sigma_1-\sigma_0$, whereas the two right members depend for their correctness on the values for the strain, σ being separately, precisely $2a$ and a before and after impact, respectively. The uniqueness of (9) in ranging from a to $2a$ is thus required by the independence of orthogonal forces being necessary to make the rates of work of (54) and (55) equal $-Q/2$ and Q as indicated.

§17. *Conclusions.*

1. When Newtonian mechanics and elasticity theory are relied upon according to the geometrical weight method, the heat conductivity distribution function for the uniform pressure case takes the form

$$f=\frac{1}{\alpha^3 b\pi^{3/2}(1+\sigma\cos\theta)^4}\exp\left(\frac{-c^2}{\alpha^2(1+\sigma\cos\theta)^2}\right), \quad . \quad (1)$$

where the temperature is given in terms of α by the familiar $k\mathrm{T}=\frac{1}{2}m\alpha^2$ and b is related to the impact strain "a" according to (10), whereas σ is a variable strain that obtains between impacts.

2. This distribution is limaçoidal in that the exponents, when set equal to the constants $\frac{-c'^2}{\alpha^2}$, are loci of heterogeneous strain in velocity space, being equal probability "limaçoids" of revolution symmetric about the direction of the temperature gradient, and whose trace in each meridian plane is the limaçon $c=c'(1+\sigma\cos\theta)$ given by (3) and fig. 1.

3. These limaçoids represent strains in velocity space due to forces like (44) making twice as great an angle

with the temperature gradient direction as the velocity vector does. This doubling of the angle θ results from the balance of torques (fig. 4) as well as forces.

4. The field of force in velocity space due to these forces is a one-parameter family of circles (in each meridian plane) of diameter $D=c'/\sin\theta'$ (fig. 6). Molecules of a spherically symmetric Maxwell distribution are displaced along these circular paths in velocity space under operation of *temperature gradient* forces like (44), according to transformations (3), (50), and (52) (whereby random jumps are excluded) till they reach corresponding positions on the limaçoids (3) of the distribution (1).

5. The distribution (1) comprises a single infinity of distributions, one for each group of molecules having traversed the ρ fractional part of their several free paths since last previous impact. These distributions differ by each one's characteristic amount of strain $\sigma=a(1+\rho)$, which varies from $\sigma=a$ just after impact ($\rho=0$) to $\sigma=2a$ just before impact ($\rho=1$). Also the molecular concentration along the free paths increases with ρ according to (7) from its least value just *after* impact to its maximum value just *before* impact. As impacts take place and are compensated by free path shifts of position, a molecule's motion under temperature gradient forces (exclusive of random jumps) is back and forth along the circular lines of force (fig. 7) between the after and before impact limaçoids under operation of the forces (44) and (47).

6. The limaçoidal distribution (1) represents two basic laws of impacts: (*a*) a strain law, and (*b*) a displacement law :—

(*a*) At a given place in the gas the temperature gradient strain per impact $a=\Delta s/c'$ given by (33) is a constant magnitude for all molecular speeds and directions, being related to temperature gradient by $a=-\frac{\lambda}{2T}\frac{dT}{dx}$, and having numerical value ordinarily about one-millionth This impact strain makes twice the angle that the velocity does with the direction of the temperature gradient.

(*b*) The impact displacements (37) of the strain law $\Delta s = ac'$ *due* to temperature gradient are constants, independent of temperature and position along the heat stream. Thus the increases of "a" as temperature falls are in inverse proportion to the lowering of the agitation velocity c' along the heat stream.

7. The total internal energy $U = \frac{3}{2}nkT$ is the same as that of the unstrained Maxwell distribution at the same temperature from which (1) is obtained under the strain law (33). But the *kinetic* energy density, which is still $\frac{3}{2}p$, and the pressure $p = nkT/b$, being the flux of momentum, are smaller by the factor $1/b$, and the internal potential energy due to the strains represented by the strain law is $P = U - \frac{3}{2}p = \frac{3}{2}\frac{nkT}{b}(b-1)$.

8. The entropy per gram molecule is less by about 10^{-5} C.G.S. units than under equilibrium conditions at the same temperature, as is to be expected, since the latter involve maximum strain (entropy).

9. To a degree of accuracy corresponding to the gas law and Maxwell's velocity distribution, the limaçoidal distribution (1) meets the following requirements :—

First, the five (§ 3) elementary requirements are met :—

(*a*) Normal law.

(*b*) Symmetry.

(*c*) Normalization.

(*d*) Mass flow is zero.

(*e*) Pressure is the momentum flux.

Secondly, it is an exact solution of Boltzmann's equation, which yields precisely the collision forces (44) calculated to strain a Maxwell distribution over into (1) under temperature gradient conditions. Thus continuity and mechanics check one another.

Thirdly, the mechanics of collisions that cause (1) to change from a distribution before impact of strain

$2a$ to one of strain "a" after impact, is shown to be in accord with :—

(a) Conservation of energy.

(b) Action and reaction.

(c) Equilibrium of torques.

(d) Equipartition of energy.

(e) Persistence of velocities.

10. The *uniqueness* of the distribution (1) is closely tied up with action and reaction and the independence of orthogonal forces. Equilibrium of torques represents equipartition of energy for the case in hand.

11. The collision force (44) emerging from the collision term of Boltzmann's equation yields, upon integration, a temperature gradient stress (53), $f=pa$, proportional to the impact strain a, indicating the pressure as the elastic modulus *, as it is also in the case of viscosity and so many other stress-strain relations applicable in gas theory. This stress is counterbalanced by the rates of change and stresses like (47) representing free molecular trips *between* impacts.

12. The heat conductivity coefficient is

$$\mathrm{K}=\frac{8}{9}n\lambda mc\mathrm{C}_v=\frac{4}{3}n\lambda k\bar{c},$$

and the ratio between it and the product of the specific heat and viscosity coefficient (by the geometrical weight method) is

$$\epsilon=\frac{\mathrm{K}}{\eta\mathrm{C}_v}=\frac{64}{9\pi}=2{\cdot}263.$$

The mechanics of collisions, especially action and reaction, is shown to require this value for the accuracy in question in case of monatomic gas, indicating that the 2·5+ of Chapman † and Enskog ‡ is too large. If the uncertainty in the experimental data, which is of the order of magnitude of the difference between 2·5 and 2·263, were attributed to leakage in heat-conduction measurements, the smaller value of ϵ would be indicated as the more accurate.

* Kimball, *loc. cit.* (see eq. (91), p. 44 ; see also item 4, p. 49).
† Chapman, *loc. cit.*
‡ Enskog, *loc. cit.*

IX. *The Cataphoresis of Particles of the Fatty Acids and Related Compounds.* *By* T. Alty, *D.Sc., Professor of Physics, and* O. Johnson, *M.Sc., University of Saskatchewan, Canada* *.

Introduction.

THE cataphoretic mobility of colloidal particles and suspensions of various kinds is generally considered to be due to the presence of a double electric layer surrounding each particle of the suspension, the inner layer being more or less rigidly attached to the particle and the outer one having the form of a diffuse cloud in the surrounding liquid. Thus each charged particle is surrounded by an excess of ions of opposite sign, just as in the Debye-Hückel theory of strong electrolytes [1], and this theory gives an expression for the velocity of the particles in an electric field in the form

$$v = \mathrm{C}.(\mathrm{D}\mathrm{X}\zeta/\eta),$$

where ζ is the potential difference across the double layer, D and η the dielectric constant and the viscosity of the surrounding liquid, X the electric field strength, and C is a constant varying with the shape of the particle. Henry [2] has also derived the equation for the velocity and has criticized Debye and Hückel's conclusion regarding the dependence of C on particle shape. He shows that for an insulating particle C is independent of particle shape and has the value $1/4\pi$, while for a particle having the same conductivity as the surrounding medium Debye and Hückel's formula is valid. Consequently, for an *insulating* particle of any shape, we may write

$$v = \mathrm{D}\mathrm{X}\zeta/4\pi\eta. \quad . \quad . \quad . \quad . \quad . \quad . \quad (1)$$

There are two views of the origin of the double electric layer. The first ascribes the charge to the preferential adsorption of ions of one sign on to the particle surface, leaving an excess of ions of the other sign in the liquid, while the second view is that some of the molecules in the surface of the particle dissociate, one ion remaining on the particle and the other leaving it and entering the liquid. If the substance of which the particle is formed

* Communicated by the Authors.

is very inert, and does not readily dissociate, we might expect any charge appearing on its surface to be due to adsorption, while, if it is readily dissociated, this dissociation would be expected to be the origin of the charge.

In the present work a systematic examination has been made of the electrokinetic properties of the fatty acids and some related compounds. The physical and chemical properties of these substances have been investigated in great detail in recent years, so that the size, shape, etc., of the molecules are known with considerable accuracy. They therefore provide a convenient means for the investigation of the variation of cataphoretic mobility with molecular structure.

In the case of these long organic molecules which have an active group at one end of a long hydrocarbon chain, the double layer might be due either to the dissociation of the active groups in the water, or to adsorption of ions on the hydrocarbon chains, or to both.

X-ray analysis by Müller and Shearer [3] indicates that when a mass of one of the fatty acids is allowed to solidify slowly in air the molecules in the surface orientate themselves parallel to each other, the length of the long hydrocarbon chains being inclined steeply to the air-acid interface. The experiments of Adam and Jessop [4] on the contact angle between such a surface and water show further that the active-end groups of the molecules in the surface layer are directed towards the acid side and the long chains towards the air side of the interface. If, therefore, a small mass of a fatty acid is allowed to solidify in air and then is immersed in water, the latter will be in direct contact only with the long chains of the surface molecules, so that this acid-water interface will be quite similar to the interface between water and a saturated hydrocarbon whose molecule contains no active group.

If the electrokinetic behaviour is controlled by the structure of the acid-water interface only, then the mobility of fatty acid and hydrocarbon particles should be identical; if, however, the active group at the inner end of the long molecule is able to exert any influence, there will be a marked difference between the mobilities of the different particles. Examination of the mobilities of small cylinders of a series of these substances has

shown that the latter is the case. The end groups are found to influence the mobility greatly in spite of the fact that, in many of the substances used, they must be 15 Å. to 25 Å. from the actual water interface. It appears further from the results that the mobility varies in a regular manner both with the length of the hydrocarbon chain, with the nature of the active group in the molecule, with the position of the latter in the molecule, and with the conductivity of the surrounding liquid.

In order to investigate the variation of the mobility with chemical composition it is advisable to use the simplest possible system. The constitution of the double layer will be influenced by many factors, such as the concentration of each type of ion in the solution and the concentration of neighbouring solid particles. In order, therefore, to be able to associate a variation of mobility with one definite cause, the number of variables must be made as small as possible. For this reason the measurements were made in pure water containing only one fatty acid particle at any one time.

Experimental.

The method used was a modification of that employed some years ago [5] in the examination of the cataphoresis of air-bubbles. The experimental vessel consists of a cylindrical glass cell whose ends are closed by large plane platinum electrodes. This is filled with water and made to rotate about its axis, which is accurately horizontal. During the steady rotation, any small particle of low density will take up an equilibrium position on the axis and can be moved along the latter to any desired position by tilting the cell slightly. Its cataphoretic velocity can be examined by measuring its velocity along the axis when an electric potential is applied between the two platinum electrodes. In order to compensate for any small gravitational effects, the velocity is measured first with the potential applied in one direction and then with it reversed, the average of these being taken as the true velocity of the particle.

In order to obtain measurements of any value it is essential that the rotation of the cell shall be very uniform, as any angular acceleration causes the particle to move non-uniformly along the axis even in the absence

of any electric field. To secure the necessary uniformity a large synchronous motor with a heavy flywheel was used to drive the cell. The flywheel greatly decreases the difficulty of starting the motor and helps to prevent accidental stoppage. In the earlier work the motor used was driven by the intermittent current from an electrically maintained tuning-fork, and considerable difficulty was experienced in keeping the fork running smoothly for the length of an experiment. In the present work the fork has been dispensed with entirely, the synchronous motor being driven directly from the A.C. mains of the

Fig. 1.

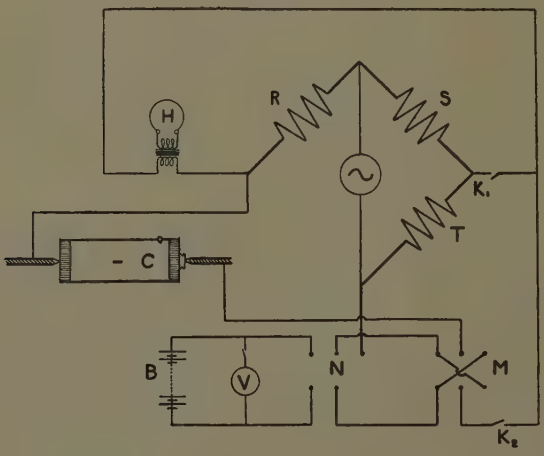

city electric supply. This supply is now very accurately controlled and uniform, and will drive the motor very smoothly and for an indefinite period.

In order to measure the electrical conductivity of the cell an A.C. bridge was used in the usual manner. The electrical connexions are shown in fig. 1. By means of the key N the cell C could be connected either to the battery B supplying the D.C. voltage, or to the A.C. bridge RST. When it was connected to B the key K_1 was opened and K_2 was closed. When the conductivity was to be determined N was reversed, K_1 closed, and K_2 opened. The head-phones H were used to balance

the bridge, while the voltmeter V gave the applied potential difference.

The small cylinders to be examined were formed by forcing the pure substance through a 1 mm. hole in a brass plate. Paraffin wax cylinders formed in this way were quite satisfactory, and their cataphoretic velocity could be determined without difficulty. When, however, similar cylinders of the fatty acids, such as palmitic or myristic acid, were used, it was impossible to obtain any satisfactory measurements, as the cylinders were barely stable on the axis, and the slightest jar caused them to vibrate about it and sometimes leave it altogether. It is evident that the density of these substances at 20° C. is too near to that of water to give a strong restoring force when the cylinder is displaced from the axis. This was somewhat unexpected, as the density of palmitic acid at 62° C. is only 0·85.

The difficulty was overcome by replacing the solid fatty acid cylinders by cylinders of paraffin wax coated with the acid. This process reduces the effective density considerably and renders the axial position of the cylinder quite stable. In order to obtain reproducible results the process of coating the paraffin cylinders must be carried out in a standardized manner. If the wax cylinder is dipped into the liquid acid, the quantity adhering, and, therefore, the diameter of the resulting cylinder, will depend both on the temperature of the solid paraffin and on that of the liquid acid. To ensure uniform conditions the acid was kept in a small thermostat at a temperature of a few degrees above its melting-point, and the paraffin cylinder was cooled in an ice-bath for a few minutes and was then dipped into the acid and quickly removed. In this way the thickness of the coating could be controlled quite satisfactorily.

Measurements were also made with the uncoated cylinders of paraffin wax. To make these quite comparable with the acid cylinders they were given the same treatment before use, *i.e.*, the cylinder, after being pressed through the 1 mm. hole, was cooled and dipped in liquid paraffin. An incidental advantage of this dipping process is that it removes any sharp edges or rough areas from the cylinders and gives them all a smooth and uniform surface. In addition, the application of the acids in the the liquid form ensures the orientation of the surface-

layers of molecules; if the acid cylinders were used as they emerged from the 1 mm. hole, this orientation would not be present. Adam and Jessop [4] have shown, however, that the orientation is satisfactory when the surface has been formed by solidification from the liquid.

Each substance was examined iu pure water and in dilute solutions of hydrochloric acid, so that the variation of mobility with the hydrogen ion concentration could be observed. Any electrolysis in the cell produces gas-bubbles which collect on the axis and interfere with the motion of the particle being examined. Therefore in all the experiments the HCl solution was so dilute that there was no observable formation of gas-bubbles at the electrodes. The maximum conductivity which could be used under these conditions was about 15×10^{-6} ohms^{-1} cm.$^{-1}$, so that the available conductivity range was from 15×10^{-6} ohms^{-1} cm.$^{-1}$ to 1×10^{-6} ohms^{-1} cm.$^{-1}$.

Endosmotic Effect.

When an electric field is applied to the ends of a cylindrical cell filled with water there will be a definite flow of the liquid along the walls under the influence of the field. The theory of this endosmotic flow, which is due to the presence of a double layer on the glass-liquid interface, is quite similar to that of cataphoresis, and Henry [2] has shown that the velocity of the liquid near the wall will be given by the formula

$$W=DX\zeta/4\pi\eta, \quad . \quad . \quad . \quad . \quad . \quad . \quad (2)$$

so that the endosmotic velocity of a liquid along the wall is equal in magnitude to the cataphoretic velocity of a particle of the same material as the wall immersed in the same liquid.

Now, in a closed vessel the total flow across any cross-section must be zero, so that the flow in one direction along the walls must be balanced by an equal flow in the opposite direction along the central portion of the tube. The actual observed velocity (V_0) of a particle on the axis will thus be the algebraic sum of its true cataphoretic velocity (V_c) relative to the surrounding water, and the velocity (W) of this water itself due to the endosmotic flow at the walls. Hence

$$V_0=V_c+W,$$

and it appears that it is necessary to measure W before the true value of V_c can be obtained from the cataphoresis observations.

Smoluchowski [6] has shown that the velocity distribution due to endosmosis is a parabolic function of the distance from the axis, and for a cell of the type used in the present work Currie [7] obtained the expression

$$W_r = W_R(2r^2/R^2 - 1) \quad . \quad . \quad . \quad . \quad . \quad (3)$$

for the endosmotic velocity W_r at a distance r from the axis in terms of the velocity W_R at the wall. It follows from this expression that the endosmotic velocity is zero at a distance $R/\sqrt{2}$ from the axis, and that *on* the axis it is equal in magnitude but opposite in direction to that at the wall of the cell. But the latter is equal to the cataphoretic velocity of a particle of the same material as the walls, so that the observed velocity of such a particle *along the axis* will be equal to twice the endosmotic velocity at the wall.

Before any work on the fatty acids was commenced, the endosmotic velocity was measured in the manner indicated above. A small hollow glass cylinder, of the same glass as the cell itself, and having the same dimensions as the paraffin particles, was examined in the experimental cell. Its velocity under a known electric field was measured and the endosmotic velocity (W_{glass}) was taken as equal to one-half of this value. This was confirmed by measuring the velocity of a palmitic acid cylinder, first in the clean glass cell and then in a cell coated with palmitic acid. In the first experiment the observed velocity V_{01} would be

$$V_{01} = V_c + W_{glass},$$

and in the second the velocity V_{02} would be

$$V_{02} = 2V_c,$$

so that

$$W_{glass} = (V_{01} - \tfrac{1}{2}V_{02}).$$

Since V_c is large in comparison with W, this is not so accurate as the direct measurement with the glass cylinder. The agreement was, however, quite satisfactory.

The mobilities of the different particles quoted in the results following are all the true cataphoretic mobilities after being corrected for endosmosis. All the particles

moved in the electric field as if they bore a negative charge.

Results.

1. *Endosmosis.*

The cataphoretic velocity of a small glass cylinder was measured as a function of the conductivity of the dilute HCl solution in which it was placed, and the endosmotic velocity at the glass wall was taken as one-half of the observed velocity. It was found that this velocity decreased steadily with increasing concentration of HCl, and when the specific conductivity was 15×10^{-6} ohms^{-1}

Fig. 2.

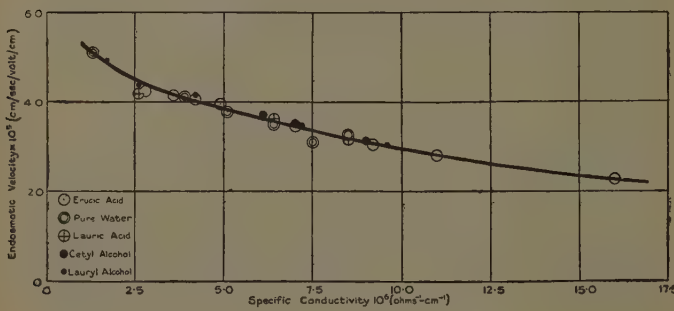

cm.$^{-1}$, the endosmotic velocity was only about one-half that in pure water.

A number of organic substances examined were slightly soluble in water (*e. g.*, lauric acid, cetyl alcohol), and it was thought possible that the dissolved organic molecules might affect the constitution of the double layer at the glass wall and so alter the endosmotic effect. For this reason the endosmotic velocity-conductivity curve was obtained first in pure water and then in the saturated solutions of the different organic materials. These solutions were prepared by heating a little of the solid in distilled water and filtering out the excess solid when it had cooled. The conductivity was varied in the different experiments by adding HCl to these saturated solutions.

The results of the endosmosis measurements are shown in fig. 2, the measurements in different saturated solu-

tions being indicated by different symbols. It will be seen that the presence of the organic compounds in the solution has no appreciable effect on the endosmotic velocity. It is, therefore, permissible to take the endosmotic correction from fig. 2, even if the particle under consideration is slightly soluble in the water.

2. *Time Variation of the Cataphoretic Mobility.*

In obtaining the endosmotic results in the cell coated with palmitic acid, an unexpected variation of the velocity with the age of the acid layer was observed. If the velocity was measured in the same cell every few hours for two or three days there appeared to be a progressive diminution in its magnitude until, finally, a steady equilibrium value was reached. It was noticed that the water did not wet the palmitic acid coating when the latter was freshly applied, but that when the final equilibrium value was attained the acid was wetted by the liquid. It therefore appears that the water slowly soaks into the surface, and that this process is accompanied by a marked reduction in the electrokinetic potential at the interface.

This effect was examined more closely in the clean uncoated glass cell. A newly prepared palmitic acid cylinder was inserted and its cataphoretic velocity was measured as a function of the time. It was found to remain practically constant for several hours, after which it decreased quite rapidly and finally settled down to a steady very small value. Similar particles which had been kept under distilled water for a month also gave this same velocity when placed in the experimental cell, so that it seems to be a permanent equilibrium value. The experiment was repeated in water of different conductivities, and the results of three such experiments are shown in fig. 3. To prevent overlapping of the curves a constant term of $2{\cdot}0\times10^{-5}$ cm./sec./volt/cm. has been added to each observation in water of conductivity 9×10^{-6} ohms^{-1} cm.$^{-1}$ and one of $4{\cdot}0\times10^{-5}$ cm./sec./volt/cm. to each observation at $1{\cdot}0\times10^{-6}$ ohms^{-1} cm.$^{-1}$. The true zeros of these curves are indicated by the dotted horizontal lines in the figure. It will be seen that in these three experiments the cataphoretic velocity in dilute solutions of hydrochloric acid is eventually reduced to less than one-tenth of its original value.

It is fortunate that at all conductivities there is no important variation in mobility for several hours after a new particle has been introduced. The time effect may therefore be eliminated by using a fresh particle for each experiment. As the latter can usually be completed in about half an hour after the introduction of the particle, the time variation will be quite negligible.

It should be noted that the time effect was not peculiar to palmitic acid. It was observed with paraffin wax and other fatty acids as well. It might be thought that the final small velocity is the true velocity characteristic of

Fig. 3.

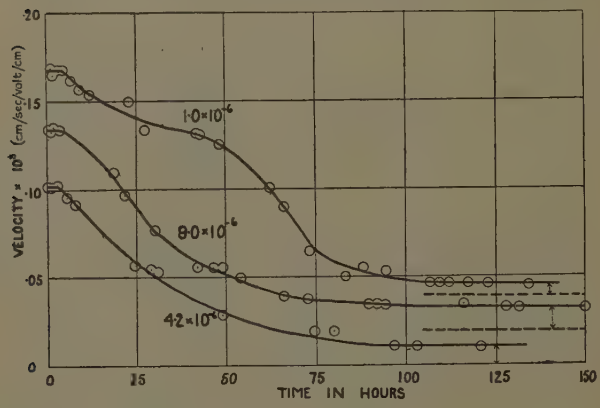

the acid, and that the initial greater speed is due to an air-film on the newly introduced particle. This is rather unlikely, as the water used had previously been boiled to free it from dissolved air, so that any air-film on the particle would be quickly absorbed by the water. It is, of course, possible that an adsorbed gas-layer may be tightly bound to the surface and only very slowly removed by the water. If this were the case it would be necessary to suppose that the removal of this gas-film enables the water to wet the particle.

3. *Effect of Length of Hydrocarbon Chain on Cataphoretic Mobility.*

The best quality palmitic, myristic, and lauric acids as supplied by the Eastman Co. of Rochester, N.Y., were

used in these experiments without further purification. These substances have long hydrocarbon chains containing 15, 13, and 11 carbon atoms respectively, with the active —COOH group at the end of the chain. As these end groups are the same for all the acids, any variation in the mobility must be due to the length of the chain. Palmitic and myristic acids are not soluble in water, but lauric acid dissolves slowly until the specific conductivity has risen from that of pure water to about $3{\cdot}5\times10^{-6}$ ohms^{-1} cm.$^{-1}$. The experiments with lauric acid were therefore performed in water previously saturated with the acid so as to avoid complications due to the solution of the particle during an experiment. Hence no measurements could be obtained at conductivities below $3{\cdot}5\times10^{-6}$

Fig. 4.

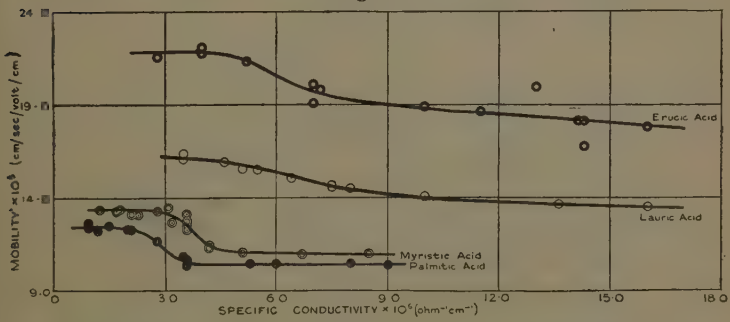

ohms^{-1} cm.$^{-1}$. The velocities of particles of these acids were measured in water of different conductivities, and the cataphoretic mobilities deduced therefrom are shown in fig. 4. This indicates that the length of the hydrocarbon chain exerts a very pronounced influence on the mobility, which becomes steadily greater as the chain-length is reduced. The significance of this result will be considered later, as will the erucic acid curve shown in fig. 4. The mobility of the different acids in pure water is given in Table I.

Further confirmation of this variation with chain-length was obtained by comparing cetyl alcohol and lauryl alcohol. Particles covered with these substances again indicate that the cataphoretic mobility increases as the chain-length is reduced (fig. 5). The lauryl alcohol

results are interesting, as this substance is not solid at the temperature of the experiment. The measurements were obtained with a particle formed by dipping a paraffin cylinder into the liquid alcohol and using this in water previously saturated with the alcohol The alcohol film remained on the particle surface, and the results shown

TABLE I.

Acid.	No. of carbon atoms in chain.	Mobility $\times 10^5$ cm./sec./volt/cm.
Lauric	11	16·20
Myristic	13	13·33
Palmitic	15	12·45

Fig. 5.

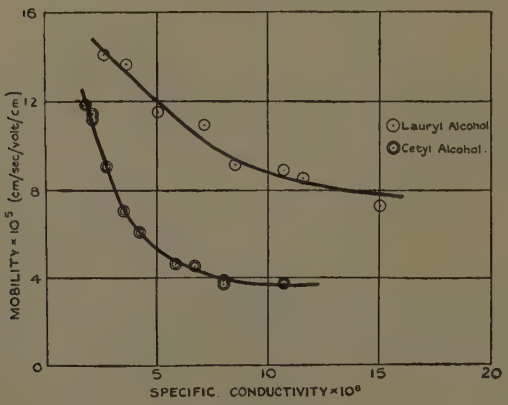

in fig. 5 were obtained. With a liquid film of this nature, the surface molecules will be free to re-orientate themselves in the interface on entering the water, so that the results will not be strictly comparable with those obtained with solid cylinders. In so far as a comparison may be made, however, they do confirm the results given by the series of fatty acids.

4. *Effect of the End Group on the Mobility.*

For the purpose of examining the change of mobility with the nature of the active group in the molecule the only substances available were palmitic acid, with an end group $-COOH$; palmitamide, with a group $-CONH_2$; cetyl alcohol, with a group $-CH_2OH$; and a hard paraffin wax melting between 60° C. and 68° C. While the length of the molecules in the wax will be greater than those in the other substances, it should serve to give the mobility of the long hydrocarbon chain in the absence of any distinctively active group.

The mobilities of the above substances in pure water are shown in Table II., whence it appears that the replacement of the end group $-COOH$ in the palmitic

TABLE II.

Substance.	Mobility $\times 10^5$ cm./sec./volt/cm.
Palmitic acid	12·45
Palmitamide	16·87
Cetyl alcohol	12·00
Paraffin wax (60°–68°)	19·60

acid by the group $-CONH_2$ in the amide results in a large increase in the mobility of the particle. Further, the very inactive paraffin wax has a mobility greater than that of any of the more active substances. Since the cetyl alcohol is slightly soluble in water, the result given in Table II. is for the motion of a particle in the alcohol-saturated water.

The variation of the mobility of these substances with hydrogen ion concentration is shown in fig. 6. This variation is very distinctive for the different molecules. In the case of the paraffin the mobility is almost constant for all conductivities of the HCl solution, and in that of palmitic acid the reduction in mobility with increasing concentration is not very pronounced. The mobilities of the palmitamide and the alcohol, however, are extremely sensitive to the HCl concentration, and decrease very

rapidly with increasing conductivity. In the more concentrated solutions the palmitic acid and palmitamide have almost identical mobilities.

5. *Effect of a Double Bond in the middle of the Hydrocarbon Chain.*

The influence of the chain-structure on the mobility was examined by using particles of erucic acid. This substance has the formula $C_8H_{15}CH : CH(CH_2)_{11}COOH$(cis), so that it differs from the other acids used in having a double bond in the middle of the chain. It will be noted

Fig. 6.

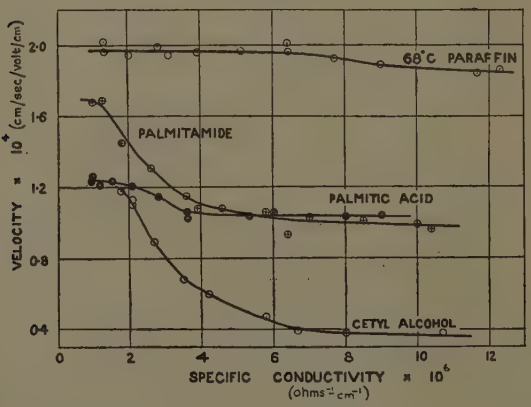

that erucic acid contains more carbon atoms in the chain than do any of the other acids employed, so that, in accordance with the previous results, it might be expected that its mobility would be smaller than that of palmitic acid. However, the altered structure of the molecule has a very pronounced effect and, in practice, this acid was found to have a higher mobility than any of the other substances used, the magnitude in pure water being $21{\cdot}8 \times 10^{-5}$ cm./sec./volt/cm. The variation of this mobility with hydrogen ion concentration is very similar to that of the other acids, and is shown, with the curves for those acids, in fig. 4.

6. *The Mobility of Water-soaked Particles.*

The variation of the mobility with conductivity has been measured for lauric acid particles which had been kept in distilled water for several weeks, so that the particle surface had attained its equilibrium condition and was wetted by the water. The velocity was very small ($1{\cdot}5 \times 10^{-5}$ cm./sec./volt/cm.) and, as in the case of fresh lauric acid particles, did not vary greatly with increasing conductivity of the solution. These results are shown in fig. 7, in which figure some measurements with water-soaked palmitic acid and a single experiment with water-soaked paraffin are also recorded. It may be

Fig. 7.

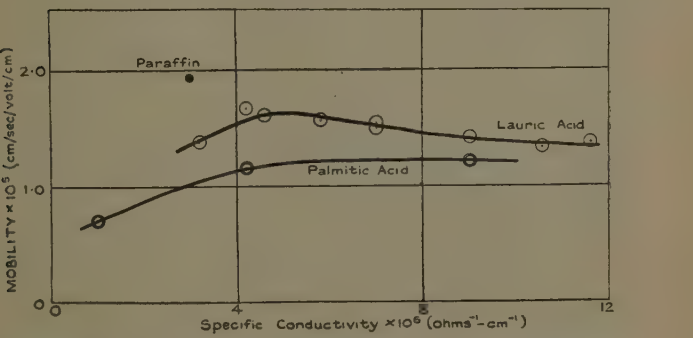

noted that, in this final equilibrium state, the mobilities of these substances are still arranged in the same order as in the case of freshly prepared particles.

Discussion.

A consideration of the above results indicates that both the long hydrocarbon chains, and also the water soluble groups in the fatty acid molecules, have a definite effect on the electrokinetic behaviour of the particle. It is interesting to compare these cataphoretic results with other characteristics of fatty acid surfaces. As already stated, Adam and Jessop [4] found that the active groups in the molecules in an orientated surface were without effect on the contact angle between the fatty acid and water. It is, therefore, somewhat surprising that these active groups, which are buried too far below the actual

interface to affect its contact angle, should have such a pronounced cataphoretic effect. On the other hand, the present results are more in agreement with the observation of Adam, Morrell, and Norrish [8] that the rate of combination of ethylene and chlorine is greater when in contact with a fatty acid surface than when this is replaced by a surface of paraffin wax. This indicates that these gases must be able to penetrate the surface and so approach the —COOH group at the inner end of the molecules.

It should be noted that, since the cross-section of the hydrocarbon chains is the same in all the acids, the number of molecules per square centimetre of surface will be the same for all, so that the only change in passing from the higher to the lower acids is a shortening of the chain-length with a consequent increase in the accessibility of the water soluble group. The experimental results show that the mobility increases with decrease of chain-length, so that a part at least of this mobility must arise from the increasing interaction between the —COOH group and the liquid as the ease with which the latter can reach the group increases.

The very pronounced variation of the mobility with the time of immersion of the particle is interesting. It is accompanied by a large change in the angle of contact between the surface and water. Adam and Jessop [4] found that the contact angle of many substances was lowered when they were allowed to crystallize in contact with water, and they ascribe this change to the presence of water-molecules entrapped between the chains. The cylinders used in the present experiments were always prepared in air and were not brought into contact with the water until the process of solidification was complete. The steady change in the contact angle must, therefore, be due to interaction with the water after solidifaction. This matter is being examined further.

In conclusion, we wish to express our thanks to Professor Sir J. J. Thomson, O.M., F.R.S., for his very helpful criticism of the paper.

Summary.

The cataphoretic behaviour of single particles of a number of the fatty acids and related compounds has

been examined in pure water and in dilute HCl solutions, and it has been shown that the mobility of the particle depends partly on the nature of the water soluble group in the molecule and partly on the length of its hydrocarbon chain. For molecules having a constant chain-length the mobility decreases as the nature of the end group is altered in the order $-CONH_2$, $-COOH$, $-CH_2OH$, the last two being almost equal. The mobility of molecules having the same end group ($-COOH$) decreases as the length of the hydrocarbon chain is increased, while the presence of a double bond near the middle of the chain, as in erucic acid, increases the mobility of the particle.

The mobilities of all the substances examined decreased with increasing hydrogen ion concentration of the surrounding liquid.

References.

(1) Debye and Hückel, *Physik. Zeits.* xxv. p. 49 (1924).
(2) Henry, Proc. Roy. Soc. A, cxxxiii. p. 106 (1931).
(3) Müller and Shearer, J. C. S. p. 3156 (1923).
(4) Adam and Jessop, J. C. S. p. 1863 (1925).
(5) Alty, Proc. Roy. Soc. A, cvi. p. 315 (1924).
(6) Smoluchowski, Bull. Acad. Sci. Cracovie, p. 182 (1903). (See also Freundlich, 'Kapillarchemie,' p. 325 (Leipzig, 1922)).
(7) Currie, Phil. Mag. [7] xii. p. 429 (1931).
(8) Adam, Morrell, and Norrish, J. C. S. p. 2793 (1925).

X. *Studies in Photomagnetism.*

By Prof. D. M. Bose, *M.A., Ph.D., and* P. K. Raha *.

In a previous paper [1] an account was given of the effect of light absorption in changing the susceptibility of paramagnetic solutions containing ions belonging to the Iron Group. The method used was to suspend from the arm of a delicate torsion balance a small glass bulb containing the solution, in a strong inhomogeneous field, and to neutralize the action of the field on the solution by attaching a bismuth ball of suitable size to the lower side of the bulb. On allowing light of suitable wave-length to impinge on the solution, a deflexion of the torsion balance was observed, which indicated an increase of susceptibility of the solution.

* Communicated by the Author.

The increase in susceptibility observed was interpreted in the following way. In the solutions the paramagnetic cat-ion existed in the form of a hydrated complex $[Me, mH_2O]^{n+}$ in which, due to the interpenetration of charges between the ion and the associated water molecules, the orbital moment of the ion was more or less quenched and the magnetic moment of the ion was due chiefly to the spin moment of the electrons present on the latter's incomplete *d*-shell. Due to light absorption the complex was temporarily dissociated into the free ion Me^{n+} and mH_2O. To the magnetic moment of the former both the spin and the orbital moment of the electrons contributed, resulting in an increase in its value. In a subsequent paper [2], the results obtained were applied to the interpretation of the mechanism of light absorption in these complex ions. So far the results obtained were only of a qualitative nature. The arrangement used, though very sensitive, was incapable of giving any quantitative results.

The present paper describes a method of quantitative measurement of the photomagnetic effect which, though not so sensitive as the previous one, gives reproducible results. It is based on a modification of the O-tube method used by Hector and Wills [3] to measure the susceptibility of gases. The O-tube arrangement is filled partly with the paramagnetic solution under investigation and the rest of the tube is filled with air, the pressure on which can be varied. The meniscus, separating the liquid and the air, is contained in the horizontal capillary part of the O-tube, and is placed between the pole pieces of a powerful electromagnet. On being illuminated with light of suitable wave-length it is found that the position of the meniscus shifts, and by increasing the air pressure it can be brought back to its original position in the field of view of a telemicroscope.

The experimental arrangement consists, therefore, of the following parts :—(1) The O-tube with the accessory arrangements for levelling the tube, for varying the gas pressure inside it, and for measuring the latter ; (ii.) the optical arrangement for observing the position of the meniscus and for illuminating the paramagnetic solution, near the meniscus, with light of suitable wave-length ; (iii.) arrangement for measuring the amount of light energy absorbed in the paramagnetic solution.

Experimental Arrangement.

ABCD is the O-tube (fig. 1), partly filled with air and partly with the paramagnetic solution under investigation. AB is the horizontal capillary tube of 1·8 mm. bore, which is placed between the pole-pieces of an electromagnet, the O-tube itself being mounted on a triangular base provided with levelling screws. E is

Fig. 1.

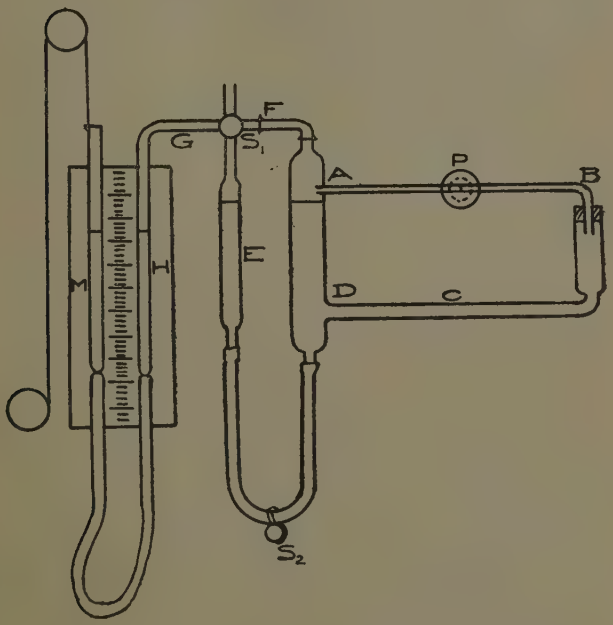

a tube of the same diameter as D and is connected by flexible rubber tubing to the bottom of D and to a three-way stop-cock S. The other parts connected to the stop-cock by flexible rubber tubings are (i.) the top of the tube D, and (ii.) the manometer tube MH filled with water—the difference in the height of water in the two legs of which is read on a millimetre scale. By means of a pulley arrangement, the leg M of the manometer can be raised or lowered by the observer while reading the

position of the meniscus between the pole-pieces of the electromagnet.

Adjustment.

The O-tube is disconnected from E and F, and taken out. A small funnel is inserted to the free end of the rubber tube connected to the bottom of D, and the paramagnetic solution is introduced into the O-tube. The rubber tube is then closed by the pinch-cock S_2, and by several jerks the pocket of air which invariably collects at the joint B is removed. The O-tube is then mounted on the base and the connexion E is completed and the pinch-cock opened. By means of a spirit-level and by adjusting the levelling screws the capillary tube is made nearly horizontal ; the quantity of liquid in the apparatus is so adjusted that there is none in the capillary tube. The electromagnet is excited and E is raised up. A long thread of the solution rises into the capillary past the homogeneous portion of the field between the pole-pieces. By lowering E the meniscus is brought very near to the edge of the flat portion of the pole-pieces, on the side away from B. After the preliminary adjustment is complete, the tube E is gradually lowered by means of a micrometer screw arrangement till the meniscus is placed in the most sensitive part of the field. This is indicated by a comparatively large shift of the position of the meniscus, when the micrometer screw head is given a minute rotation. The photomagnetic effect is now qualitatively sought for, and if obtained the connexion at F is completed. The stop-cock S_1 is then so turned that the connexion with the outer air is cut off and E and F are put in connexion with the manometer tube H. By the optical arrangement to be described below the liquid meniscus is illuminated by light from a mercury arc lamp. Any change in the susceptibility of the paramagnetic solution causes a shift in the position of equilibrium of the meniscus, and by either raising or lowering the level of the liquid in the arm M of the manometer tube MH, the volume of air contained in the tubes D and AB is either compressed or dilated till the meniscus returns to its original position in the field of view. From the change of pressure of the air column the change of susceptibility of the liquid can be calculated, as will be shown later.

Optical Arrangement.

Hg is a mercury-vapour arc, whose radiation is focussed by means of a lens L on the capillary tube B. P is the trace of the pole-pieces between which the capillary tube is placed. The image of the meniscus in B is reflected in a horizontal direction by means of the mirror M to the telemicroscope T, which has a micrometer scale in its eye-piece. F is a glass filter vessel 2 cm. thick containing a paramagnetic solution of the same substance with which the capillary tube is filled up. The initial position of the meniscus is read on the micrometer scale of the eye-piece when the solution is illuminated by light which has passed through the filter F, and from which, therefore, the absorbable portion has been cut off. The filter is then

Fig. 2.

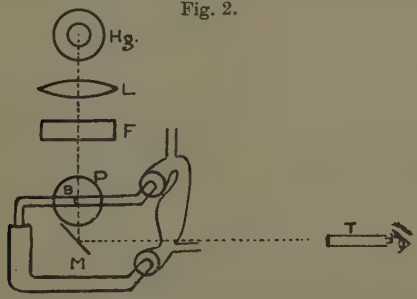

removed, and it is found that the meniscus quickly takes up a new position. The manometer is manipulated till the meniscus returns to its old position on the micrometer scale, and the difference of pressure is read off on the manometer scale. Originally an additional filter to cut off the infra-red radiation was used, but as it was found that a positive deflexion was obtained indicating an increase of susceptibility of the paramagnetic solution even without cutting off the infra-red rays, and that the use of the infra-red filter diminished the total deflexion produced, the use of the latter was discontinued. The maximum deflexion observed was about 1·5 scale divisions of the micrometer scale, and a prolonged exposure to the light was accompanied by a diminution of deflexion, indicating a rise of temperature of the liquid in the capillary tube.

The electromagnet used was of the Rutherford type for the investigation of the magnetic deflexion of α-particles. The pole-pieces were rebuilt with the addition of two cylindrical sliding horizontal pole-pieces with the tapering ends 1 cm. diameter. The sides of the capillary were ground flat, so that the air-gap was only 4 mm. With a current of 5 amp. the field was about 40,000 gauss. Originally we used a Weiss's electromagnet built by Max Kohl. But with a current of 11 amp. a field of about 30,000 gauss was produced, and it was not sufficient for the observation of the photomagnetic effect.

Measurement of the Absorption Coefficient of the Paramagnetic Solutions.

During the course of this investigation two kinds of light absorption measurements were made :—

Fig. 3.

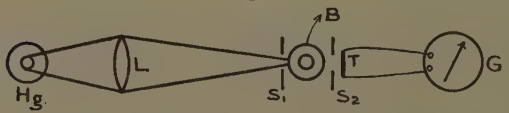

(i.) To get a comparative table of the percentage of radiation from a mercury arc absorbed by the same thickness of the different paramagnetic solutions, containing equimolecular concentration of the salts. For this purpose a glass cell of 5 mm. thickness, filled with the different solutions, was placed between the light source and a Moll's linear thermopile connected to a Moll's galvanometer.

(ii.) To obtain an estimate of the total amount of radiation from the given light source, which was absorbed by a given solution of $CrCl_3$ contained in the capillary portion of the O-tube arrangement under the actual experimental condition.

For this purpose the Moll's thermopile system was calibrated by means of a standard Hefner lamp, using Gerlach's value of the amount of energy radiated across unit area at a distance of 50 cm. from the source. The mercury arc, the lens L, and a capillary tube B, of the same bore as that used in the O-tube, were placed at

the same relative distances apart as in the actual photomagnetic experiment. Since the source of light was a broad one, an extended image of the latter was formed at B. In order to prevent any stray radiation, other than that passing through the absorbing liquid, falling on the slit S_2 of the thermopile T, a slit S_1 of the same aperture, 1·8 mm., as the diameter of the capillary tube is placed in front of the latter (fig. 3). On tracing the path of the beam after it emerges from the capillary it is found to come to a line focus and then diverge into a band. The intensity distribution along the width of the band was measured, by mounting the thermopile with the slit S_2 on a base which could be shifted parallel to the width of the slit by means of a micrometer screw. It was found that the intensity of the band remained constant over an area 1·5 times the width of the slit S_2. In order to get the total intensity of the radiation emerging from the capillary liquid column the thermopile reading is multiplied by the correction factor 1·5. The capillary tube is filled *in situ*, first with water and then with the paramagnetic solution of the same concentration as used in the photomagnetic experiment, and the corresponding readings of the thermopile were taken.

Experimental Results.

The experimental results obtained can be divided into three groups : (I.) preliminary observation on substances, whose photomagnetic effect had not been recorded in the previous paper ; (II.) a comparative study of the photomagnetic effect found in aqueous and ammoniacal, and acid solutions containing paramagnetic ions ; (III.) more detailed study of the photomagnetic effect in $CrCl_3$ solution in relation to the light energy absorbed. The spectral terms corresponding to the absorption spectra of the Cr^{+++} ion in solution are known, and since the percentage change of susceptibility due to light absorption is the largest in the solutions of chromic salts, it seemed worth while to attempt a more detailed quantitative study with the solution.

I. *Preliminary Observation on Substances.*

A.—The absorption spectra of the V^{+++} and V^{++} ions in solution have been studied by S. Kato [5] and

correlated with certain transition of the respective ions, *e. g.*, for V^{+++}, $^3F \rightarrow {}^1D$, ^1G, and for V^{++}, $^4F \rightarrow {}^2P$, ^2G, ^2H. Ammonium vanadate was treated with HCl, when a deep brown solution was formed. This solution was reduced with a zinc-mercury couple, till there was no more reaction. A deep greenish-violet solution was obtained which evidently contained both the ions V^{+++} and V^{++}. On introducing the solution in the apparatus an increase of susceptibility was observed under light absorption. As it was not possible to obtain solutions containing only one kind of vanadium ion, the investigation was not carried on further.

B.—Photomagnetic effect in paramagnetic crystals : So far the effect has been observed in paramagnetic solutions only. It was thought worth while to try to see if the effect could be observed with a crystal. For this purpose a small crystal of $NiSO_4$, $7H_2O$ was grown in a cylindrical form on the end of a stiff glass fibre and suspended from the arm of a sensitive torsion balance, in the inhomogeneous magnetic field of an electromagnet. The attraction of the field on the crystal was neutralized by means of a bismuth ball of suitable size attached to the latter by soft wax, in the way mentioned in the previous paper. An increase of susceptibility under light absorption was noted.

C.—The same experiment was repeated using dehydrated crystals of $NiCl_2$. The salt was obtained as a crystalline powder. A small quantity was taken in a thin glass bulb, with a bismuth ball of required dimension attached below it. After mounting the bulb on the arm of the torsion balance and illuminating it with light from a mercury arc, no perceptible deflexion was noted. As mentioned in the previous paper, in the inhomogeneous field of the electromagnet the torsion balance makes a continuous oscillatory motion. The anhydrous chlorides show very strong surface absorption and scattering. It is difficult to state whether any appreciable absorption took place in the body of the salt crystals.

II. *Experiments with Paramagnetic Solutions.*

In our investigations with different paramagnetic solutions the procedure followed was to observe the change, due to light absorption, in the position of the

image of the meniscus of the paramagnetic solution on the micrometer scale in the eye-piece of the telemicroscope, and then to alter the pressure of the air enclosed in the O-tube till the meniscus was brought back to its original position. The increase in the hydrostatic pressure was a measure of the increase in the paramagnetic susceptibility of the solution. The accuracy with which this change could be measured was dependent upon the amount of the change. Under the most favourable conditions a change of 1·5 scale divisions could be obtained, but the arrangement then became unstable and the readings obtained were not reproducible. For deflexions of the order of 1 scale division the arrangement was stable and the results obtained reproducible. In an experiment with a solution of $CrCl_3$ the mean error for a series of seventeen readings was about 8 per cent. With solutions which gave smaller photomagnetic effect the accuracy of reading was proportionately less. For some of the solutions a qualitative change could be observed, but no quantitative readings were possible.

A set of readings was taken of the rise of temperature in a solution of $CrCl_3$, by introducing a fine thermo-couple inside the solution; there was a rise of temperature for about 9 seconds at the rate of 0°·0014 C. per second, after which the temperature became steady.

The paramagnetic solutions investigated contained in the ions Cr^{+++}, Co^{++}, and Ni^{++}; the orbital moments in the ground state, of all of these ions are the same, viz., F. These salts were dissolved either in water, dil. HCl, or ammonia. The results obtained are given in Table I.

The observed P.M.E. given in column (4) is the difference in the readings of the two legs of the water manometer MH necessary to bring the meniscus of the paramagnetic solution to its initial position, when the latter is absorbing radiation from a mercury arc—it is a measure of the change in the paramagnetic susceptibility of the given solution. Column (5) gives the percentage of the total radiation from the mercury arc absorbed by a layer of the given solution 2 mm. thick—it is assumed that the actual amount of radiations absorbed by the different solutions in the capillary tube of 1·8 mm. diameter, in the photomagnetic experiment, are proportional to the values given in (5). The latter are

TABLE I.

Ground term.	(1) Salt.	(2) Solvent.	(3) Gm. of cat. ion per c.c.	(4) Observed P.M.E.	(5) Percentage of radiation absorbed.	(6) P.M.E. / Radiation absorbed.	(7) P_1 (cal.).	(8) P_1 (exp.).
$^4F_{3/2}$	$CrCl_3, 6H_2O$	water	·0075*	2·4	99·4	2·52	25·8	18–19
	,,	,,	·07927*	2·5	,,			
	,,	HCl	·04923*	Barely perceptible.	98·3	—	—	18–19
$^4F_{9/2}$	$CoCl_2, 6H_2O$	water	·09605*	very small	63	—	25·8	25–26
	,,	,,	·07201*	,,	52·7			
F_4	$NiCl_2, 6H_2O$	water	·1551*	1·73	59·16	2·92	22·1	16
	,,	,,	·1030*	1·08	44·8	2·41		
	,,	,,	·1178†	1·08	44·8	2·41		
	,,	Dil. HCl	·1030*	very small	83·9	—	—	14·1
	,,	NH_4OH (soln.)	·0942†	1·55	90·1	—	—	15·5
,, ...	$NiSO_4, 6H_2O$	water	·1028*	1·22	50·07	2·4		
	,,	,,	·1122†	1·22				
	'	NH_4OH	·0763†	·92	92	—	—	15·5

* The strength of the solution has been calculated.
† The strength of the solution has been estimated.

arrived at in the following way: solutions of the different salts containing ·1125 gm. molecules per litre were made and the percentage of radiations absorbed from the mercury arc by 5 mm. thickness of these solutions, was measured by Moll's thermopile. Then assuming the truth of Beer's Law, the percentage of radiation which would be absorbed by a 2 mm. thickness of the solution, of concentrations used in the photomagnetic experiments, was calculated and these values entered in (5). Column (6) gives the ratio of the observed P.M.E. to the radiation absorbed, in arbitrary units. Column (7) gives the magneton number of the ions in Weiss's units as calculated from Van Vleck's formula

$$n_W = 4{\cdot}97\sqrt{4s(s+1)+l(l+1)}. \quad . \quad . \quad . \quad . \quad (1)$$

Column (8) gives the experimentally determined magneton numbers of these paramagnetic solutions.

Discussion of Results.

From a scrutiny of Table I. the following conclusions can be drawn :—

(i.) The photomagnetic effect is the largest in aqueous solutions and the least in the HCl solutions.

(ii.) For different ions in aqueous solutions the effect observed is minimum in cobaltous solutions and much greater in solutions containing Cr^{+++} and Ni^{++} ions. On comparing the magneton number of these ions given in columns (7) and (8), it will be found that the difference between calculated and the observed values of the magneton numbers is the smallest for the cobaltous ion and the largest for the Cr^{+++} ion. There appears to be some correlation between the photomagnetic effect shown by aqueous solution of a given ion and the deviation of the experimentally observed value of the magneton number from that obtained by calculation. On the other hand, though in the HCl solutions this deviation is the maximum, such solutions show very little photomagnetic effect.

We shall now try to interpret these results in terms of a theory correlating the absorption spectra of a paramagnetic solution with its paramagnetic moment, a preliminary account of which was given in a previous paper.

The paramagnetic salts and their solutions are usually coloured. The first successful attempt to correlate the absorption spectra of these solutions with the spectral terms of the paramagnetic ion in the ground state was made by M. N. Saha [4] for the Cr^{+++} ion, and later for other ions by S. Kato [5]. S. Datta [6] has measured the absorption spectra of some of these ions in dil. HCl and in alcohol solutions. He has also made similar measurements for the Ce^{+++} ion in solutions [2]. It is found that for (i.) aqueous solutions of salts belonging to the Iron group the absorption spectra are shifted to the shorter wave-length side of that due to the corresponding free ions ; (ii.) in the case of the Ce^{+++} ion the shift is towards the longer wave-length side ; (iii.) and in the acidic and alcoholic solutions of the ions of the Iron group there is very little shift in the position of the absorption maxima with respect to that due to the free ion.

The above results can be interpreted in the following way :—If W_1 and W_2 are the energies of the free ion in the ground and the excited state respectively, and ν_0 the absorption frequency for transition between these two states, then we have

$$h\nu_0 = W_2 - W_1 ; \quad . \quad . \quad . \quad . \quad . \quad (2)$$

in the state of solution, due to the interaction with the surrounding atoms and molecules, the energy of the ion in the two states can be put as $W_1 - A_1$ respectively $W_2 - A_2$, and the absorption frequency ν of the solution is given by the equation

$$h(\nu - \nu_0) = A_1 - A_2. \quad . \quad . \quad . \quad . \quad . \quad (3)$$

Therefore, from the frequency shift of the absorption maxima in the solution, with respect to that of the free ion, we can get an estimate of the relative values of the energy of binding of the ion in the two states.

We can distinguish between three possible cases :—
(i.) $A_1 > A_2$, then $\nu > \nu_0$, and the absorption maxima shifts towards the ultra-violet side. Here the interaction of the ion with its neighbour is less in the excited than in the initial state. This type of absorption is shown by the aquo, amino, and other complexes of the paramagnetic ions of the first transition group.

(ii.) $A_1 < A_2$, then $\nu < \nu_0$, a typical example of which is the absorption of the $[Ce, 6H_2O)^{+++}]$ complex [5] for

the transition $4^2F \rightarrow 5^2D$, where the absorbing electron is initially inside the (5 s, p.) octet shell; in the excited state its position is outside the latter, and there it is subject to interaction with the water molecules.

(iii.) $A_1 \sim A_2$, the absorption maxima, is very slightly shifted with respect to ν_0, the absorption frequency of the free ion. This type of absorption is found in alcohol and HCl solutions of the chlorides of the paramagnetic ions, and has been shown to be due to absorption by the undissociated chloride molecules.

We shall consider how the interaction between the paramagnetic ion with its neighbouring atoms and molecules affects the magnetic moment of the former. For this purpose we shall consider two different types of interaction: (i.) between the paramagnetic ion and the molecules associated with it in the hydrated, amino. and other complexes; and (ii.) in dil. HCl solution, in which the paramagnetic salt can be shown to exist as undissociated molecules $MeCl_n$, and a different type of interaction will be found to exist between the cat-ion and the an-ion. In a previous paper only the former type of interaction was considered.

i. (*a*). In this class of compounds $A_1 > A_2$, *i. e.*, the interaction in the excited state is small compared to that in the ground state. For the free ions belonging to the Iron Group, Van Vleck has deduced the following expression for their magnetic moments, on the assumption that the energy of separation of the fine structure of the ground-level of ion is small compared to kT

$$p_1 = \sqrt{4s_1(s+1)+l_1(l_1+1)}. \quad . \quad . \quad . \quad . \quad (4)$$

If the ion forms part of a crystal or of a solution it is subject to the influence of its neighbours; one consequence of such interaction is the well-established fact that the experimentally determined values of p_1 are always less than that given by the above formula, the limiting lower value being

$$p_1 = \sqrt{4s_1(s_1+1)} \quad . \quad . \quad . \quad . \quad . \quad . \quad (5)$$

when the orbital moment is totally quenched. We take account of this loss of the orbital moment by assuming that the quenching is proportional to the loss of potential energy A, due to the interaction between the paramagnetic ion and its neighbouring atoms and molecules. The

expression for the moment of the ion then takes the form

$$p_1=\sqrt{4s_1(s_1+1)+l_1(l_1+1)\cdot f\left(\frac{A_1}{T}\right)}, \quad . \quad . \quad (6)$$

where $$f\left(\frac{A_1}{T}\right)=0 \text{ ; for } \frac{A_1}{T}=\infty$$

$$=1 \text{ ; for } \frac{A_1}{T}=0.$$

Stoner [7] has shown that the experimentally determined values of the magnetic moment of this group of paramagnetic ions lie between (4) and (5). The deviation of the values from that given by (4) is a measure of the energy of coupling A.

If n be the number of ions per c.c. of the solution, the volume susceptibility is given by

$$K=\frac{n_0 {p_1}^2}{3kT}.$$

If now the solution is illuminated and, as a result of light absorption, n_2 of the ions are promoted to the excited state and $n_1=n_0-n_2$ remain in the ground state, then the change in the volume susceptibility of the solution is given by

$$\Delta k=\frac{n_2({p_2}^2-{p_1}^2)}{3kT},$$

where $$p_2=\sqrt{4s_2(s_2+1)+l_2(l_2+1)f\left(\frac{A_2}{T}\right)}$$

the moment of the ion in the excited state. Then

$$\Delta k=\frac{n_2}{3kT}\left[4(s_2-s_1)(s_2+s_1+1)+f\left(\frac{A_2}{T}\right)l_2(l_2+1)\right.$$

$$\left.-f\left(\frac{A_1}{T}\right)l_1(l_1+1)\right]. \quad . \quad . \quad (7)$$

We shall apply this formula to the discussion of the P.M.E. in the hydrated complexes of the Cr^{+++}, Co^{++}, and Ni^{++} ions.

Ion.	Ground state.	Excited state.
Cr^{+++}	$^4F_{3/2}$	^2G, ^2H
Co^{++}	$^4F_{9/2}$	
Ni^{++}	$^3F_4$	

Let us take the case of Cr^{+++} ion first. For this ion $s_1=\frac{3}{2}$ and $s_2=\frac{1}{2}$ and therefore the first term in (7) inside

the square bracket is negative ; it is known that for this ion the magnetic moment in the ground state is due entirely to the spin moment, *i. e.*, $f\left(\frac{A_1}{T}\right)=0$, the ion also shows a positive P.M.E., *i. e.*, $\Delta k>0$. This implies that the value of $f\left(\frac{A_2}{T}\right)$ in excited state is $>>0$, and we can reasonably suppose it to be unity, *i. e.*, in the process of light absorption the coupling between the ion and the water molecules breaks down and the ion in the excited state is entirely free.

Co^{++} ion—the spin and orbital moments of this ion are the same as those for the Cr^{+++} ion. In a previous paper (1) it was shown that there is good ground for assuming that in all the paramagnetic ions of this group with multiplicity greater than two, the process of light absorption is accompanied by lowering of multiplicity by two units. On this assumption the value of the first term inside the bracket in (7) is the same for Cr^{+++} and Co^{++}. The value of p_1 for Co^{++} given in columns (7) and (8) of Table I., show that for this ion there is very little quenching of the orbital moment, *i. e.*, $f\left(\frac{A_1}{T}\right)\sim 1$. Therefore $f\left(\frac{A_1}{T}\right)$ and $f\left(\frac{A_2}{T}\right)$ are both of the same order of magnitude, and the very small value of the P.M.E. obtained for this ion is due to the small difference in the values of $f\left(\frac{A}{T}\right)$ in the two states.

Ni^{++} ion shows a larger P.M.E. than Cr^{+++}. In aqueous solution Ni^{++} ion has a magneton number of 16, while the "spin only" value for it is 14·1. This shows that the ion has a higher residual orbital moment than Cr^{+++}, *i. e.*, for it $f\left(\frac{A_1}{T}\right)>0$. In spite of this the former shows a larger P.M.E. than the latter. This is due to the fact that in (7) the value of $4(s_2-s_1)\ (s_2+s_1+1)$ is

$$4(\tfrac{1}{2}-\tfrac{3}{2})\ (\tfrac{1}{2}+\tfrac{3}{2}+1)=-12 \text{ for } Cr^{+++},$$

and

$$4(0-1)\ (0+1+1)=-\ 8 \text{ for } Ni^{++},$$

i. e., the diminution in the spin moment contribution due to light absorption is greater for Cr^{+++} than for Ni^{++}.

Thus, on the assumption that in the hydrated complexes the process of light absorption leads to a dissociation of the latter with the restoration of the orbital moment to the paramagnetic ion, a satisfactory explanation of the observed P.M.E. in this class of solution is obtained.

i. (*b*). Ammoniacal solution of nickel salts :—

In the solid state the magnetic moment of the two amino complexes [8] have been measured, viz. $[Ni(NH_3)_4]^{++}$ with $p=13$ and $[Ni(NH_3)_6]^{++}$ with $p=16$. We tried to see if the tetramine complex of nickel with completely quenched orbital moment would give a larger P.M.E. in solution. Solutions of $NiCl_2$ and $NiSO_4$ in water, saturated with ammonia, were used for photomagnetic measurements. It was found that these solutions absorb a much larger percentage of the mercury radiation without a corresponding increase in the P.M.E. value as compared with similar aqueous solutions. Direct measurements of the susceptibilities of these ammoniacal solutions showed that the Ni^{+++} complex had the same magneton number as in an aqueous solution ; evidently we have to do with the $[Ni(NH_3)_6]^{++}$ complex in the solutions.

III. *The Photomagnetic Effect in dil. HCl solution of $CrCl_3$ and $NiCl_2$.*

As shown in Table I., the effect is very small, though the percentage of light absorption is much greater than in the aqueous solutions. This is explicable according to (7) if A_1 and A_2, the energies of coupling of the paramagnetic ion with its neighbours in two states, are of the same order of magnitude. From absorption and Raman spectra evidence, S. Datta [6] has concluded that at room temperature in alcohol and HCl solutions the paramagnetic chlorides exist as undissociated simple molecules of the type $MeCl_n$, so that the interaction of the paramagnetic ion is now with the Cl ions and not with the dipole molecules like H_2O, NH_3, etc. From the photomagnetic evidence given above it is concluded that $A_1 \sim A_2$, and since

$$h(\nu - \nu_0) = A_1 - A_2$$

it follows that the position of the absorption maxima in these solutions will be only slightly displaced with respect to that due to the free ion. We shall show that this conclusion is verified in the case of the absorption

by the Cr^{+++} ion in the various states of aggregation, for which necessary data are available and are given in Table II.

It is known that the emission and absorption spectra of Cr^{+++} in the visible region, both in the state of vapour and also in crystals and solutions, can be represented as due to transitions between $^4F \rightarrow {}^2G$, ^2H levels. The data for the third column of Table II. are taken from the absorption measurements in $CrCl_3$ vapour, made by Saha and Deb [9]. They found a series of band heads with frequency range given above followed by continuous absorption near 300 mμ. In the fourth column the position of the absorption maxima in a dil. HCl solution

TABLE II.

Transition.	Emission ν cm.$^{-1}$. Cr^{+++} ion,	Absorption ν cm^{-1}. $CrCl_3$ vapour.	Cr^{+++} in dil. HCl.	Cr^{+++} in H_2O.
$^4F-{}^2G$	14781 14456 14422	—	15100	17500
$^4F-{}^2H$	20078 20329 20469	21689 to 23883	21050 21700	23800

of $CrCl_3$ is given ; in addition to these we get a region of continuous absorption, beginning from 305 $m\mu$. In the fifth column is given the absorption maxima due to $CrCl_3$ in water. It is supposed that both in the $CrCl_3$, $6H_2O$ crystals, as well as in its aqueous solution, the absorption in the visible region is due to the $[Cr, 6H_2O]^{+++}$ complex. Hence from the relation $h(\nu-\nu_0)=A_1-A_2$, since $\nu-\nu_0=3000$ cm.$^{-1}$ it is concluded that $A_1>>A_2$, *i. e.*, in the upper level the complex is dissociated into a free Cr^{+++} ion and water molecules. From the similarity of the position of the absorption regions, shown in (3) and (4), and from other evidence, it is concluded that in (4) the absorption maxima are due to the undissociated $CrCl_3$ molecule, and their positions are only slightly shifted with respect to ν_0. The undissociated $CrCl_3$ molecule is held together by covalent bonds between

the two ($4s$) and one ($3d$) electrons of the Cr atom and one ($2p$) electron in each of the three Cl atoms. The absorption is due to the inner incomplete $3d$ shell of Cr with three electrons in it giving rise to the electron transitions

$$^4F \rightarrow {}^2G \quad \text{and} \quad {}^4F \rightarrow {}^2H,$$

together with associated interatomic vibrations. During these transitions the $CrCl_3$ molecule is not dissociated, so that we can reasonably assume that the energy of interaction between electrons in the $3d$ shell of Cr with its neighbours is not appreciably altered during the process of light absorption, *i. e.*, $A_1 \sim A_2$.

The absence of P.M.E. in the acid solution of $NiCl_2$ can be explained in exactly the same way, only the term levels of Ni^{++} giving rise to absorption in the visible region are not known. It will be noticed (Table I.) that the orbital moment of Ni^{++} is completely quenched in the HCl solution.

The quenching of orbital moment of the paramagnetic ions has been explained by Van Vleck [10] and his fellow workers on the assumption that the degenerate energy levels of the paramagnetic ion is split up by the electric field due to the distribution of atoms and molecules round the latter. This field can be of different types of symmetry—for hydrated complexes in crystals, it is found necessary to assume a field of predominantly cubic symmetry, with a small additional rhombic field. Presumably the same type of field will exist in the case of hydrated ions in aqueous solution. On these assumptions a fairly satisfactory calculation of the temperature variation of susceptibility of these ions has been given. For paramagnetic molecules Van Vleck has given a qualitative explanation of the quenching of moment on a similar assumption, viz., that the anisotropic field is due to the distribution of atoms held by covalent bonds to the paramagnetic atom.

In order to account for the existence of P.M.E. in the hydrated ions and its absence in the halide molecules, it will be necessary to assume different mechanisms by which the anisotropic electric field is created in the two cases. In the former in the process of light absorption the cubic field is destroyed, leading to release of the orbital moment of the paramagnetic ion. Since the distribution of the dipole water molecules round the latter

remains unchanged, we have to suppose that the cubic field inside the hydrated ion was originally produced by a rearrangement of the electric charges between the *d*-shell of the ion and the dipole molecules associated with it. In the paramagnetic halides, on the other hand, the absence of P.M.E. is due to the continued existence of the anisotropic field both in the ground and in the excited states of the molecules. This indicates that there is little interaction between the *d*-shell of the paramagnetic atom and the chlorine atoms bound to it. The absorption spectra in both cases are in agreement with these conclusions.

Magnitude of the Change of Magnetic Susceptibility of the Solutions due to Light Absorption.

We shall now consider more in detail the relation between the magnitudes of the light absorption in relation to the change of susceptibility produced in an aqueous solution of $CrCl_3$. For a given solution we have the following data,

Wt. of Cr^{+++} ion per c.c.	K (volume susceptibilities).	P.M.E.	ΔK.
0·78 gm.	$13{\cdot}4\times10^{-6}$	2·4 cm.	7×10^{-11}

The solution has two absorption maxima at

$$\lambda=6100\ (^4F\rightarrow{}^2G), \quad \text{and} \quad \lambda=4300\ (^4F-{}^2H),$$

and for simplicity we assume that all the radiation from the Hg-arc is absorbed in equal parts in both these regions, and therefore if we take ν to be the mean frequency corresponding to these two absorption maxima, and ΔE the amount of energy absorbed per unit volume of the solution, then the number of photons N_2 absorbed per sec. is given by $\Delta E = N_2 . h\nu$. There ought to be some relation between the number of photons absorbed per second in the solution and the number of the ions which are in the two metastable states ^2G and ^2H respectively. We again make the assumption that equal number of ions are present in the two states.

From the relation

$$\Delta K=\frac{n_2}{3kT}(p_2{}^2-p_1{}^2),$$

we can calculate the value of n_2, provided we make some assumption about the mean value of p_2 in the excited state.

In Table III. we give the spectral terms of Cr^{+++} and also the magneton numbers to be expected for Cr^{+++} according to different assumptions.

In the ground state the experimental value p_1 found for Cr^{+++} is 3·8, and if for the excited state Van Vleck's formula holds then

$$\bar{p}_2 = 5{\cdot}28\,\mu_B, \quad . \quad . \quad . \quad . \quad . \quad . \quad . \quad (a)$$

and if Hund's formula holds then

$$\bar{p}_2 = 4{\cdot}97\,\mu_B. \quad . \quad . \quad . \quad . \quad . \quad . \quad . \quad (b)$$

For n_2 we get the values :

$$n_2 = {\cdot}76 \times 10^{16} \text{ according to } (a)$$
$$= {\cdot}99 \times 10^{16} \quad ,, \quad (b)$$

TABLE III.

Spectral terms.	$p=\sqrt{4s(s+1)}$	$=\sqrt{4s(s+1)+l(l+1)}$.	$=g\sqrt{j(j+1}$
^4F	3·8	5·2	·78
^2G	1·73	4·8	3·42 5·53
^2H	1·73	5·75	4·43 6·5

If the rise in temperature of the solution due to light absorption per second be ΔT, and the time taken for a single reading be t seconds, then the diminution of susceptibility of the solution due to rise of temperatures is

$$\Delta K = -\frac{n_0 p_1^2}{3k} \cdot \frac{\Delta T}{T^2} \cdot t.$$

ΔT is ·0014° and t is taken as 3″ and $n_0 = 9{\cdot}2 \times 10^{20}$ then

$$\Delta K = -13 \times 10^{-11}.$$

Introducing this correction, the value of n_2 is increased to 2·3 and $3{\cdot}0 \times 10^{16}$ resp.

To find the number N_2 of photons absorbed per second, we measured, according to the method described above, the amount of energy ΔE absorbed per second in unit volume of the given solution of $CrCl_3$. The value of ΔE is found to be 20×10^4 ergs per sec.

The value of

$$N_2 = \frac{\Delta E}{h\nu} = 5{\cdot}36 \times 10^{16}.$$

It is thus found that these two quantities, n_2 and N_2, are of the same order of magnitude, and this indicates that the mean life of the ion in the excited metastable state is rather high. We have tried to obtain an estimate of the value of N_2 from Einstein's formula ; but without introducing a term to take into account the effect of the collision in reducing the number of metastable ions, we get the result that about half the ions are in the upper state.

Summary.

The present paper gives a further account of investigations on the increase in the paramagnetic susceptibilities (photomagnetic effect) of crystals and solutions containing ions of the iron group of elements. A new apparatus, which is a modification of the well-known O-tube arrangement, is described ; it is not so sensitive as the torsion balance described in a previous paper ; but it enables quantiative measurements to be made. Amongst the results obtained are :—

(i.) Increase in susceptibility due to light absorption of a solution containing vanadium ions of different valencies and of a crystal of $NiSO_4$, $7H_2O$.

(ii.) The P.M.E. in aqueous solutions containing ions Ni^{++}, Cr^{+++}, Co^{++} have been measured quantitatively, and their magnitudes for the same amount of light absorbed are found to diminish in the order in which the ions are arranged. It is found that the effect is roughly proportional to the quenching of the orbital moment of these ions in their ground states.

(iii.) Solutions of Cr^{+++} and Ni^{++} in dil. HCl solutions were found to give negligibly small P.M.E. even with increased absorption of light energy by these solutions. This behaviour is attributed to the presence of undissociated paramagnetic molecules in these solutions which absorb the light and in which the orbital moment of the paramagnetic ion is equally quenched both in the initial and in the final states.

(iv.) In a solution containing ·078 gm. Cr^{+++} per c.c. with $K = 13{\cdot}4 \times 10^{-6}$ the increase in volume susceptibility

is found to be 7×10^{-11} C.G.S. units On certain assumptions as to the state of the ions in the excited state it is found that about 10^{16} ions out of a total of 10^{20} Cr^{+++} ions are in the excited state. From a measurement of the amount of light energy in the solution it is concluded, on certain assumptions, that about $5{\cdot}4\times10^{16}$ photons are absorbed per second per c.c. of the solution. A theoretical discussion of the effects observed under (ii.) and (iii.) is given.

References.

(1) Bose and Raha, *Zeits. f. Phys.* lxxx. p. 361 (1933).
(2) Bose and Datta, *Zeits. f. Phys.* lxxx. p. 376 (1933).
(3) Hector and Wills, Phys. Rev. xxiii. p. 209 (1924).
(4) M. N. Saha, 'Nature,' cxxv. p. 163 (1930).
(5) Kato, Sc. P. Inst. Phys. Chem. Res. xiii. p. 22 (1930).
(6) S. Datta, Phil. Mag. xvii. p. 585 (1934).
(7) Stoner, Phil. Mag. viii. p. 250 (1929).
(8) Bose, *Zeits. f. Phys.* lxv. p. 693 (1930).
(9) Saha and Deb, All. Acad. Sci. i. p. 8 (1932).
(10) Van Vleck, 'Electric and Magnetic Susceptibilities,' p. 287 ; Phys. Rev. xli. p. 208 (1932); Penney and Schlapp, *ibid.* xli. p. 194 (1932).

University College of Science,
Calcutta.

XI. *The Oscillations of Atmospheric Mercury Arcs.* By Vivian Voss, *M.A., Ph.D.* (*Senior Lecturer in Physics, University of Pretoria*) *.

[Plate I.]

An attempt was made some time ago in this laboratory to get mercury arcs of the "atmospheric" type to run off a source of a.c. supply. A very simple form of arc-tube was mainly used in these experiments. Two vertical pyrex tubes of diameter approximately 5 mm. were joined below by a horizontal capillary tube. Mercury was introduced and strongly heated. By sucking the mercury from side to side bubbles of gas were removed. The current was passed through iron wires dipping into the mercury in the vertical side-tubes.

It is well known that if a small current, say 0·1 amp., from a d.c. supply of, say, 220 volts is passed through

* Communicated by the Author.

this capillary then, if the mercury in the capillary is heated till the thread breaks, an arc will form at that point and will burn indefinitely, the heat of the arc keeping the threads separated. These arcs are useful in the laboratory for spectroscopic work, but as the town supply in Pretoria is 250 volts a.c. it would be more convenient to be able to run these arcs off an a.c. circuit than from a d.c. generator.

Arc-tubes of various shapes and sizes were constructed. In each of them it was found possible to run a d.c. arc, but in only two or three would an a.c. arc run for any length of time. In a d.c. circuit the arc runs smoothly and silently when the capillary is of fine bore. With coarser bores the arc runs with a hammering noise. Originally pyrex tubing only was used. The finest pyrex capillary available in this laboratory had a diameter of about 0·8 mm. This tubing was heated and drawn out to a finer bore, but naturally it was not possible to get this quite uniform along the tube. By chance one of the first arc-tubes constructed allowed an a.c. arc to run steadily for an indefinite period; but other tubes of approximately the same dimensions would not allow the a.c. arc to run at all, or only for short periods of time. It was then decided to investigate the whole problem very thoroughly for both d.c. and a.c. arcs.

D.C. Arcs.

An arc which was hammering slightly was examined in a rotating mirror, and it was immediately seen that the arc-gap was opening and closing in a very regular manner. To obtain a photographic record of the oscillation a simple camera of the following type was constructed (see fig. 1, elevation).

The camera-box was of wood, painted black inside and out. L was a lens taken from a photographic enlarger, C a cardboard cap fitting loosely over the lens; D was a wooden drum turning freely on a horizontal axle; *a*, *b*, *c*, *d*, etc. were eight nails driven in horizontally in a circle concentric with the axis of the drum. The diameter of the wooden drum was 3·75 inches, and its width was 2 inches. P was a steel projection screwed into the drum; E an elastic band with a loop at each end, one loop being slipped over a hook, *h*, and the other

over one of the nails, *a*. At H a brass tube passed horizontally through the side of the box. A brass rod, longer than the tube and fitting it closely, passed through the tube. The rod could be slightly withdrawn and the drum rotated counter-clockwise till P was in contact with the left side of the stop S, fixed to the base of the box. If the rod were now pushed in it would prevent the drum from rotating. A strip of white paper was pinned to the drum, the cap C removed, and the camera adjusted till a sharp image of the arc to be photographed was visible on the white paper. The room was now darkened and a strip of photographic film passed round the drum and fixed to it by a drawing-pin pushed through its overlapping ends into the wooden drum. The lid of the box was now put on, cap C replaced, and the loaded

Fig. 1.

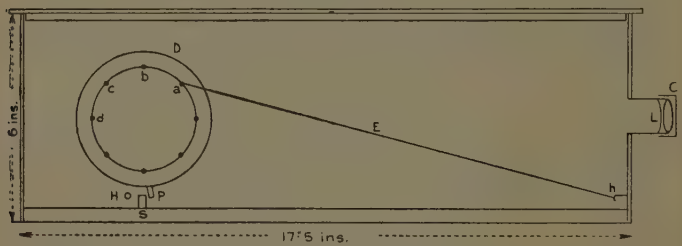

camera was ready for an exposure. The arc would be restarted, the cap C removed, the rod pulled out slightly, and the elastic band E would then cause the drum to rotate till P was stopped by S.

When the arc which was hammering slightly was photographed with this camera it was seen (Pl. I. (i.)) that the arc-gap collapsed to nothing in between flashes. The arc starts at one of the lower jagged edges, the gap widens to a maximum and then decreases to nothing (as indicated by the sharp points on the tops of the flashes). If the current is increased the amplitude of the oscillation increases and it may happen that the arc-gap no longer closes in between flashes (Pl. I. (ii.)). If this happens the "hammering" ceases completely. The hammering is thus no doubt due to the mechanical

impact of the two threads of mercury when the gap closes.

The timing of the frequency of the oscillation was done with a stroboscopic disk. This was a white disk with an outer ring of 16 equidistant black spots. Inside this ring was another containing 12 spots, and inside this again one with 8 spots. The disk was rotated by means of an electric motor. After every 100 revolutions of the disk a bell rang, and this interval could be timed with a stop-watch. The speed of rotation could be regulated with a rheostat, but a finer adjustment could be got by holding a finger lightly against the edge of the disk.

It was thought at first that if some of the mercury from the side-tubes were removed the period of oscillation would be altered, as the mass of oscillating mercury would be decreased. It was found, however, that even when the head of mercury in the side-tubes was altered from, say, 4 cm. to 1 cm. that the period was not affected appreciably. On considering the matter more carefully it was realized that the mass of oscillating mercury was that contained in the *capillary* tube, the head of mercury in the side-tubes merely affecting the pressure in the arc-gap. The column of oscillating mercury in the capillary tube bears some resemblance to the column of air in an organ-pipe. Any "end-effect" would probably be negligibly small, as the length of the capillary was always very great compared to its diameter.

Preliminary experiments showed that the period of oscillation depended upon (1) the length of the capillary, (2) the diameter of the capillary, (3) the pressure in the arc-space, (4) the amplitude of the oscillation. Before considering a theory to account for the continuous oscillations which take place we must first determine how the rate of electrical heating in the arc-space depends upon the length of that space The source of d.c. supply was a generator giving 218 volts. An ammeter and a rheostat were connected in series with the arc. Pairs of readings were taken on the ammeter with and without the arc running; from these the resistance of the arc could be calculated and so the rate of electrical heating. The arc was oscillating, but the gap closed periodically as in (Pl. I. (i.)). Suppose, *e. g.*, the current when the arc was running was 0·105 amp. and 0·127 when the arc

was not running. If i_0 were the current when the gap was a maximum, then, roughly, $\frac{i_0+0{\cdot}127}{2}=0{\cdot}105$, *i. e.*, $i_0=0{\cdot}083$ amp. Again, if resistance of rheostat were R ohms and maximum resistance of arc were r ohms then $0{\cdot}083=\frac{218}{R+r}$, and $0{\cdot}127=\frac{218}{R}$ $\therefore$ $r=910$ ohms,

Maximum length of gap.	Current when arc not running.	"Mean" current when arc is running.	i_0.	Rate of electrical heating for max. gap-length.
8·5 mm.	0·127 amp.	0·105 amp.	0·083 amp.	$(\cdot083)^2\times910$ $=6{\cdot}3$ watts
10·5 mm.	0·163 amp.	0·132 amp.	0·101 amp.	$(\cdot101)^2\times821$ $=8{\cdot}4$ watts
15·0 mm.	0·189 amp.	0·141 amp.	0·093 amp.	$(\cdot093)^2\times1191$ $=10{\cdot}3$ watts
18·0 mm.	0·210 amp.	0.150 amp.	0·090 amp.	$(\cdot090)^2\times1385$ $=11{\cdot}2$ watts
22·0 mm.	0.236 amp.	0·162 amp.	0·088 amp.	$(\cdot088)^2\times1553$ $=12{\cdot}0$ watts
28·0 mm.	0·271 amp.	0.172 amp.	0·073 amp.	$(\cdot073)^2\times2182$ $=11{\cdot}6$ watts

Fig. 2.

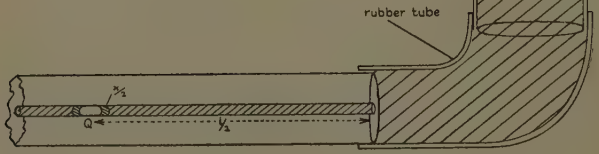

and the rate of electrical heating would be $(0{\cdot}083)^2\times910$ $=6{\cdot}3$ watts when the gap was at its maximum length.

For each pair of readings the maximum arc-length was determined with a low-power telemicroscope having an eyepiece scale.

For currents above this the gap does not close. It is evident that for moderate arc-lengths the rate of electrical heating increases with the length of the arc-space.

To account for the oscillations of the arc we must explain: (1) why the arc should oscillate at all; (2) why it should go on oscillating indefinitely; (3) how the oscillation period varies with the length of the oscillating column, the diameter of the column, and the pressure in the arc-space.

Suppose for the moment that the arc could stop oscillating. The gap would then adjust itself till the rate at which heat was lost by conduction and by radiation was just equal to the rate of electrical heating. When equilibrium obtains the vapour pressure in the gap will be $p=(\mathrm{H}+h)\rho g+\frac{2\mathrm{S}}{r}$, where H is the barometric height in cm. of mercury, h the head of mercury in the side-tubes, ρ and S the density and surface tension respectively of mercury, and r the radius of the capillary.

Suppose now that the tube is jarred and that as a result the arc-gap Q (fig. 2) is, say, slightly lengthened. The electrical heating increases, causing a further lengthening. The expansion occurs very suddenly, and we may regard the mercury vapour as behaving approximately like a gas. The adiabatic expansion causes a lowering of the vapour pressure, and when this outweighs the effect of the electrical heating the outward movement of the mercury columns ceases and the external pressure forces them inwards. As the gap shortens the electrical heating gets less, causing further shortening, but there is an adiabatic increase in pressure, and this will arrest the inward movement of the columns. With the larger currents the photographs (*e. g.*, Pl. I. (ii.)) show that the columns never actually touch each other, but when the current is reduced they do (Pl. I. (i.)). But of course this does not necessarily mean that the vapour space vanishes entirely. The mercury columns may merely touch peripherally, leaving a vapour space inside.

The above argument explains why the arc should oscillate and go on oscillating indefinitely.

If the mean volume of the arc-space is v, the pressure p, and the ratio of the specific heats of mercury γ, then $pv^{\gamma}=$constant.

$$\therefore \quad -\delta p=\frac{\gamma p}{v}\,.\,\delta v.$$

If a simple expression is to be found for the oscillation

period then, as in so many other types of oscillation, only small amplitudes must be considered. For small amplitudes the average length of the arc-space is of the order of the bore of the capillary tube. Thus the mean volume v may be written $\pi r^2 . kr$, where k is small.

Then

$$-\delta p = \frac{\gamma p \pi r^2 x/2}{k\pi r^3} = \frac{\gamma p x}{2kr} \text{ (see fig. 2).}$$

This gives the decrease in pressure in the arc-space; therefore the retarding force acting on the mercury column in the capillary is

$$\frac{\gamma p x}{2kr} . \pi r^2,$$

and this must be equal to

$$-\pi r^2 \frac{l}{2} . \rho . \frac{d^2x}{dt^2};$$

$$\therefore \quad \frac{d^2x}{dt^2} + \frac{\gamma p x}{krl\rho} = 0.$$

Therefore period of oscillation is

$$T = 2\pi \sqrt{\frac{k\rho}{\gamma} . \frac{rl}{p}}.$$

Variation of T *with* l.

To find experimentally the variation of T with l a length of 48·5 cm. of capillary tubing was chosen, diameter 0·059 cm. Soft-glass capillary tubing was used, as no fine-bore pyrex was available. The coarser pyrex capillary tubing could not be drawn down, as it was of course necessary to have the radius constant if the length was to be varied. Vertical side-tubes of about 5 mm. diameter were joined to the horizontal capillary by rubber tubing (as in fig. 2). The method adopted to get rid of bubbles after the mercury had been introduced was the following: the whole of the horizontal tubing was heated by moving a pointed flame back and forth along it; the thread broke up into innumerable gaps; by repeatedly pinching one of the rubber connexions sharply these bubbles could be driven over to the opposite side-tube; after repeating this three or four times the

arc would burn steadily when started, but without this treatment it would not burn at all.

The arc would be set going near the stroboscopic disk in an otherwise dark room. The speed of the disk would be increased till the outer ring of 16 spots appeared stationary, with their true spacing, for the first time. This will for convenience be referred to as the " normal speed " of the disk. By glancing at the inmost ring of 8 spots it is immediately possible to tell whether the disk is rotating at the normal or at twice the normal speed. If the former, then there appear to be 16 stationary spots in the inmost ring, if the latter then 8 stationary spots. The most convenient way to proceed to shorter lengths of capillary tubing was found to be to make two file-scratches the required distance apart on the horizontal tubing. One end would now be raised till the mercury had dropped below that file-mark. The tube would then be broken there, the short piece removed, and the side-tube reattached by rubber tubing. The process would be repeated at the other end. In this way no new mercury was introduced, and so no bubbles had to be removed.

Length of capillary tubing.	Time for 100 revs. of disk.
48·5 cm.	$2 \times 50{\cdot}8$ sec.
40·4 cm.	$2 \times 47{\cdot}6$ sec.
32·2 cm.	$2 \times 41{\cdot}6$ sec.
24·4 cm.	$2 \times 35{\cdot}6$ sec.
16·4 cm.	$2 \times 29{\cdot}2$ sec.
10·0 cm.	$2 \times 23{\cdot}4$ sec.
6.6 cm.	$2 \times 19{\cdot}0$ sec.

The times for 100 revolutions are multiplied by 2 because the disk was run at twice the " normal " speed. The oscillation periods will of course be proportional to the times of revolution. When log T is plotted against log l (fig. 3) the slope comes to 0·49, *i. e.*, T varies nearly as $\sqrt{l}$. In each case the amplitude was kept as small as possible, *i. e.*, the maximum arc-length was always about 5 mm. In a previous experiment, performed

before it was realized that the amplitude had to be kept small, a set of readings of T and l were taken with the maximum arc-length 13 mm. in every case. On plotting log T against log l the points lay very nearly on a straight line of which the slope was 0·47.

Fig. 3.

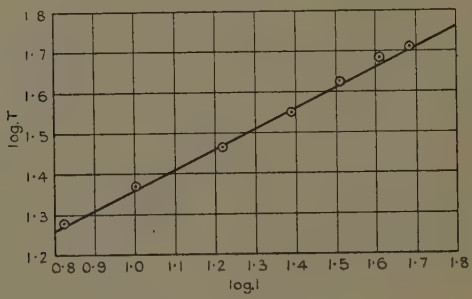

Variation of T *with Pressure.*

The pressure of the vapour in the arc-space is

$$p=(\mathrm{H}+h)\rho g+\frac{2\mathrm{S}}{r}.$$

In the experiment below the extreme values of h were 3·7 and 98·3 cm. The capillary tube used had a diameter of 0·043 cm. and was 10 cm long. When the barometer height is 65·7 cm. and the head of mercury in the side-tubes is 3·7 cm. the pressure in the arc-space is 69·4 cm. of mercury if we neglect the surface tension term. At 354° C. the pressure of mercury vapour is 69·4 cm. of mercury, and so, if we regard 354° C. as being approximately the temperature of the ends of the mercury columns bounding the arc-space, we can calculate the surface tension of this mercury from the formula $\mathrm{S}_t=\mathrm{S}_0-0{\cdot}379\,t$. Taking S_0 to be 450 dynes per cm., we find S_{354} to be 316. Similarly when h=98·3 cm. the temperature of the vapour will be a little more than 400° C., and we find S_{400} to be approximately 300 dynes per cm. If we consider only the mean value of the surface tension, 308 dynes per cm., then

$$\frac{2\mathrm{S}}{r}=\frac{2\times308}{0{\cdot}0215\times13{\cdot}6\times980}=2{\cdot}2 \text{ cm. of mercury.}$$

Thus the pressure in the arc-space is $(65{\cdot}7+2{\cdot}2+h)$ cm. of mercury.

Head of mercury.	Pressure in arc-space.	Time for 100 revs.
3·7 cm.	71·6 cm. of mercury	2×21 sec.
9·9 cm.	77·8 cm. ,,	2×20·1 sec.
15·6 cm.	83·5 cm. ,,	2×19·2 sec.
27·5 cm.	95·4 cm. ,,	2×17·6 sec.
34·6 cm.	102·5 cm. ,,	2×16·9 sec.
46·8 cm.	114·7 cm. ,,	2×16·4 sec.
57·2 cm.	125·1 cm. ,,	2×16·0 sec.
74·5 cm.	142·4 cm. ,,	2×15·0 sec.
98·3 cm.	166·2 cm. ,,	2×13·6 sec.

Fig. 4.

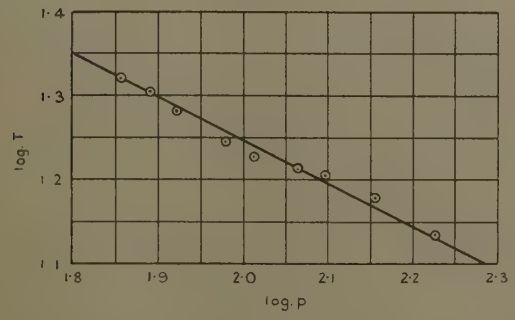

In each case the timing of 100 revolutions of the disk was repeated several times, and in column 3 the mean times are given. The actual times, for example, when $h=3{\cdot}7$ cm., were: 21·1, 20·8, 20·9, 21·0, 21·0, 20·9, 21·0 sec.

As before the amplitudes were always kept constant and as small as possible.

When log T is plotted against log p (fig. 4) the slope is found to be $-0{\cdot}51$, which is very near the theoretical value $-0{\cdot}50$.

Variation of T *with r.*

Before the theoretical expression for the oscillation period had been obtained an attempt had been made to determine experimentally how the period varied with the diameter of the tube. The periods of oscillation were determined for tubes of different bore, keeping the maximum arc-length (which we shall call λ) constant in each case. Various sets of readings were taken. More sets were also taken in which λ was kept as small as possible. In each case log T was plotted against log diameter, and a straight line drawn lying as evenly as possible between the points. Rather low haphazard values were obtained for the slopes of these lines. When the matter was reconsidered in the light of the theoretical expression for the period it was realized that not only had the amplitudes to be small but the mean arc-length had in each case to bear a constant ratio to the diameter of the tube.

Six tubes were now selected, with diameters varying from 0·485 to 1·314 mm. Each tube was cut to a length of 40 cm. A seventh shorter tube of diameter 0·814 mm. was included in this set. A length of only 18·65 cm. of this tubing could be obtained, but the oscillation period for a length 40 cm. could be calculated, since it had been shown experimentally that the period varied as the square root of the length of the capillary. The diameter of each tube was determined by weighing a mercury thread of measured length in it. A set of readings of T and λ was taken with each tube. λ was determined by means of a low-power telemicroscope with an eyepiece scale, and observing through a piece of smoked glass. The values of the divisions in the eyepiece were determined in each case by sighting on a mm. scale placed directly below the tube being tested. T was plotted against λ for each tube, so that the values of T for a constant ratio λ/d could be obtained for all the tubes. Since the values of T for small λ's could not be determined accurately (because here the arc was on the point of going out) it was obviously difficult to decide the exact course taken by the curves, for small λ's, and hence the values of T determined by *extrapolation* (for example for $\lambda=3d$), were inaccurate. So, rather, the smallest *observed* value of T for the tube of smallest diameter (0·485 mm.) was chosen as a starting-point, and for this tube $\lambda/d=15$.

Then for each of the other tubes the value of T for the same ratio λ/d was determined by interpolation. The actual readings for the different tubes were as follows (the head of mercury in the side-tubes was always 3 cm.; the small changes in the surface tension term, which itself was small, were neglected; for these long tubes the stroboscopic disk was always run at four times the "normal" speed):—

TUBE *a*: diameter $4{\cdot}85\times10^{-2}$ cm.; 10 scale-divisions in eyepiece correspond to 6·3 mm.

λ in scale-divisions	26·8	24·5	22·0	18·5	16·5	15·0	14·5	11·5
T (to be multiplied by 4) ..	25·8	25·2	24·7	24·4	24·0	23·4	23·0	22·5 sec.

TUBE *b*: diameter $5{\cdot}89\times10^{-2}$ cm.; 10 scale-divisions correspond to 6·35 mm.

λ in scale-divisions	31·0	25·6	23·5	21·0	19·0	16·4	14·0
T (to be multiplied by 4) ..	29·4	27·8	27·2	26·6	26·3	25·6	25·1 sec.

TUBE *c*: diameter $8{\cdot}14\times10^{-2}$ cm.; 10 scale-divisions correspond to 6·3 mm. This tube 18·65 cm. long.

λ in scale-divisions	39·0	34·5	31·0	27·0	22·8	19·0	17·8	17·2	13·5
T (to be multiplied by 4) ..	23·8	23·0	22·3	21·8	20·7	20·2	19·9	20·1	19·2 sec.

TUBE *d*: diameter $9{\cdot}80\times10^{-2}$ cm.; 10 scale-divisions correspond to 6·45 mm.

λ in scale-divisions	41·0	34·0	31·0	29·0	26·0	21·5	18·5	18·0	15·0
T (to be multiplied by 4) ..	36·2	33·9	32·8	32·4	31·6	30·8	30·5	30·2	29·8 sec.

TUBE *e*: diameter $10{\cdot}60\times10^{-2}$ cm.; 10 scale-divisions correspond to 6·24 mm.

λ in scale-divisions.....	45·0	40·75	40·25	35·5	29·5	26·5	26·0	21·5	16·0
T (to be multiplied by 4)..	38·1	37·2	37·0	36·0	34·4	33·6	33·5	31·65	29·9 sec.

TUBE f: diameter $12{\cdot}24\times10^{-2}$ cm.; 10 scale-divisions correspond to 6·45 mm.

λ in scale-divisions	41·5	39·0	31·0	24·0	18·2	15·0
T (to be multiplied by 4)..	39·5	37·8	35·5	33·6	32·55	32·2 sec.

TUBE g: diameter $13{\cdot}14\times10^{-2}$ cm.; 10 scale-divisions correspond to 6·25 mm.

λ in scale-divisions	38·0	34·0	33·0	29·2	25·0	22·0	18·2
T (to be multiplied by 4)..	40·0	38·8	38·6	37·47	36·0	35·4	34·44 sec.

The following are the values of T for the different tubes corresponding to the ratio $\frac{\lambda}{d}=15$ for each tube:—

Tube.	Diameter.	T.
a	$4{\cdot}85\times10^{-2}$ cm.	22·50 sec.
b	$5{\cdot}89\times10^{-2}$ cm.	25·10 sec.
c	$8{\cdot}14\times10^{-2}$ cm.	29·42 sec. (corresponding to length 40 cm.)
d	$9{\cdot}80\times10^{-2}$ cm.	30·95 sec.
e	$10{\cdot}60\times10^{-2}$ cm.	33·30 sec.
f	$12{\cdot}24\times10^{-2}$ cm.	34·58 sec.
g	$13{\cdot}14\times10^{-2}$ cm.	38·15 sec.

When log T was plotted against log d the seven points lay approximately along a straight line (fig. 5), and the slope of this line was 0·50. This result gives further experimental support for the theoretical expression for T. We may test the expression further by making a direct substitution of the values obtained with one of the tubes, say tube b above. The "normal" speed of rotation of the stroboscopic disk is $4\times25{\cdot}1$ sec. The oscillation period is therefore $\frac{4\times25{\cdot}1}{1600}$ sec.$=0{\cdot}063$ sec. In the expression $2\pi\sqrt{\frac{k\rho}{\gamma}\cdot\frac{rl}{p}}$, kr is the mean length of the

arc-space, and is therefore roughly one-half the observed *maximum* length (from the nature of the case this can only be approximately true). Thus $kr=\lambda/2$, *i. e.*, $k=\lambda/d=15$. The density $\rho=13{\cdot}6$ gm. per c.c., radius $r=2{\cdot}945\times10^{-2}$ cm., length $l=40$ cm., ratio of specific heats $\gamma=1{\cdot}67$, pressure $p=70\times13{\cdot}6\times980$ dynes per sq. cm. approximately. On substituting these values in the expression we obtain the value 0·055 sec. It is difficult to assess the agreement between this value and the actual oscillation period 0·063 sec., owing to the uncertainty in the value of k. The theoretical expression does, at any rate, give an oscillation period which is of the right order.

Fig. 5.

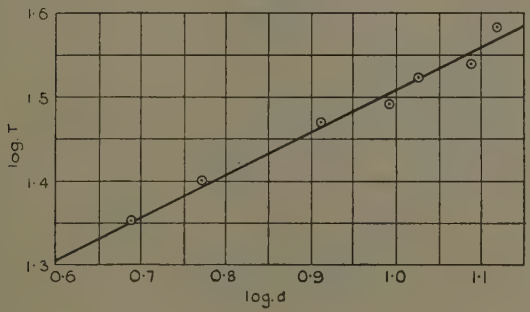

Non-oscillating Arc.

An arc-tube was next constructed of pyrex (fig. 6). The capillary was about 8 cm. long and had a diameter of just under 1 mm. Side-tubes, 1 cm. diameter, were sealed on. Mercury was introduced and heated to remove all bubbles. A fine hole was made with a hot pin in each of two corks, which were then pushed down the side-tubes till they touched the mercury. Iron wires were then pushed through the holes and sealing-wax was run in on top of the corks. If direct current from a 218 volt generator were passed through this tube, with an ammeter and rheostat in series, and the mercury thread in the capillary were split with a pointed flame (some mercury being forced up into tiny orifices in the cork), an arc would burn quite steadily and with great brilliancy.

The ammeter showed 0·16 amp. when the arc was not running and 0·06 amp. with the arc running. With the side-tubes open and the arc oscillating the ammeter read 0·14 amp.

It can be shown from these readings that the steady arc with the smaller current consumes more than twice the watts used by the oscillating arc with the larger current.

These non-oscillating arcs are most useful in the laboratory, as they burn with great brilliancy and show no tendency to go out. They can be constructed in a few minutes. If the arc is used continuously for a long time it gradually creeps in the direction of the positive

Fig. 6.

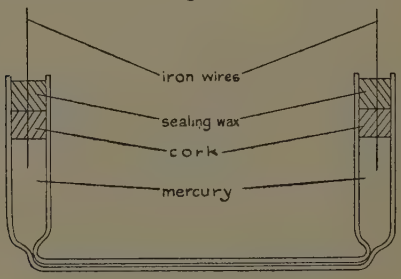

mercury column. This is due to the positive being the hotter end, the mercury gradually distilling over to the other end of the arc-space. When this arc is examined in a rotating mirror the horizontal line of light is drawn out into a vertical band of constant width which shows a remarkable resemblance to the light from an electrical discharge passing through a gas at low pressure. Even the well-known "striations" appear to be present and make the similarity more striking. Of course this similarity is spurious, as these apparent "striations" are parallel to the *length* of the arc. They are evidently fluctuations in the intensity of the arc, but they occur with extraordinary regularity. Pl. I. (iii.) shows a photograph taken with the camera described above. These intensity fluctuations were also frequently observed with oscillating arcs. When such an arc was examined in a rotating mirror these high-frequency

intensity fluctuations would sometimes be clearly visible in the drawn-out band of light. In the case of the steady arc the intensity-fluctuations are so distinct that their frequency can be determined with the stroboscopic wheel. There are indications that the effect may be due to a commutator ripple from the generator, but this explanation does not seem to be wholly satisfactory. The matter is still being investigated.

A.C. Arcs.

Among the earlier arc-tubes which had been constructed of pyrex one was found which allowed an arc to run indefinitely in an a.c. circuit. The frequency of the town mains here is 50 cycles per sec., *i. e.*, 100 alternations per sec. When the frequency of the arc-flashes was determined with the stroboscopic disk it was found to be exactly 50 per sec. for all currents at which the arc would run (Pl. I. (iv.)). The next photograph (Pl. I. (v.)), was taken with the same tube but with a larger current flowing. It will be seen from the photographs that the arc ceases abruptly when the alternating voltage drops below a critical value. The mercury columns have not drawn together sufficiently to allow the arc to strike when the voltage rises in the reverse direction. In the succeeding half-cycle, however, the arc flashes on again. A d.c. ammeter was now put in series with the arc, and showed that the current was indeed unidirectional. The gap would almost certainly close up in between arc-flashes, but the point was settled experimentally by putting the steady arc described above immediately behind the a.c. arc. When the a.c. arc-flash ceased the steady arc shone through the gap, and the photographs show clearly that the gap closed completely (Pl. I. (vi.) and (vii.)). The latter was taken after the elastic band in the camera had been tightened. It is obvious that in Pl. I. (vi.) the steady arc was somewhat to one side of the a.c. arc. If the current through the intermittent arc be small it can be readily understood that the gap-opening might not be complete each time, *i. e.*, that when the columns spring apart a narrow film of mercury might occasionally persist along the glass wall. When this happens the rectified current might reverse in direction. These occasional

reversals were actually found to occur with small currents. For larger currents, however, as might be expected, no such reversal took place. It was thought that further light might be thrown on the process if it could be determined whether, in the event of the a.c. current being suddenly stopped, the gap would open spontaneously. The steady arc was again mounted directly behind the a.c. arc. Just after the drum in the camera had been released a switch was opened in the a.c. arc-circuit. The negative (Pl. I. (viii.)) showed that the gap opened and shut four times after the alternating current had been stopped. Another negative showed five subsequent openings of the gap. In considering the process that takes place an analogy may be useful. Imagine a metal cylinder resting on a horizontal plate. The bottom of the plate, below the cylinder, is struck at regular intervals with a hammer. If the cylinder has time to descend, in between blows, then it will jump with the frequency of the blows. If the frequency of the blows is increased the cylinder frequency will increase at exactly the same rate up to a certain point. Beyond this stage the cylinder will not have time to descend in between successive blows, and its jumping frequency will suddenly drop to half the value of the blow frequency. It will now follow at half the frequency up to a further point, when it will suddenly drop to one-third of the blow frequency, and so on. Of course the analogy is not exact; there are not, strictly, electrical *impulses* corresponding to the *blows* of the hammer. Each arc-flash lasts for an appreciable portion of the total time between successive closings of the gap. This latter time we shall refer to as the period of the forced vibration.

To study these forced oscillations the 218 volts d.c. generator was used, and the current interrupted by means of a Cohen interrupter. The frequency of the interruptions was gradually increased from some low value, and the arc-flashes were found to remain exactly in step up to a certain point. Then the frequency of the flashes dropped to exactly half that of the interruptions, and remained half till some higher limiting frequency was reached, when it suddenly dropped to one-third that of the interruptions. At a still higher frequency it dropped to one-fourth that of the interruptions. The frequency of the interruptions was determined by passing the current

through a neon lamp through the Cohen interrupter and measuring the frequency of the neon flashes with the stroboscopic wheel. During these experiments the maximum arc-lengths were kept constant. To consider the analogy for a moment, suppose the frequency of the hammer-blows is three times that of the cylinder. Keep the frequency constant but decrease the strength of the blows. The height to which the cylinder jumps will decrease, and presently the frequency of the cylinder will suddenly increase to one-half that of the blows. If the strength of the blows is further decreased the frequency of the cylinder will suddenly increase to exactly that of the blows. A similar thing was done with the interrupted d.c. arc. The frequency of the interruptions was, say, three times that of the flashes. Now either the mercury cup on the interrupter was lowered away from the platinum prong (thus decreasing the time of flow of the current) or the resistance in the circuit was increased, either of these decreasing the amplitude of the arc oscillation. The arc would begin to flicker uncertainly and then suddenly settle down to a steady oscillation once more, with a smaller amplitude. Its frequency is now half that of the interruptions. If the process of decreasing the amplitude is continued the arc will begin to flutter again and then suddenly settle down with a very small amplitude and the same frequency as the interruptions—which is all as we should expect. The suddenness and definiteness with which the arc settles down, with a steady buzz, is quite striking. It is possible to get the interrupted d.c. arc to run with a much smaller amplitude than was possible with the continuous d.c. oscillating arc. It is actually possible in some cases to decrease the amplitude to such an extent that the arc becomes a little yellow glowing point of light, so faint that it will not illuminate the stroboscopic disk sufficiently to allow a timing to be done.

To return to the analogy, the time taken by the cylinder to fall back from its maximum height to the plate is always proportional to the total time from the instant the blow is struck, *i. e.*, when the cylinder leaves the plate, till the cylinder gets back to the plate. Now in the case of the arc, although the arc-flash does not last merely for an instant as the hammer-blow does, still the symmetry with which the gap is seen to open and close, about

the dotted line, in Pl. I. (vi.) makes it reasonable to assume that the time taken for the gap to close after its maximum opening is proportional to the total time from the instant the gap opens till it closes again, *i. e.*, to the period of the forced oscillation.

Interrupted d.c. arcs. Variation of T *with l.*

Suppose now that interrupted arcs are run in tubes of different lengths but all of the same diameter. Let the maximum opening be the same in each case, and be denoted by s. Suppose t is the time taken for the columns to come together again after their maximum separation, and α their relative acceleration. Theoretically we again consider only very small amplitudes.

Then, for two tubes of different lengths,

$$s=\tfrac{1}{2}\alpha_1 t_1^2=\tfrac{1}{2}\alpha_2 t_2^2;$$

$$\therefore \quad \frac{t_1^2}{t_2^2}=\frac{\alpha_2}{\alpha_1}.$$

But if P is the restoring pressure acting on the mercury columns, r the common radius of the capillaries, and l_1 and l_2 their lengths, then, the restoring force being equal to the product of mass by acceleration, we have

$$\mathrm{P}\,.\,\pi r^2=\pi r^2 l_1\rho\alpha_1=\pi r^2 l_2\rho\alpha_2;$$

$$\therefore \quad \frac{\alpha_2}{\alpha_1}=\frac{l_1}{l_2};$$

$$\therefore \quad \frac{t_1}{t_2}=\sqrt{\frac{l_1}{l_2}},$$

i. e., the periods should vary as the square roots of the lengths of the capillary tubes.

In testing this result experimentally the maximum lengths of arc-flashes were kept equal for all lengths of capillary tubing used by observing the interrupted arc through the telemicroscope. The maximum arc-length was always adjusted to correspond to eight divisions in the eyepiece scale. For instance, with a certain length of capillary tubing the wire on the Cohen interrupter was gradually tightened, thus increasing the

frequency of the interruptions. The rheostat in the arc circuit and the mercury cup on the Cohen interrupter were also both adjusted until the maximum frequency consistent with an arc-length eight divisions had been reached. The frequency of the arc-flashes was determined with the stroboscopic disk, and also the frequency of the interruptions. This was done, as before, with the help of a neon lamp. The two frequencies were found to be identical. As a check on this result the wire would be tightened considerably and the frequency of the flashes drop to half that of the interruptions. The maximum frequency of the interruptions under these circumstances would be determined as before. The process could be continued with the wire still tighter. It was sometimes difficult to get the arc to run long enough to enable the timing to be done with the stroboscopic disk. This difficulty was circumvented very easily as follows :—The neon lamp and the interrupted arc would be arranged so as to illuminate the stroboscopic disk simultaneously. The neon lamp would now be screened and the disk speeded up until there were 16 stationary spots in the outer ring and 8 in the inmost ring as seen by the light from the arc. Now the neon lamp would be uncovered and the arc screened. There might now appear to be 16 spots in both rings. This would tell us immediately that the frequency of the interruptions was twice that of the arc-flashes. Similarly a 1 : 1 ratio, or a 3 : 1 ratio (by observing the middle ring of 12 spots) could be detected immediately. The frequency of the neon-flashes could now be determined at leisure. The following readings were obtained. (In column 2 are the times for 100 revolutions when only the neon lamp illuminated the disk, and in column 3 when only the arc shone on the disk. With the longer lengths of capillary it was difficult, if not impossible, to reduce the frequency of the interruptions so as to be equal to that of the arc-flashes, unless, of course, the maximum arc-lengths were allowed to become less than eight scale-divisions.)

Log T was plotted against log l (fig. 7) and the slope found to be 0·47. Consider next an interrupted arc run in a capillary tube of constant diameter and fixed length but with various heads of mercury in the side-limbs.

The amplitude is again kept constant. For a small expansion δv of the gap we have

$$-\delta p = \frac{\gamma p}{v} \cdot \delta v.$$

Length of capillary.	T (neon-flashes).	T (arc-flashes).	Mean T (arc-flashes).
20·1 cm.	26·2 17·8	$2\times 26\cdot 2 = 52\cdot 4$ $3\times 17\cdot 8 = 53\cdot 4$	52·9
17·1 cm.	23·8 16·0	$2\times 23\cdot 8 = 47\cdot 6$ $3\times 16 = 48\cdot 0$	47·8
13·7 cm.	21·6 14·4	$2\times 21\cdot 6 = 43\cdot 2$ $3\times 14\cdot 4 = 43\cdot 2$	43·2
10·55 cm.	19·0 13·6	$2\times 19\cdot 0 = 38\cdot 0$ $3\times 13\cdot 6 = 40\cdot 8$	38·0 (uncertain)
7·85 cm.	32·4 17·2 11·9	32·4 $2\times 17\cdot 2 = 34\cdot 4$ $3\times 11\cdot 9 = 35\cdot 7$	33·4 (uncertain)
6·9 cm.	31·6 16·1 11·5	31·6 $2\times 16\cdot 1 = 32\cdot 2$ $3\times 11\cdot 5 = 34\cdot 5$	31·9 (uncertain)
6cm.	29·0 14·5	29·0 $2\times 14\cdot 5 = 29\cdot 0$	29·0

Fig. 7.

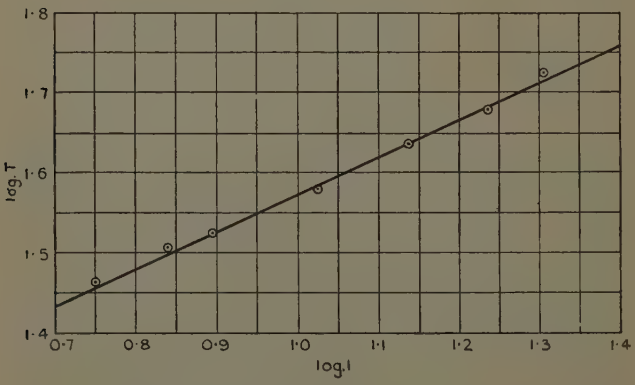

This decrease in pressure is the restoring pressure on the mercury columns, and, since the amplitudes are

kept equal, will therefore be proportional to the total pressure p, which is equal to $(H+h)\rho g+\frac{2S}{r}$. Let the restoring pressure be equal to cp, where c is a constant.

$$\frac{t_1^2}{t_2^2}=\frac{\alpha_2}{\alpha_1}.$$

But

$$cp_1 \cdot \pi r^2=\pi r^2 l\rho\alpha_1,$$

and

$$cp_2 \cdot \pi r^2=\pi r^2 l\rho\alpha_2 ;$$

$$\therefore \quad \frac{\alpha_2}{\alpha_1}=\frac{p_2}{p_1};$$

$$\therefore \quad \frac{t_1}{t_2}=\sqrt{\frac{p_2}{p_1}},$$

i. e., the periods should vary inversely as the square roots of the total pressures.

In the readings below the maximum arc-lengths were again constant and equal to eight scale divisions. The frequency of the interruptions was so chosen that it was always equal to the frequency of the arc-flashes. $\frac{2S}{r}$ was very nearly 2 cm. of mercury.

Head of mercury.	Total pressure p (65·7+2·0+head).	T.
4·0 cm.	71·7	36·6
13·8 cm.	81·5	32·5
24·0 cm.	91·7	31·6
31·9 cm.	99·6	30·0
48·8 cm.	116·5	28·5
61·1 cm.	128·8	27·0
77·6 cm.	145·3	25·6
97·5 cm.	165·2	24·0

Log T was plotted against log p (fig. 8) and the slope found to be $-0{\cdot}49$.

Variation of T *with Diameter.*

Consider next the case where the length of the capillary and the head of mercury are kept constant but the diameter is varied. The small change in the surface tension term is neglected.

As before,

$$-\delta p = \frac{\gamma p}{v} \cdot \delta v.$$

If the tube considered has a radius r_1 we may again write $v = k\pi r_1^3$. If the increase in volume δv means a

Fig. 8.

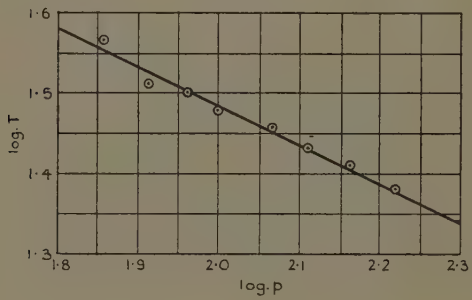

widening of the gap by a small amount s_1, then $\delta v = \pi r_1^2 \cdot s_1$;

$$\therefore \quad -\delta p_1 = \frac{\gamma p \cdot \pi r_1^2 \cdot s_1}{k\pi r_1^3} = k' \frac{s_1}{r_1},$$

where k' is a constant, since p will be the same for all the tubes.

Similarly for another tube

$$-\delta p_2 = k' \frac{s_2}{r_2}.$$

The restoring force on the mercury columns in the first tube will be

$$\frac{k' s_1}{r_1} \cdot \pi r_1^2 = \pi r_1^2 l \rho \alpha_1,$$

and similarly

$$\frac{k's_2}{r_2} \cdot \pi {r_2}^2 = \pi {r_2}^2 l \rho \alpha_2 ;$$

$$\therefore \quad \frac{s_1\alpha_2}{s_2\alpha_1} = \frac{r_1}{r_2}.$$

The ratio $\frac{s_1}{s_2}$ will be the ratio of the maximum openings of the gap.

Thus

$$\frac{s_1}{s_2} = \frac{\frac{1}{2}\alpha_1 {t_1}^2}{\frac{1}{2}\alpha_2 {t_2}^2},$$

$$\therefore \quad \frac{{t_1}^2}{{t_2}^2} = \frac{s_1\alpha_2}{s_2\alpha_1} = \frac{r_1}{r_2};$$

$$\therefore \quad \frac{t_1}{t_2} = \sqrt{\frac{r_1}{r_2}}.$$

In testing this result experimentally the maximum arc-lengths had to be chosen proportional to the diameters of the tubes.

Diameter of capillary.	Max. arc-length in scale-divs.	T (neon-flashes).	T (arc-flashes).	Mean T (arc-flashes).
$6{\cdot}61 \times 10^{-2}$ cm.	9·9	42 sec. 21 sec.	42 sec. $2 \times 21 = 42$ sec.	42·0
$5{\cdot}42 \times 10^{-2}$ cm.	8·1	37·8 sec. 18·9 sec.	37·8 sec. $2 \times 18{\cdot}9 = 37{\cdot}8$ sec.	37·8
$4{\cdot}81 \times 10^{-2}$ cm.	7·2	35·6 sec. 18·2 sec.	35·6 sec. $2 \times 18{\cdot}2 = 36{\cdot}4$ sec.	36·0
$4{\cdot}11 \times 10^{-2}$ cm.	6·2	32·4 sec.	32·4 sec. (tube cracked)	32·4
$2{\cdot}48 \times 10^{-2}$ cm.	3·7	26 sec. 13 sec.	26·0 sec. $2 \times 13 = 26{\cdot}0$ sec.	26·0

Log T was plotted against log d (fig. 9) and the slope found to be 0·49.

The above investigations throw some light on the difficulty originally experienced in getting an arc to run in an a.c. circuit. It is evident from the foregoing discussions as to the nature of the oscillation process that the frequency of an interrupted d.c. arc will not be very different to that of a continuous d.c. arc running in a tube of the same dimensions and at the same pressure. The factors controlling the oscillation frequency are (1) the diameter of the capillary, (2) its length, (3) the pressure, (4) the amplitude. It is easily possible to select the first three, so as to give us an intermittent arc of required frequency, and we are allowed considerable

Fig. 9.

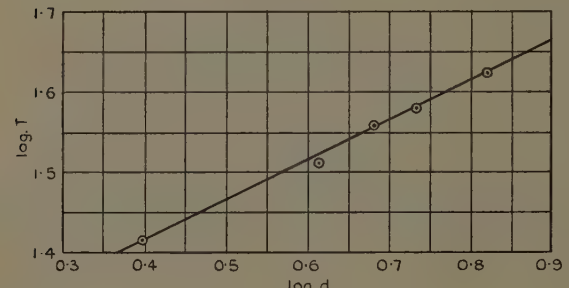

latitude in this selection because (4) controls the intermittent arc-frequency over such a wide range. In the first attempts to run a.c. arcs the diameter of the capillary was anything but uniform. In that case it becomes nearly impossible to select the other factors so as to give a required frequency; for while an arc is running it does not remain absolutely in one spot, but hunts lightly from side to side. If the bore is not uniform the frequency will be upset and the arc may get out of step with the electrical "impulses" and go out. But there is no difficulty at all in getting an a.c. arc to run in a uniform capillary. For capillary tubing of given diameter an estimate of the length necessary for a given frequency can be made by using the theoretical expression for the oscillation period. For instance, one of the capillaries used in the last set of experiments had

a diameter of 0·0248 cm. Suppose it was desired to run an arc at a frequency of 50 in this tubing. If the maximum arc-length is to be about 2 mm. then k will be about 8. The length of capillary required then comes to about 12 cm. If we wished the arc to run at a frequency of 100 the length would have to be a quarter of what it was for frequency 50, *i. e.*, about 3 cm. This was tested experimentally. A length of 5 cm. of this tubing was used. A d.c. ammeter was included in the circuit. It was easily possible, by adjusting the resistance in the circuit, to run an arc at a frequency of 50 per second off the town mains. This arc buzzed quite steadily and showed no tendency to go out or even to flicker. The ammeter showed a unidirectional current. Next the resistance in the circuit was increased. The arc flickered and then settled down sharply, with a smaller amplitude, to a frequency of 100. It was allowed to run for over an hour, and during this time showed no sign of flickering. The frequency was timed, as usual, with the stroboscopic wheel. The d.c. ammeter of course registered nothing. A photograph of the arc oscillating at a frequency of 100 is shown in Pl. I. (ix.).

Finally, it was found to be easily possible to get the arc to run off the a.c. mains at other frequencies besides 100 or 50. A tube of diameter 0·054 cm. was used and length about 8 or 9 cm. By adjusting the rheostat the arc was first made to run quite steadily at a frequency of 50 per second. The d.c. ammeter then showed a unidirectional current. The resistance was now decreased, and the arc fluttered and settled down, quite steadily, at a frequency of $33\frac{1}{3}$ per second. The d.c. ammeter, by registering nothing, indicated alternating current. The resistance was further decreased, and the arc settled down once more at a frequency of 25 per second. It again ran quite steadily, and the ammeter indicated a unidirectional current.

Incidentally we have in the a.c. arc a very simple method of " rectifying " small alternating currents.

I am indebted to Mr. M. N. S. Immelman and to Mr. S. Langerman, of this laboratory, for much helpful discussion during the course of this work.

XII. *Note on the "Bending" Properties of Symmetrical Electrical Networks.* *By* E. Selach, *Eng.* (*Leningrad*) *.

§ 1. *Introduction.*

THE bisection properties of a class of symmetrical networks have been frequently investigated in the pages of this magazine †. Here we intend to consider some still more general properties of symmetrical net-

Fig. 1.

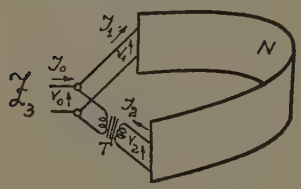

Fig. 2.

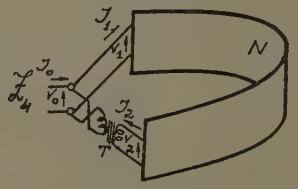

Fig. 3.

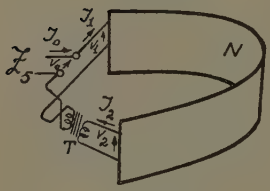

Fig. 4.

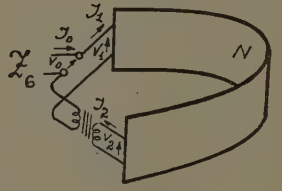

Fig. 5.

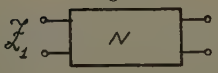

Fig. 6.

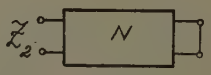

works referring to the schemes of figs. 1, 2, 3, and 4. These schemes have recently appeared in the literature ‡, and the following analysis of them should be of interest.

§ 2. *The "Bending" Theorem.*

By analogy with Bartlett's bisection theorem the following thesis may be stated :—

* Communicated by the Author.

† A. C. Bartlett, Phil. Mag. i. p. 553 (1926); iv. p. 902 (1927). O. Brune, Phil. Mag. xiv. p. 806 (1932).

‡ G. A. Campbell, Bell Syst. Techn. Journ., Nov. 1922. W. Cauer, *El. Nachr. Technik*, vii. (1929); v. (1932); Physics, ii. p. 242 (1932). Niquist and Brand, Bell Syst. Techn. Journ., July 1930.

If a symmetrical network with characteristic impedance Z_0 and propagation constant θ is "bent" according to figs. 1, 2, 3, and 4, T being an ideal transformer of 1 : 1 ratio, then

$$Z_3=\tfrac{1}{2}Z_0 \coth \frac{\theta}{2}, \quad . \quad . \quad . \quad . \quad . \quad . \quad (1)$$

$$Z_4=\tfrac{1}{2}Z_0 \tanh \frac{\theta}{2}, \quad . \quad . \quad . \quad . \quad . \quad . \quad (2)$$

$$Z_5=2Z_0 \coth \frac{\theta}{2}, \quad . \quad . \quad . \quad . \quad . \quad . \quad (3)$$

$$Z_6=2Z_0 \tanh \frac{\theta}{2}, \quad . \quad . \quad . \quad . \quad . \quad . \quad (4)$$

where Z_3, Z_4, Z_5 and Z_6 are the impedances of the two-terminal networks formed from the original one *.

The proof is very simple. Let V_1 and I_1 be the input voltage and current of the network N, V_2, and I_2, the output ones, and let V_0 be the voltage impressed on and I_0 the current entering the two-terminal networks of figs. 1, 2, 3 and 4. Then

$$\left.\begin{aligned} V_1&=V_2 \cosh \theta+I_2Z_0 \sinh \theta, \\ I_1&=V_2 \frac{1}{Z_0} \sinh \theta+I_2 \cosh \theta\,; \end{aligned}\right\} \quad . \quad . \quad . \quad . \quad . \quad (7)$$

$$\left.\begin{aligned} V_0&=I_0Z_3=V_1=V_2, \\ I_0&=I_1-I_2\,; \end{aligned}\right\} \text{ for fig. 1 only.} \quad . \quad . \quad (7a)$$

$$\left.\begin{aligned} V_0&=I_0Z_4=V_1=-V_2, \\ I_0&=I_1+I_2\,; \end{aligned}\right\} \text{ for fig. 2 only.} \quad . \quad . \quad (7b)$$

$$\left.\begin{aligned} V_0&=I_0Z_5=V_1+V_2, \\ I_0&=I_1=-I_2, \end{aligned}\right\} \text{ for fig. 3 only.} \quad . \quad . \quad (7c)$$

$$\left.\begin{aligned} V_0&=I_0Z_6=V_1-V_2, \\ I_0&=I_1=I_2. \end{aligned}\right\} \text{ for fig. 4 only.} \quad . \quad . \quad (7d)$$

* The notations Z_1 and Z_2 will be used further for the "open" and "closed" impedances of the network (see figs. 5 and 6). Remember that

$$Z_1=Z_0 \coth \theta, \quad . \quad . \quad . \quad . \quad . \quad . \quad . \quad . \quad . \quad (5)$$

$$Z_2=Z_0 \tanh \theta. \quad . \quad . \quad . \quad . \quad . \quad . \quad . \quad . \quad . \quad (6)$$

Solving together (7) with each of the equations (7 *a*), (7 *b*), (7 *c*), and (7 *d*), we get (1), (2), (3) and (4), containing the thesis.

Call it for brevity the bending theorem.

On the basis of the bending theorem the bisection theorem can be easily derived. Indeed, in a particular case, if the network N consists of two electrically similar parts, the "electrical midst" of the network will be evidently under "open condition" in the scheme of fig. 1, and under "closed condition" in the scheme of fig. 2. Thus

$$Z_3=\frac{A}{2}, \quad Z_4=\frac{B}{2}, \quad . \quad . \quad . \quad . \quad . \quad (8)$$

A and B being the "open" and "closed" impedances of each of the halves of the network N, measured (or calculated) from its original terminals.

Substituting (8) in (1) and (2), we get

$$A=Z_0 \coth\frac{\theta}{2}, \quad B=Z_0 \tanh\frac{\theta}{2}, \quad . \quad . \quad . \quad (9)$$

i. e., we obtain the bisection theorem.

§ 3. *Cases when the Ideal Transformer can be omitted.*

The most interesting cases for practice are those where the ideal transformer in figs. 1, 2, 3, and 4 can be omitted.

The sole purpose of this transformer is to make the input currents of the network N equal—in other words, to make it a "two-terminal pair." Naturally no transformer is needed when this equality of currents is assured without it.

On the basis of the author's former paper * it can be easily shown that the ideal transformer can be omitted in the following cases :—

(1) In all schemes of figs. 1, 2, 3, and 4 if N represents a "broken" network. We have given this name to a system that has no galvanical nor electrical coupling between the input and the output terminals. As an example, take a network containing a real transformer (fig. 7).

* E. Selach, *El. Nachr. Technik*, vii. (1931).

(2) In schemes of figs. 1 and 4 if N represents a so-called "three-pole" (fig. 8).

(3) In schemes of figs. 1 and 2 if the network N is symmetrical as to its longitudinal axis; and

(4) In the scheme of fig. 1 if the network N is symmetrical as to its transversal axis.

Fig. 7.

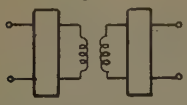

Fig. 8.

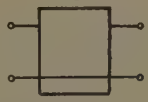

In all these cases the schemes of figs. 1, 2, 3, and 4 may be redrawn as in fig. 9.

Fig. 9.

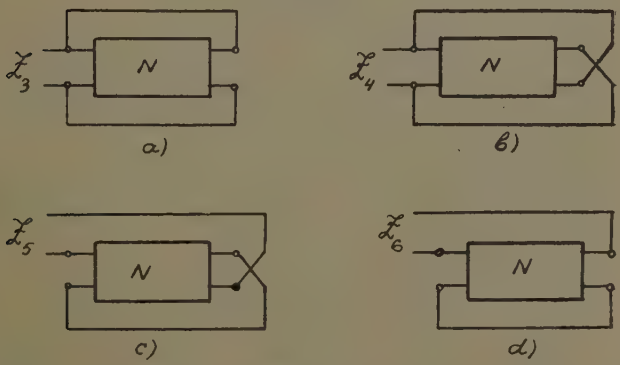

The list referred to, though not exhaustive, includes, however, most of the networks encountered in practice.

§ 4. *Relations between the Impedances* $Z_1, Z_2, Z_3, Z_4, Z_5, Z_6$.

From (1)–(6) simple relations between the impedances $Z_1, Z_2, Z_3, Z_4, Z_5, Z_6$, can be found:

$$Z_3 = \tfrac{1}{4} Z_5, \quad . \quad . \quad . \quad . \quad . \quad . \quad . \quad . \quad . \quad (10)$$

$$Z_4 = \tfrac{1}{4} Z_6, \quad . \quad . \quad . \quad . \quad . \quad . \quad . \quad . \quad . \quad (11)$$

$$Z_3 + Z_4 = Z_1, \quad . \quad . \quad . \quad . \quad . \quad . \quad . \quad . \quad . \quad (12)$$

$$Z_5+Z_6=4Z_1, \quad . \quad . \quad . \quad . \quad . \quad . \quad . \quad (12a)$$

$$\frac{1}{Z_3}+\frac{1}{Z_4}=\frac{4}{Z_2}, \quad . \quad . \quad . \quad . \quad . \quad . \quad . \quad . \quad (13)$$

$$\frac{1}{Z_5}+\frac{1}{Z_6}=\frac{1}{Z_2}, \quad . \quad . \quad . \quad . \quad . \quad . \quad . \quad . \quad (13a)$$

$$Z_1=\frac{4Z_3^2}{4Z_3-Z_2}, \quad . \quad . \quad . \quad . \quad . \quad . \quad . \quad . \quad (14)$$

$$Z_6=2\left[Z_1-\sqrt{Z_1(Z_1-Z_2)}\right], \quad . \quad . \quad . \quad (15)$$

and so on.

It may be seen now that a symmetrical network is completely determined by any pair of its impedances Z_1, Z_2, Z_3, Z_4, Z_5, Z_6 (except the pairs Z_3, Z_5 and Z_4, Z_6).

Due to this fact, many applications of the theory referred to are possible, such as determination of constants of symmetrical networks, construction of equivalent networks, analysis of electrical filters, etc.

§ 5. *Determination of Constants of Symmetrical Networks.*

The constants of a symmetrical network can be determined in an easy and rapid way when using the formulæ of the table derived from the equations (1)–(6).

Here are some typical examples.

Example 1.—To calculate the Z_0 and θ of the bridge network of fig. 10.

Fig. 10.

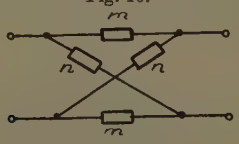

This problem can be solved by "bisection" or by "bending." The solution by "bisection" is given by Brune *, so we can deal here with the solution by the second method only.

Let us "bend" the network according to schemes (1) and (2), after being previously convinced that ideal transformers can be omitted in these schemes, because the

* *Loc. cit.*

TABLE.

Formulæ for determining Z_0 and θ.			Networks for which the ideal transformers of figs. 1, 2, 3, and 4 can be omitted.
$Z_0=2\sqrt{Z_3(Z_1-Z_3)}$,	$\tanh\frac{\theta}{2}=\sqrt{\frac{Z_1-Z_3}{Z_3}}$.	(16)	(1) "Broken" networks; (2) "three-poles"; (3) networks symmetrical as to their longitudinal axis; (4) networks symmetrical as to their transversal axis.
$Z_0=2Z_3\sqrt{\frac{Z_2}{4Z_1-Z_2}}$,	$\tanh\frac{\theta}{2}=\sqrt{\frac{Z_2}{4Z_3-Z_2}}$.	(17)	
$Z_0=2\sqrt{Z_1(Z_1-Z_4)}$,	$\tanh\frac{\theta}{2}=\sqrt{\frac{Z_4}{Z_1-Z_4}}$.	(18)	(1) "Broken" networks; (2) networks symmetrical as to their longitudinal axis.
$Z_0=2Z_1\sqrt{\frac{Z_2}{4Z_4-Z_2}}$,	$\tanh\frac{\theta}{2}=\sqrt{\frac{4Z_4-Z_2}{Z_2}}$.	(19)	
$Z_0=2\sqrt{Z_3Z_4}$,	$\tanh\frac{\theta}{2}=\sqrt{\frac{Z_4}{Z_3}}$. . .	(20)	
$Z_0=\sqrt{Z_5(Z_1-\frac{1}{4}Z_5)}$,	$\tanh\frac{\theta}{2}=\sqrt{\frac{4Z_1-Z_5}{Z_5}}$.	(21)	(1) "Broken" networks.
$Z_5=\frac{1}{2}Z_5\sqrt{\frac{Z_2}{Z_5-Z_2}}$,	$\tanh\frac{\theta}{2}=\sqrt{\frac{Z_2}{Z_5-Z_2}}$.	(22)	
$Z_0=\sqrt{Z_4Z_5}$,	$\tanh\frac{\theta}{2}=\sqrt{\frac{4Z_4}{Z_5}}$. . .	(23)	
$Z_0=\frac{1}{2}\sqrt{Z_6Z_6}$,	$\tanh\frac{\theta}{2}=\sqrt{\frac{Z_6}{Z_5}}$. . .	(24)	
$Z_0=\sqrt{Z_6(Z_1-\frac{1}{4}Z_6)}$,	$\tanh\frac{\theta}{2}=\sqrt{\frac{Z_6}{4Z_1-Z_6}}$.	(25)	(1) "Broken" networks; (2) "three-poles."
$Z_0=\frac{1}{2}Z_6\sqrt{\frac{Z_2}{Z_5-Z_2}}$,	$\tanh\frac{\theta}{2}=\sqrt{\frac{Z_6-Z_2}{Z_2}}$.	(26)	
$Z_0=\sqrt{Z_3Z_6}$,	$\tanh\frac{\theta}{2}=\sqrt{\frac{Z_6}{4Z_3}}$. .	(27)	

network is symmetrical as to its longitudinal axis (see table). Then

$$Z_2=\tfrac{1}{2}n, \quad Z_4=\tfrac{1}{2}m. \quad . \quad . \quad . \quad . \quad . \quad (28)$$

Putting (28) into (20), we get at once

$$Z_0=\sqrt{mn}, \quad \tanh\frac{\theta}{2}=\sqrt{\frac{m}{n}}.$$

Example 2.—To calculate Z_0 and θ of the network represented on fig. 11.

It is obvious that this problem cannot be solved by bisection. For this reason we shall apply the "bending."

Fig. 11.

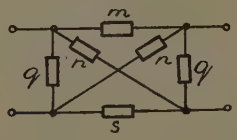

Bearing in mind that the network is symmetrical as to its transversal axis (see table), we compute by inspection

$$\left.\begin{aligned} Z_2&=\frac{q\left(\dfrac{mn}{m+n}+\dfrac{ns}{n+s}\right)}{q+\dfrac{mn}{m+n}+\dfrac{ns}{n+s}}, \\ Z_3&=\frac{1}{2}\cdot\frac{nq}{n+q}. \end{aligned}\right\} \quad . \quad . \quad . \quad . \quad (29)$$

Substituting (29) in (17), we find the result:

$$Z_0=q\sqrt{\frac{n}{n+q}\cdot\frac{mn+2ms+ns}{mn+2ms+ns+q(m+2n+s)}},$$

$$\tanh\frac{\theta}{2}=\sqrt{\frac{n+q}{n}\cdot\frac{mn+2ms+ns}{mn+2ms+ns+q(m+2n+s)}}.$$

Note that the method of determination of Z_0 and θ with the aid of the table can be considered as a

generalization of the classical " open and closed " method, with its well-known relations

$$Z_0 = \sqrt{Z_1 Z_2}, \quad \tanh\theta = \sqrt{\frac{Z_2}{Z_1}}. \quad . \quad . \quad (30)$$

Fig. 12.

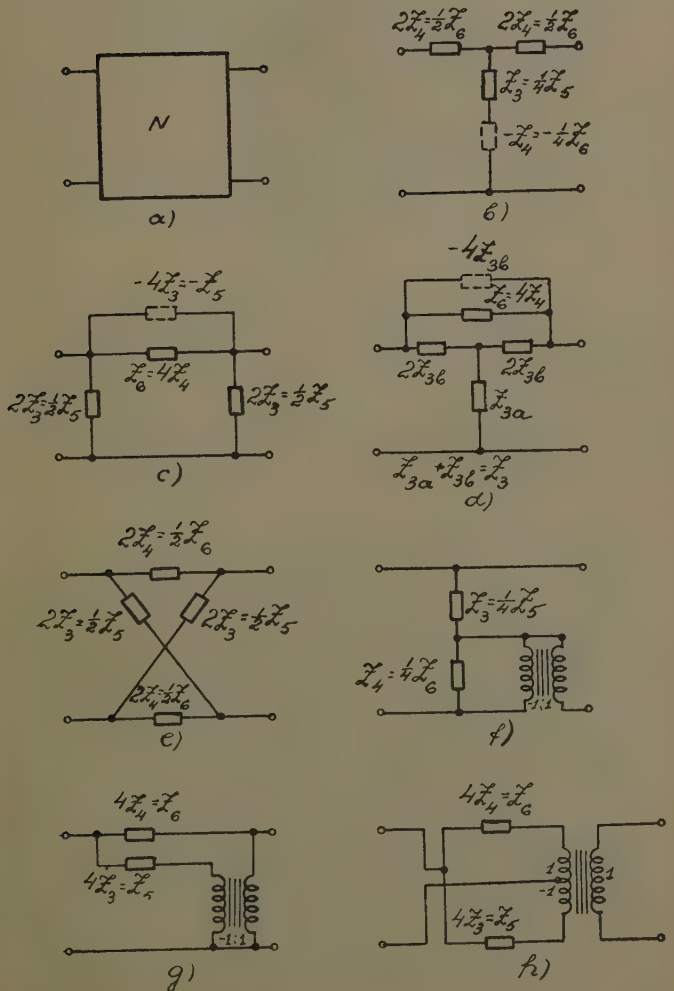

In many cases the values of Z_1, Z_2, Z_3, Z_4, Z_5, Z_6, instead of being calculated, can be determined with the aid of measurements only. In such cases, as a detailed analysis * has shown, the use of the "bending" impedances enables us to measure greater values of θ than the classical "open and closed" method.

§ 5. *Construction of Equivalent Networks.*

Now apply the "bending" impedances to construct networks equivalent to a given one.

Two sets of such networks, expressed in the terms of the "bending" impedances, are shown in figs. 12 and 13, N being the given symmetrical section. The

Fig. 13.

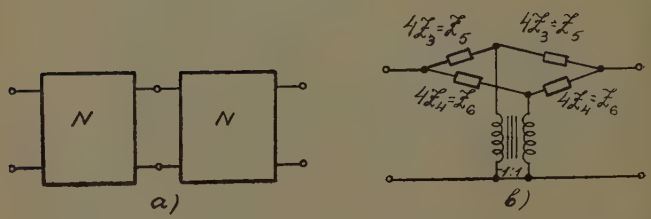

equivalence of the networks in each set can be easily proved by bisection or by "bending."

It may be seen that the schemes of fig. 12, *b*, *c*, *d*, cannot be physically realized, except definite cases. The structures of fig. 12, *e*, *f*, *g*, *h*, and fig. 13, *b*, however, are always realizable, provided that transformers sufficiently approximating to an ideal one can be constructed.

As to the ideal transformers in the impedances Z_3, Z_4, Z_5, and Z_6, they may be frequently omitted if the impedances are suitably chosen. So for the network of fig. 14, *a*, an equivalent network without transformers can be constructed, employing the impedances Z_3 and Z_4 (fig. 14, *b*), but it cannot be done with the aid of the impedances Z_5 and Z_6, all the more with the aid of bisection.

* Published in a separate paper by the same author.

§7. *Analysis of Filters.*

Finally, illustrate how the "bending" impedances can be applied to the analysis of electrical filters. There are usually two types of filters: the balanced type (that is, symmetrical as to its longitudinal axis) and the unbalanced one (that is, a "three-pole"). In both the ideal transformers can be omitted when using Z_3 and Z_4 for the balanced type and Z_3 and Z_6 for the unbalanced one.

Now $$\theta=\alpha+j\beta,$$

and

$$\tanh\frac{\theta}{2}=\frac{\sinh\alpha+j\sin\beta}{\cosh\alpha+\cos\beta}=\sqrt{\frac{Z_4}{Z_3}}=\sqrt{\frac{\frac{1}{4}Z_6}{Z_3}}. \quad (31)$$

Fig. 14.

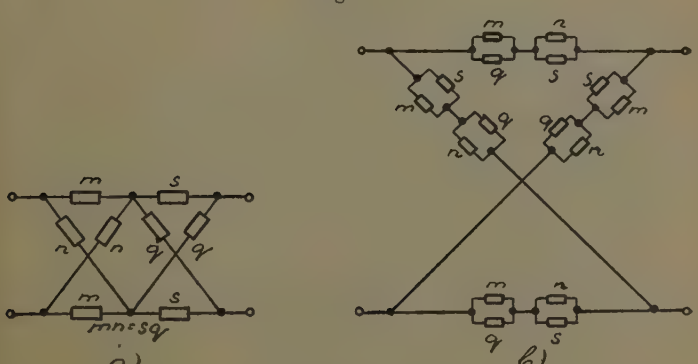

A discussion of (31), provided Z_3, Z_4, and Z_6 are pure reactances, leads to the following conclusions * :—

(1) The frequencies for which Z_4 (or $\frac{1}{4}Z_6$) and Z_3 are of opposite sign pass through the filter without attenuation, and

(2) the frequencies for which Z_4 (or $\frac{1}{4}Z_6$) and Z_3 have the same sign are highly attenuated by the filter; particularly is the attenuation infinite when

$$Z_3=Z_4, \text{ or } Z_3=\tfrac{1}{4}Z_6. \quad . \quad . \quad . \quad . \quad (32)$$

* *Cf.* A. Jaumann, *Veröff. aus d. Gebiete d. Nachrichtentechnik* (*Siem. u. Halske*), iv. p. 248 (1932).

Take, for instance, the bridged-T network of fig. 15. Compute its impedances Z_3 and Z_6, which can be easily done by inspection,

$$Z_3 = j\left(\omega L_2 - \frac{1}{\omega}\cdot\frac{2C_1+C_2}{2C_1C_2}\right), \quad Z_6 = j\frac{\omega L_1}{1-\frac{1}{2}\omega^2 L_1 C_1}. \quad (33)$$

Fig. 15.

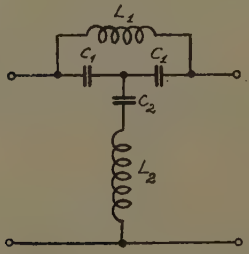

Now draw Z_3 and $\frac{1}{4}Z_6$ as functions of frequency according to three different arrangements of the network (fig. 16).

We see at once that in the first case (fig. 16, *a*) the network passes the frequency bands $0 \ldots f_1$ and $f_2 \ldots 0$,

Fig. 16.

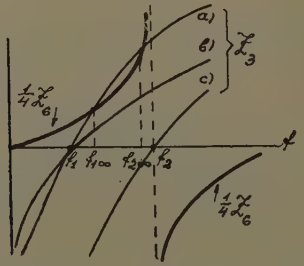

and attenuates the band $f_1 \ldots f_2$, having an infinite attenuation for the frequencies $f_{1\infty}$ and $f_{2\infty}$. In the second case (fig. 16, *b*) the bands hold, but the frequencies $f_{1\infty}$ and $f_{2\infty}$ vanish. Finally, in the third case the network is no more a filter, passing freely all the frequencies. The values of f_1, f_2, $f_{1\infty}$, and $f_{2\infty}$ can be easily found on the basis of (33).

Thus a simple method to determine the location of transmitted and attenuated bands is obtained. In comparison with the well-known method, confined to ladder and lattice structures only *, the above method is directly applicable to filters of any construction.

Scientific Research Institute for
Electrical Communication, Leningrad, U.S.S.R.
January 1935.

XIII. *Notices respecting New Books.*

Inequalities. By G. H. Hardy, J. E. Littlewood, and G. Polya. (Cambridge University Press. Price 16*s*.)

IT has been customary among Mathematical Analysts until quite recently, to regard inequalities as propositions whose importance and interest are mainly derived from the particular results with which they are connected. A consequence of this has been that analysts in the past have obtained a knowledge of inequalities by meeting them individually and unsystematically as they appear. Although it would be generally agreed that this method of acquiring the requisite knowledge yields a satisfactory intimacy with the subject-matter, it has long been felt that the subject should be available in collected form. Further, no one would deny that inequality theory possesses an elegance in itself, both in statement and proof, which is far from common in modern developments of pure mathematics. For these reasons, a work devoted entirely to inequalities is most welcome to those who find the subject æsthetically satisfying, to those who require inequalities as ready and powerful weapons, and to those who meet the subject for the first time. It is, additionally a source of satisfaction that this book, the first of its kind, should come from three authors who have done as much in the subject as any other living persons.

The book opens with a complete account of the inequalities which have become part of the everyday equipment of the modern analyst ; the inequalities bearing the names of Holder and Minkowski may be regarded as typical. Alternative proofs are given, the alternatives being chosen from amongst the many possibilities, to show additional aspects of the inequalities. Many extensions of the original unelaborated inequalities are given, and even if the newcomer to the subject

* G. A. Campbell, *l. c.*, or T. E. Shea, 'Transmission Networks and Wave Filters,' p. 240, London (1929).

might be well advised to leave the elaborations alone, yet the older hand will be glad to have them available in case of need, or as a piece of reading for an empty hour. The remainder of the work is devoted to inequalities which as yet are not as well known as their elder brethren and which lead up to certain types of function theory in particular, to work in Fourier's Series and Complex Variable theory. In order to restrict themselves to the field imposed by the title of their book, the authors have excluded all save mere reference to the function theory itself, so that this final section must be regarded as an introduction to inequalities of function theory type. For this purpose the references given are ample.

As is customary with these authors, the true inwardness of their subject-matter is never sacrificed to over rigid meticulousness of style ; this is of great importance in a book on inequalities, for a complete grasp of an inequality always demands a complete grasp of the proof, and the proof is usually of a concentrated type, savouring of the lightning flash of inspiration rather than of the virtues of diligence. The work may be safely regarded as a never failing source of inspiration, enjoyment, and encouragement to all who read it. It is compendious without being dull, detailed while never overwhelming. The authors must be justly satisfied with their product.

Monographs on Biochemistry : *The Carbohydrates.* By E. F. Armstrong and K. F. Armstrong. [Pp. 247.] (London : Longmans, Green & Co., Ltd., 1934. Price 15*s.* net.)

In 1910 the senior author of this work, whose investigations in the laboratory of Emil Fischer enabled him to write with authority, published the first edition of ' The Simple Carbohydrates and the Glucosides,' of which further editions appeared in 1912, 1919, and 1924. On account of the rapid expansion which has recently taken place in our knowledge of carbohydrate chemistry, the division of the book became necessary, and ' The Glycosides ' appeared in 1931.

The authors state " it is primarily our object to appeal to those interested in sugar chemistry from a biological aspect, and we have therefore confined our attention to the natural sugars and their derivatives and restricted as much as possible the discussion of intricate structural problems."

This aim has been entirely fulfilled, and the ever increasing importance of these compounds in both plant and animal physiology is apparent on almost every page. The very valuable lists of references appended to each chapter deal, moreover, with most of the latest work. The manner in which

the unsolved problems of sugar chemistry are discussed is particularly valuable and will afford a constant stimulus to research.

The authors state in their preface "we have ..... purposely avoided a discussion of sugar metabolism, muscle contraction and fermentation." The latter subject receives, nevertheless, a certain amount of attention, and on p. 225 an attempt is made to give a very brief account of the course of events in alcoholic fermentation, the importance of the hexosephosphates in this process being indicated. No hint is given, however, that during the last two years a very much closer insight into the part played by these phosphates has been gained, due to the work of Meyerhof, Embden, and Lohmann. A detailed discussion of this would have been contrary to the authors' scheme, but a brief indication, with references, of the lines along which the recent advances have been made might, perhaps, have been inserted.

On the other hand, the recent and important work on ascorbic acid both in England and abroad is included. The relation of kojic acid to the hexoses is also touched upon.

Much interesting information is recorded concerning glycuronic and galacturonic acids. The significance of the former in its relation to the origin of xylose and the structure of xylan and the hemicelluloses is discussed; galacturonic acid has an analogous importance as regards arabinose and the pectins. Recent work on the mechanism of the formation of conjugated glycuronic acids in the animal body is also described. The researches of Heidelberger and Avory on specific carbohydrates and immunity are outlined, and here again glycuronic acid is shown to form part of the structure of two out of the three polysaccharides obtained from pneumococci. In view of the biological importance of this acid it always seemed surprising that it had not been detected in mould cultures on glucose. An observation of Kiliani, recorded on p. 229, would appear to indicate that such a formation has now been established.

While the action of moulds is being considered reference may be made to another aspect of this subject, with which the authors deal on p. 228. The remarkable results of Chrzaszcz and of Bernhauer on the mycological production of citric acid from acetic acid or acetates and from alcohol, have brought theories regarding the mechanism of this change into line with those on the breakdown of carbohydrate by yeasts and bacteria and of its metabolism in muscle.

The reader will turn with interest to those chapters which deal with the di- and polysaccharides. The structural formulæ are clearly represented, and the methods by which these have been established are briefly indicated. Then

follows an interesting discussion of the relation of the di- and trisaccharides to each other and to sucrose, from which they are presumably derived. Their occurrence and behaviour to various enzymes also receive considerable attention.

Passing to the complex polysaccharides an outline is given of Haworth's method for the determination of the molecular dimensions of cellulose, starch, and inulin. Reference is also made to the synthesis of pure cellulose by the growth of *Acetobacter xylinum* on glucose or fructose, and to the very important demonstration that the molecule of starch contains phosphoric acid residues as an integral part, yielding glucose-6-phosphoric acid on hydrolysis.

It is a matter for the deepest regret that Dr. K. F. Armstrong, for whom his colleagues prophesied a most brilliant and valuable scientific career, lost his life early this year in an Alpine accident. This is not the place to comment upon his achievements, but the writer wishes, in conclusion, to express his deep sense of the loss which chemistry and British University life have alike suffered as a result of this tragedy.

The Kinetic Theory of Gases. By Leonard B. Loeb. Second Edition. [Pp. xx+687.] (McGraw-Hill, New York and London, 1934. Price 36*s*.)

The value of the first edition of this book has been widely recognized and the appearance of a second edition, completely revised and with much new material, is very welcome. The new material is partly concerned with quantum theory developments; but by no means entirely, for the field is one in which the purely classical theory is still gaining triumphs.

The book is characterized by the detailed treatment of experimental aspects of the subject, and by the presentation of the theory with adequate explanations of the mathematical steps for the reader who is not a "professional" mathematician. The treatment throughout is by the more strictly kinetic theory methods rather than by those of statistical mechanics. The first three chapters deal with the history and the fundamental ideas of the theory. The distribution of velocities is then treated in detail; in the experimental part an account is given of the recent tests of the results by molecular ray methods. The more rigorous treatment of the equation of state is then developed. The following three chapters are concerned with transport phenomena, low pressure and surface phenomena, and the Brownian movement. Specific heats are then discussed, with a full account of the quantum theory treatment, including the work on ortho- and para-hydrogen. The last two chapters are concerned

with applications of kinetic theory to electric and magnetic susceptibilities, and to the conduction of electricity by gases, a subject to which the author's own contributions are very considerable.

The book reveals throughout the author's enthusiasm for the subject, and also his wide knowledge of the literature. Many sections, as is gracefully acknowledged, follow closely on the lines of previous books. It is pleasant to find an appreciation not only of original experimental and theoretical work, but also of methods of presentation in "secondary" sources. In some ways the book suffers from the disadvantages of being at once a "text" and a reference book; in the sense that, through anxiety to give due reference to all relevant work, the text at times is almost too full. But in no sense is the book merely a digest; the impress of the author's critical consideration of each topic is always evident.

Only very occasionally will the less mathematical reader feel hardly treated. An instance occurs in the derivation of the velocity distribution law. It would seem that the detail in which some of the simpler steps are explained is rather supererogatory if the reader can be assumed to be familiar with the functional transformation determinant, which is introduced without explanation or reference.

The price of the book, though perhaps not excessive for the matter, will place it beyond the means of many who might wish to buy it, and for this reason it might be better if the applications to gaseous conductivity and susceptibilities were dealt with separately; the two chapters, however, are in themselves admirable, and certainly add to the value of the book.

Full references are given both to original papers and to text-books, and there are useful appendices containing physical constants, molecular data, and mathematical tables.

The book will be invaluable to those who require an up-to-date reference book on kinetic theory; at the same time it is a most readable account of the subject for physicists and chemists generally.

S. T. Coleridge's 'Treatise on Method' as published in the *'Encyclopædia Metropolitana.'* Ed. Alice D. Snyder. [Pp. xxviii+92.] (London: Constable & Co., Ltd., 1934. Price 6*s.* net.)

To those who think of Coleridge as a strewer of inspired fragments it may seem strange that so unmethodical a pen should write 'A Preliminary Treatise on Method.' This 'General Introduction,' as it was printed in the 1818 edition

of the 'Encyclopædia Metropolitana' or, with slight variations, in the Cabinet Edition of 1849, though editorial alterations once made Coleridge threaten to disown it, shows that Coleridge could write as methodically as a student of method should. He was, apparently, less able to keep pace with the serial publication of the 'Encyclopædia Metropolitana' by completing other articles, or sections, at their required dates. He did write the 'Preliminary Treatise on Method.' To this, and to "the general plan" which was also considerably altered, Coleridge's share in the 'Encyclopædia Metropolitana' was confined.

The prevalent encyclopædia habit, by constructing compendiums of knowledge, stirred compilers to plan systems. Coleridge could not ignore the convenient "Alphabetical Department," in which, for instance, the "thermometer" would have its "varieties of construction" described, but "the Principles of the Thermometer" would be disclosed under "the effects of heat" because the "Philosophical arrangement" was intended to control the "Alphabetical." Coleridge's "correct Philosophical Method," however, able or unable to control the working schemes of 'Dictionaries of Science,' has its own interest as a significant item in his philosophical output. Miss Snyder, by ably editing and annotating the 'Treatise on Method,' has assisted the present interest in Coleridge's philosophy.

This short systematic survey of the domains of knowledge and their relations provides an interesting insight into Coleridge's thought. It also flashes side-lights on the science of the day—as in its reference to light and heat "as imponderable substances." Perhaps it helps to correct some impressions of Bacon through its insistence on "the completion of the Ideal System, by applying the same Method to external Nature which Plato had before applied to intellectual existence." Coleridge could hardly keep Shakespeare out if there was any excuse for bringing him in, and poetry, represented by Shakespeare, is included in the philosophical scheme with a discussion of the sciences—"Pure" or "Mixed and Applied." His remark that "Every Physical Theory is in some measure imperfect, because it is of necessity progressive," is as relevant, if not more relevant, now as it was then.

Thought has moved since the 'Treatise on Method' was written, but this little manifesto, whether it is dwelling on a now purely historical interest, or still provoking assent or dissent, displays Coleridge's penetrative mind and the qualities of his writing.

[*The Editors do not hold themselves responsible for the views expressed by their correspondents.*]

(i.).

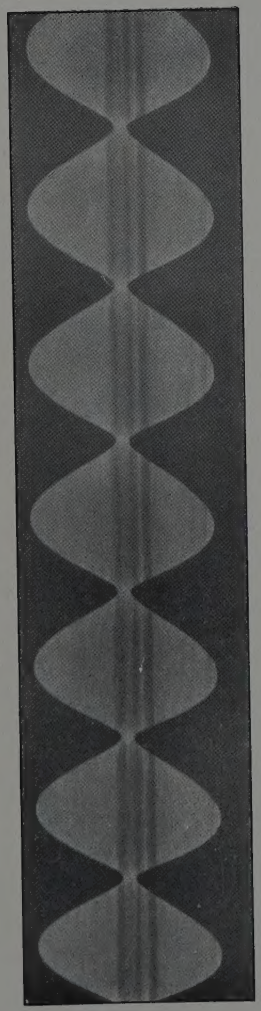

(ii.).

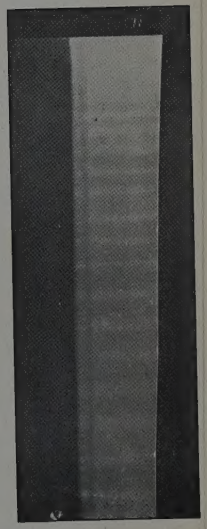

(iii.).

(iv.).

(v.).

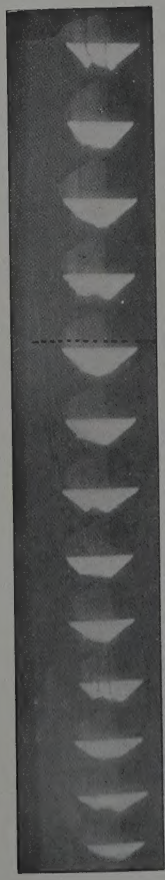

(vi.).